

THE PLEISTOCENE PLANKTONIC FORAMINIFERAL
AMINOSTRATIGRAPHY OF OCEAN DRILLING PROGRAM HOLE 625B
IN THE NORTHEAST GULF OF MEXICO

by

Beverly J. Johnson

A thesis submitted to the Faculty of the University of
Delaware in partial fulfillment of the requirements for the degree
of Master of Science in Geology

May, 1990

THE PLEISTOCENE PLANKTONIC FORAMINIFERAL
AMINOSTRATIGRAPHY OF OCEAN DRILLING PROGRAM HOLE 625B
IN THE NORTHEAST GULF OF MEXICO

by

Beverly J. Johnson

Approved: _____
John F. Wehmiller, Ph.D.
Professor in charge of thesis on behalf of the Advisory
Committee

Approved: _____
Billy P. Glass, Ph.D.
Chairman of the Department of Geology

Approved: _____
Carol E. Hoffecker, Ph.D.
Acting Associate Provost for Graduate Studies

ACKNOWLEDGEMENTS

I would like to thank my thesis advisor, Dr. John F. Wehmiller. His continued interest, feedback and support throughout the extent of this project were integral to its completion. Thanks also goes to the other members of my thesis committee, Dr. Ronald E. Martin, and Dr. Billy P. Glass for their time and efforts.

There are many people in Delaware I feel very lucky to have met, only a few of which I can acknowledge in this thesis. Brenda Spotz and Glenn Johnson taught me how to identify the foraminiferal species used and offered guidance throughout the biostratigraphic part of this study. June Mirecki and Linda York taught me how to run an HPLC and then offered valuable insights into interpreting the data. Scott Howard and Hi-Il Yi were two of the many who cheerfully helped me to meet some of my "last" deadlines. Office-mates Phil Chen, Al Fernandez, Steve Baumgardner, Greg Rubino and Khalequezzaman provided me with many smiles. Talks with Kate Butoryak, Linda York, June Mirecki, Andy Victor-Gasper, and Brenda Spotz helped me to maintain some degree of sanity. Thanks goes to Al Thompson for

sharing with me some of his philosophies on life. A warm thanks goes to William Lowe for the encouragement and support, and for many unforgettable evenings shared over a computer. A special thanks goes to Vicki Crouse (whose zest for life is contagious) for many hearty laughs (Pinkies up!) and a lot of good conversations.

My deepest thanks goes to my family, particularly Ann and Jack. Their unconditional love, unfaltering support and genuine friendship have always made every cleared hurdle along the way a triumph in life.

TABLE OF CONTENTS

	<u>page</u>
LIST OF FIGURES	ix
LIST OF TABLES	xvii
ABSTRACT.....	xviii
 <u>Chapter</u>	
1 INTRODUCTION	1
Background to Amino Acid Racemization.....	1
Introduction to Racemization/Epimerization	1
Geological Applications of Racemization/Epimerization.....	2
Objectives.....	6
Study Area.....	7
Location and Logistics	7
Past and Present Work on Site 625B.....	9
2 KINETICS OF RACEMIZATION/EPIMERIZATION	13
Introduction.....	13
First-Order Reversible Kinetics	15
Age Determinations.....	16
Paleotemperature Estimates.....	17
Diagenetic Reactions Affecting Epimerization.....	19
Hydrolysis and Epimerization.....	19
Carbonate Dissolution and Leaching.....	21
Decomposition of Amino Acids.....	22

Table of Contents (continued)

	<u>page</u>
3	METHODOLOGY 23
	Introduction..... 23
	Processing and Isolating Foraminifera..... 23
	Core Sample Processing..... 23
	Species Identification 25
	Sample Picking..... 30
	Methodology of Amino Acid Analyses..... 31
	Chemical Cleaning..... 31
	Dissolution, Hydrolysis, and Drying-Down of Samples..... 35
	High Performance Liquid Chromatography (HPLC)..... 37
	Data Reduction..... 41
	Precautions Used Against Contamination..... 43
	Numerical Age Assignment..... 45
	Data Presentation..... 46
4	RESULTS-CLEANING EXPERIMENTS..... 48
	Introduction..... 48
	Criteria For Determining Sample Cleanliness..... 49
	Hydrogen Peroxide..... 52
	Ammonium Hydroxide..... 59
	Two Cleaning Methods Compared in Foraminiferal Samples..... 66
5	RESULTS-AMINOSTRATIGRAPHY OF ODP HOLE 625B ... 80
	Epimerization Results of the Total Fraction..... 80
	<u>Orbulina universa</u> 80
	<u>Neogloboquadrina dutertrei</u> 82
	<u>Globorotalia tumida-menardii</u> Complex..... 82
	Monospecific Species Comparison..... 85
	Mixed Foraminiferal Species Assemblage..... 89

Table of Contents (continued)

	<u>page</u>
Epimerization Results of the Free and Bound Fractions.....	92
Free Fraction.....	92
Bound Fraction.....	92
6 DISCUSSION.....	95
Intercore Correlations Between Gulf of Mexico Core 625B, Mid-Atlantic Core 13519-2, and Equatorial Pacific Core V28-238.....	95
Introduction.....	95
Epimerization Trends In All Three Cores.....	97
Syn-Depositional Dissolution In All Three Sites.....	102
Post-Depositional Dissolution In All Three Sites.....	104
Quantification of Dissolution Using Amino Acid Data	112
Site 625B.....	112
Core 13519-2.....	118
Constant Bottom Water Temperature?.....	121
Intergeneric Comparisons.....	122
Amino Acids in The Clay Fraction.....	122
7 CONCLUSIONS.....	125
Cleaning Methods.....	125
Carbonate Dissolution.....	126
The Record Preserved at Site 625B.....	128
Aminostratigraphy of Site 625B.....	130
Proposed Taxonomic Study.....	138
REFERENCES.....	139

Table of Contents (continued)

page

APPENDICES

APPENDIX A: Procedure for Wet Sieving.....	150
APPENDIX B: Sample Calculation for Determining the Number of Nanomoles Amino Acid/Gram Carbonate Material.....	152
APPENDIX C: Raw Data of <u>Globigerinoides ruber</u>	154
APPENDIX D: Raw Data of <u>Orbulina universa</u>	158
APPENDIX E: Raw Data of <u>Neogloboquadrina dutertrei</u>	160
APPENDIX F: Raw Data of the <u>Globorotalia tumida-menardii</u> complex.....	162
APPENDIX G: Raw Data of the Mixed Foraminiferal Assemblage.....	164
APPENDIX H: Raw Data of the Interlaboratory Comparison Powders.....	166

LIST OF FIGURES

	<u>page</u>
Figure 1.1: General structure of an amino acid in the L- and D-enantiomers.....	3
Figure 1.2: Map of Northeastern Gulf of Mexico showing location of Site 625, seismic profile track lines (labeled 124, 126, 128), and the bathymetry of the basin (from Rabinowitz et al., 1985; after Mitchum, 1978).....	8
Figure 2.1: "Non-linear" kinetic curve of isoleucine epimerization in marine sediments, where $X = (A/A+I)$ at any time, T, and $X_E = X$ at equilibrium (modified from Wehmiller and Hare, 1971; and Wehmiller, 1982).....	14
Figure 3.1: Diagram of generalized procedures used for amino acid analysis in foraminiferal tests from ODP Site 625B.....	24
Figure 3.2.a: Percent abundance of <u>Globigerinoides ruber</u> in the upper 100 m of ODP Site 625B (from Johnson, 1988).....	26
Figure 3.2.b: Percent abundance of <u>Orbulina universa</u> in the upper 230 m of ODP Site 625B (from Johnson, 1988; Spatz, 1989).....	26

List of Figures (continued)

	<u>page</u>
Figure 3.2.c: Percent abundance of <u>Neogloboquadrina dutertrei</u> in the upper 230 m of ODP Site 625B (from Johnson, 1988; Spotz, 1989).....	27
Figure 3.2.d: Percent abundance of the <u>Globorotalia tumida-menardii</u> complex in the upper 100 m of ODP Site 625B (from Johnson, 1988).....	27
Figure 3.3: Diagram of procedures used for cleaning of foraminiferal tests from ODP Site 625B.....	33
Figure 3.4: Sample chromatogram of <u>Neogloboquadrina dutertrei</u> taken from ODP 625B core sample 3/4: 53-55 cm (22.5 m sub-bottom depth).....	39
Figure 3.5: Sample chromatogram of the <u>Globorotalia tumida-menardii</u> complex taken from ODP 625B core sample 12/6: 0-2 cm (99.5 m sub-bottom depth).....	40
Figure 3.6: Sample chromatogram of the quantitative standard.....	42
Figure 4.1: A/I ratios in samples of <u>Globigerinoides ruber</u> found at depths greater than 70.5 m in ODP Site 625B.....	53
Figure 4.2: A/I ratios in samples of <u>Globigerinoides ruber</u> found at depths between 68.00 and 70.25 m in ODP Site 625B.....	55
Figure 4.3: A/I ratios in samples of <u>Globigerinoides ruber</u> from ODP Site 625B.....	58
Figure 4.4.a: Serine/Leucine ratios in samples of <u>Globigerinoides ruber</u> from ODP Site 625B.....	61

List of Figures (continued)

	<u>page</u>
Figure 4.4.b: Glycine/Alanine ratios in samples of <u>Globigerinoides ruber</u> from ODP Site 625B.....	61
Figure 4.4.c: A/I ratios in samples of <u>Globigerinoides ruber</u> from ODP Site 625B.....	62
Figure 4.4.d: Total isoleucine concentrations (alloisoleucine + isoleucine) in samples of <u>Globigerinoides ruber</u> from ODP Site 625B.....	62
Figure 4.4.e: Total amino acid concentrations in samples of <u>Globigerinoides ruber</u> from ODP Site 625B.....	63
Figure 4.5: A/I ratios in samples of <u>Globigerinoides ruber</u> found at depths between 50.0 and 65.0 m in ODP Site 625B.....	65
Figure 4.6.a: A/I ratios in samples of <u>Orbulina universa</u> cleaned using one of two methods from ODP Site 625B.....	68
Figure 4.6.b: Serine/Leucine ratios in samples of <u>Orbulina universa</u> cleaned using one of two methods from ODP Site 625B.....	68
Figure 4.6.c: Glycine/Alanine ratios in samples of <u>Orbulina universa</u> cleaned using one of two methods from ODP Site 625B.....	69
Figure 4.6.d: Total amino acid concentrations in samples of <u>Orbulina universa</u> cleaned using one of two methods from ODP Site 625B.....	69

List of Figures (continued)

	<u>page</u>
Figure 4.7.a: A/I ratios in samples of <u>Neogloboquadrina dutertrei</u> cleaned using one of two methods from ODP Site 625B.....	73
Figure 4.7.b: Serine/Leucine ratios in samples of <u>Neogloboquadrina dutertrei</u> cleaned using one of two methods from ODP Site 625B.....	73
Figure 4.7.c: Glycine/Alanine ratios in samples of <u>Neogloboquadrina dutertrei</u> cleaned using one of two methods from ODP Site 625B.....	74
Figure 4.7.d: Total amino acid concentrations in samples of <u>Neogloboquadrina dutertrei</u> cleaned using one of two methods from ODP Site 625B.....	74
Figure 4.8: A/I ratios in ILC-B samples cleaned using one of three methods.....	78
Figure 5.1.a: A/I ratios plotted against age in samples of <u>Orbulina universa</u> through the Pleistocene and Pliocene of ODP Site 625B.....	81
Figure 5.1.b: A/I ratios plotted against age in samples of <u>Orbulina universa</u> through the Pleistocene and Pliocene of ODP Site 625B.....	81
Figure 5.2.a: A/I ratios plotted against age in samples of <u>Neogloboquadrina dutertrei</u> through the Pleistocene and Pliocene of ODP Site 625B.....	83
Figure 5.2.b: A/I ratios plotted against age in samples of <u>Neogloboquadrina dutertrei</u> through the Pleistocene and Pliocene of ODP Site 625B.....	83

List of Figures (continued)

	<u>page</u>
Figure 5.3.a: A/I ratios plotted against age in samples of the <u>Globorotalia tumida-menardii</u> complex through the Pleistocene of ODP Site 625B.....	84
Figure 5.3.b: A/I ratios plotted against age in samples of the <u>Globorotalia tumida-menardii</u> complex through the Pleistocene of ODP Site 625B.....	84
Figure 5.4.a: A/I ratios plotted against age in samples of <u>Orbulina universa</u> , <u>Neogloboquadrina dutertrei</u> , and the <u>Globorotalia tumida-menardii</u> complex through ODP Site 625B.....	86
Figure 5.4.b: A/I ratios plotted against age in samples of <u>Orbulina universa</u> , <u>Neogloboquadrina dutertrei</u> , and the <u>Globorotalia tumida-menardii</u> complex over the first 100 ka (14.5 m).	88
Figure 5.5.a: A/I ratios plotted against age in samples of the mixed foraminiferal species assemblage through ODP Site 625B.....	90
Figure 5.5.b: A composite aminostratigraphy of ODP Site 625B, including the A/I ratios measured in the monospecific samples, as well as those ratios measured in the mixed foraminiferal species assemblages.....	91
Figure 5.6.a: A/I ratios of the total and free fraction of isoleucine plotted against age in samples of the mixed foraminiferal species assemblages from ODP Site 625B.....	94

List of Figures (continued)

	<u>page</u>
Figure 5.6.b: A/I ratios of the total, free and bound (total - free) fractions of isoleucine plotted against age in samples of the mixed foraminiferal species assemblages from ODP Site 625B.....	94
Figure 6.1: A/I ratios in samples of two spinose species of the same family, <u>Globigerinoides</u> compared in three ocean basins.....	98
Figure 6.2.a: A/I ratios in samples of the non-spinose species <u>Globorotalia tumida-menardii</u> complex from Gulf of Mexico Site 625B, mid-Atlantic Core 13519-2 (from Mueller, 1984), and Pacific Core V28-238 (from King and Neville, 1977).....	99
Figure 6.2.b: A/I ratios in samples of the <u>Globorotalia tumida-menardii</u> complex from Gulf of Mexico Site 625B, mid-Atlantic Core 13519-2 (from Mueller, 1984), and Pacific Core V28-238 (from King and Neville, 1977) plotted against age.....	100
Figure 6.3: Alloisoleucine and total isoleucine (alloisoleucine + isoleucine) concentrations in samples of the <u>Globorotalia tumida-menardii</u> complex from Gulf of Mexico Site 625B, mid-Atlantic Core 13519-2 (from Mueller, 1984), and Pacific Core V28-238 (from King and Neville, 1977) plotted against age.....	103
Figure 6.4.a: Total isoleucine (alloisoleucine + isoleucine) concentrations in samples of <u>Orbulina universa</u> from Gulf of Mexico Site 625B and mid-Atlantic Core 13519-2 (from Mueller, 1984) plotted against age on a semilogarithmic graph.....	109

List of Figures (continued)

	<u>page</u>
Figure 6.4.b: Total isoleucine (alloisoleucine + isoleucine) concentrations in samples of the <u>Globorotalia tumidamenardii</u> complex from Gulf of Mexico Site 625B and mid-Atlantic Core 13519-2 (from Mueller, 1984) plotted against age on a semilogarithmic graph.....	110
Figure 6.5.a: Total isoleucine (alloisoleucine + isoleucine) concentrations in samples of <u>Orbulina universa</u> from Gulf of Mexico Site 625B.....	116
Figure 6.5.b: Total isoleucine (alloisoleucine + isoleucine) concentrations in samples of <u>Neogloboquadrina dutertrei</u> from Gulf of Mexico Site 625B.....	116
Figure 6.5.c: Total isoleucine (alloisoleucine + isoleucine) concentrations in samples of the <u>Globorotalia tumidamenardii</u> complex from Gulf of Mexico Site 625B.....	117
Figure 6.6.a: Total isoleucine (alloisoleucine + isoleucine) concentrations in samples of <u>Orbulina universa</u> from mid-Atlantic Core 13519-2.....	120
Figure 6.6.b: Total isoleucine (alloisoleucine + isoleucine) concentrations in samples of the <u>Globorotalia tumidamenardii</u> complex from mid-Atlantic Core 13519-2.....	120
Figure 6.7: A/I ratios in samples of <u>Neogloboquadrina dutertrei</u> and <u>Orbulina universa</u> from Core 625B plotted against each other.....	123
Figure 7.1: Composite stratigraphy of ODP Site 625B (modified from Johnson, 1988).....	132

List of Figures (continued)

page

Figure 7.2: Composite stratigraphy of ODP Site 625B
(modified from Johnson, 1988), including variabilities
in predicted ages associated with a 5% analytical error
in measured A/I ratios.....135

Figure 7.3.a: Concurrent A/I ratios of three species (where
Orbulina universa = 0.19, Neogloboquadrina dutertrei
= 0.28, and the Globorotalia tumida-menardii complex
= 0.32) plotted on the epimerization curves
predetermined for ODP Site 625B.....136

Figure 7.3.b: Non-concurrent A/I ratios of three species
(where Orbulina universa = 0.15, Neogloboquadrina
dutertrei = 0.28, and the Globorotalia tumida-menardii
complex = 0.45) plotted on the epimerization curves
predetermined for ODP Site 625B.....137

LIST OF TABLES

	<u>page</u>
Table 1.1: Summary of core recovery for Site 625B (from Rabinowitz et al., 1985).....	10
Table 3.1: Summary of the cleaning methods used on foraminifera in this study of ODP 625B.....	34
Table 3.2: Numerical ages assigned to the Neogene of Core 625B, as determined by Johnson (1988) and Spatz (1989).....	47
Table 4.1: Summary of epimerization results for two ILC-C powders handled differently before chemical cleaning.....	57
Table 6.1: Sub-bottom depths corresponding to samples thought to have undergone some dissolution (from Johnson, 1988), and depths corresponding to samples analyzed for total isoleucine concentrations.....	113

ABSTRACT

Amino acid analyses were performed on four planktonic species of foraminifera and a mixed foraminiferal species assemblage through the Quaternary section of Ocean Drilling Program Site 625B in the northeast Gulf of Mexico. The extent of isoleucine epimerization in the individual species increased with time as the overall rate of epimerization decreased with time. Extents of epimerization among the species in increasing order are Globigerinoides ruber, Orbulina universa, Neogloboquadrina dutertrei and the Globorotalia tumida-menardii complex. The mixed foraminiferal species assemblage was found to epimerize at a rate intermediate to the limits delineated by Globigerinoides ruber and the Globorotalia tumida-menardii complex.

A new cleaning method was devised and found to be effective at removing contaminant amino acids from foraminiferal samples. It entails a primary soak of the foraminiferal tests in dilute hydrogen peroxide for 1 hour, followed by a secondary soak in concentrated ammonium hydroxide for 36 hours.

It is possible to differentiate between dissolution of the carbonate tests as it occurs in the water column or at the sediment-water-interface (syn-depositional), and dissolution as it occurs during the earliest phases of diagenesis (post-depositional). Comparisons of total isoleucine concentrations and the extent of isoleucine epimerization between Gulf of Mexico Site 625B, mid-Atlantic Site 13519-2, and equatorial Pacific Site V28-238 reveal a higher degree of dissolution in the waters of the Pacific, followed by the Atlantic, followed by the Gulf of Mexico. Assuming a constant rate of epimerization in all three ocean basins, an inverse relationship is seen to exist between syn-depositional and post-depositional dissolution.

Recent evidence indicates that the preserved record at Hole 625B may have undergone some type of geochemical alteration at depths greater than 67 m. This alteration may be seen in the highly variable aminostratigraphy of the poorly-cleaned, fragile, spinose species Globigerinoides ruber, but does not appear to be seen in the aminostratigraphy of the well-cleaned, non-spinose species analyzed. Thus, provided the specimens are well-cleaned and robust, it appears that the aminostratigraphy at ODP Site 625B may become the reference section for future studies of aminostratigraphy in the Gulf of Mexico.

CHAPTER 1

INTRODUCTION

Background to Amino Acid Racemization

Introduction to Racemization/Epimerization

Amino acids are the building blocks of all proteins. All, except glycine, contain at least one chiral carbon to which four side groups are attached. An amine group, a carboxyl group, an R-group, and a hydrogen atom are bonded to the chiral carbon. (The R-group refers to the side-chain that is unique to each amino acid.) The relative positioning of these side-chains results in a strongly dipolar structure, and allows for easy peptide bonding of amino acids to form polypeptides.

Each amino acid can exist in one of two configurations, or enantiomers. These non-superimposable, mirror-image isomers are optically active and have identical physical properties, except for the direction of rotation of the plane of polarized light. Solutions of L- (levo, or "left-handed") enantiomers rotate plane-polarized light to the left, and solutions of D- (dextro, or "right-

handed") enantiomers rotate plane polarized light to the right. They have identical chemical properties, except toward optically active reagents. Thus, each amino acid exists either as the L-form or D-form enantiomer (Figure 1.1).

Racemization is the structural change that takes place at the alpha-carbon of the amino acid, where the L-amino acids gradually convert to an equilibrium mixture of D- and L-amino acids. Epimerization is the structural change that occurs in amino acids with more than one chiral center, such as isoleucine. (During epimerization the interconversion still takes place at the alpha-carbon, however.) Both reactions are time and temperature dependent.

Geological Applications of Racemization/Epimerization

In most living organisms approximately 100% of all amino acids are of the L-form enantiomer. After death of the organism, the L-amino acids are no longer in equilibrium with the system, and gradual interconversion to an equilibrium mixture of D- and L-form amino acids results.

A measure of the D- and L-form enantiomers, expressed as the ratio D/L, provides a method of assigning relative ages to samples based on the extent of racemization their constituent amino acids have undergone. D/L in living organisms = 0.0, and

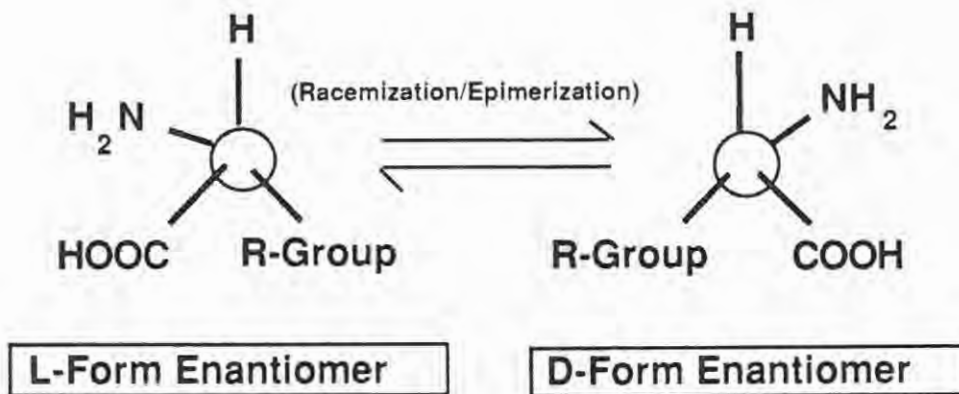


Figure 1.1: General structure of an amino acid in the L- and D-enantiomers. Racemization/epimerization results in two isomers that are non-superimposable, mirror images of each other.

D/L in samples that have reached racemic equilibrium = 1.0. Under certain conditions, racemic equilibrium is not reached until as far back as the Miocene (King and Hare, 1972).

The enantiomers of isoleucine (D-Alloisoleucine and L-Isoleucine) result from epimerization, and are easily resolved by high performance liquid chromatography (HPLC). The ratios of these enantiomers, expressed as A/I, are used to assign relative ages to samples in this study. It is important to realize that alloisoleucine is a nonprotein amino acid produced only by the epimerization of isoleucine, and that epimeric equilibrium is not achieved until A/I ratios approximate 1.25-1.40 (Hare and Mitterer, 1967, 1969).

Amino acid racemization (AAR) has been studied in a variety of organisms, including planktonic foraminifera (Wehmiller and Hare, 1971; Bada and Schroeder, 1972; King and Hare, 1972; 1972a; 1972b; King and Neville, 1977; Wehmiller, 1980; and Mueller, 1984), benthic foraminifera (Miller et al., 1983; and Sejrup et al., 1984), marine molluscs (Kennedy et al., 1982; Miller, 1985; Hearty et al., 1986; Wehmiller et al., 1988), terrestrial molluscs (Miller et al., 1987), corals (Wehmiller et al., 1976), bones, teeth (Bada, 1985), and ostrich shells (Miller, 1989; in press). Most of these sample types are dealt with more completely in Hare et al. (1980) and Wehmiller (1984; 1986).

Amino acid enantiomeric ratios can be used as an effective stratigraphic tool, an application referred to as aminostratigraphy (Miller and Hare, 1980). Similar D/L ratios in two different fossiliferous strata represent coeval units, providing that the same species are analyzed, and that the temperature and diagenetic histories are the same in both localities. The aminostratigraphy of deep-sea cores is useful as a chemical stratigraphic tool for correlation of Neogene sections, when taxa of planktonic foraminifera are used.

Quaternary foraminiferal tests from deep-sea cores have proven to be a particularly useful type of fossil for AAR analysis (Hare and Mitterer, 1969; Wehmiller and Hare, 1971; King and Neville, 1977; Mueller, 1984; Stathoplos and Hare, 1988), because the thermal variables affecting racemization are at a minimum, and there is often reliable age control down the core. Thus, D/L ratios from deep-sea cores also provide a clearer understanding of the processes and kinetics of AAR.

The aminostratigraphy of deep-sea cores in conjunction with a biostratigraphic analysis also allows for a better understanding of the depositional record preserved at the core site. It is often difficult to document the presence of an unconformity in a core solely on the basis of its biostratigraphy. An abrupt appearance or disappearance of a species may imply an

erosional contact, instead of an evolutionary change, for example. Ideally, AAR analysis of foraminiferal tests will help to identify the presence of hiatuses in a core by revealing discontinuities in trends of D/L ratios with depth.

The subject of this study entails the examination of isoleucine epimerization in selected Pleistocene and Pliocene foraminiferal tests taken from Ocean Drilling Program (ODP) Site 625B, in the northeast Gulf of Mexico. Biostratigraphic analyses reveal generally well-preserved foraminiferal tests (Johnson, 1988; Spatz, 1989), permitting isolation and analysis of single species throughout the core. The presence of species vulnerable to physical crushing and dissolution, such as Globigerinoides ruber, indicate that Site 625B is little modified by diagenesis (Johnson, 1988).

Objectives

The objectives of this research are the following:

- 1) to determine the most effective cleaning method for AAR studies in planktonic foraminifera;
- 2) to determine a preliminary aminostratigraphy of the Pliocene and Pleistocene sections of ODP 625B;
- 3) to help verify the biostratigraphy of ODP 625B;

4) to evaluate the potential utility of AAR data for regional correlation of marine sediments;

5) to compare intergeneric effects of isoleucine epimerization in foraminiferal species Globigerinoides ruber, Neogloboquadrina dutertrei, Orbulina universa, and the Globorotalia tumida-menardii complex, and to compare these to isoleucine epimerization in the mixed species foraminiferal assemblage through the core; and

6) to attempt to quantify degrees of dissolution in foraminifera tests based on amino acid composition.

Study Area

Location and Logistics

Three holes were drilled at Site 625 in the northeast Gulf of Mexico, during the Ocean Drilling Program's Leg 100 shakedown cruise of JOIDES Resolution. Core recovery was highest (94.8%) for Site 625B (Table 1.1). Site 625B is located slightly southeast of De Soto Canyon in the carbonate province of the western Florida slope, and in a water depth of approximately 890 m. The latitude/longitude of Site 625B is 28°49.9'N/87°09.6'W (Figure 1.2).

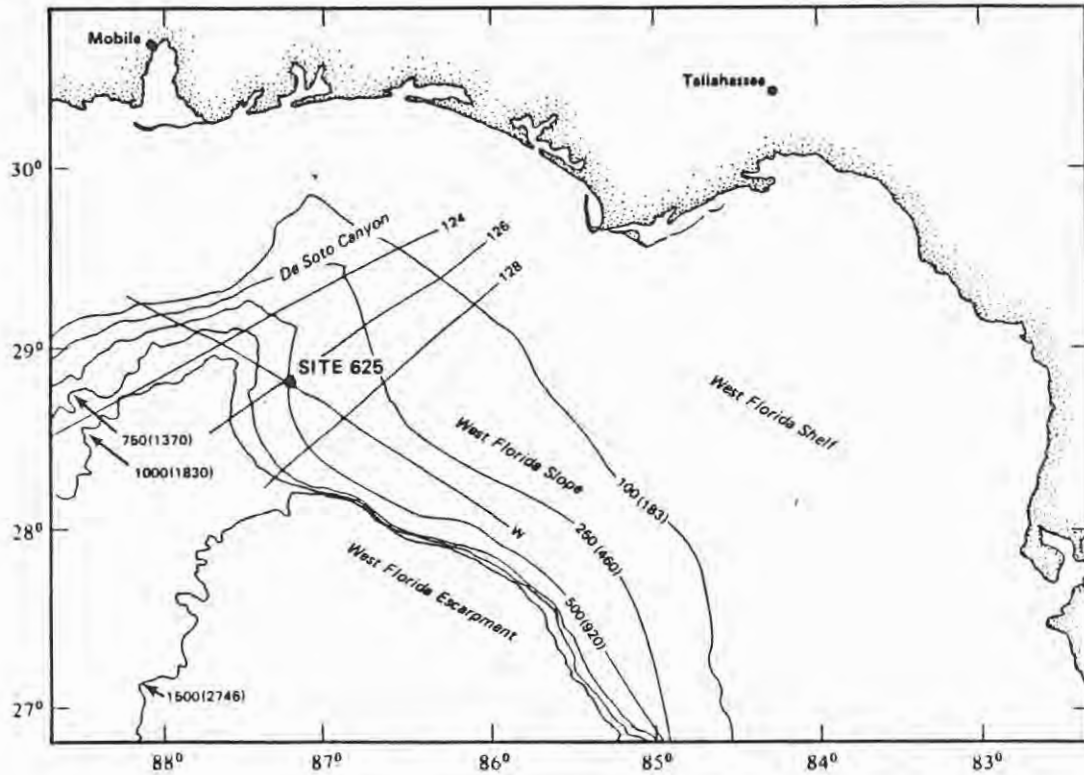


Figure 1.2: Map of Northeastern Gulf of Mexico showing location of Site 625, seismic profile track lines (labeled 124, 126, 128), and the bathymetry of the basin (from Rabinowitz et al., 1985; after Mitchum, 1978). Contours are in fathoms (meters).

There are three stratified water masses observed in the Gulf of Mexico. The Surface Waters encompass the upper 100 m of the water column, the Subtropical Waters are found between 100-300 m, and the Antarctic Intermediate Waters are found between 300-1100 m. The temperature of the bottom waters at Site 625B is thought to approximate the temperature of the Antarctic Intermediate Waters at 1000 m water-depth (6 °C). The reader is referred to Nowlin (1971) for further discussion on the water masses and circulation patterns of the Gulf of Mexico.

An advanced hydraulic piston corer (APC) was used to core the upper 197.1 m (Cores 625B-1 - 625B-23) at Site 625B. (Core 625B-3 had to be manually extruded, and represents a relatively disturbed 7.2 m of sediment). Four additional extended core barrel (XCB) cores (Cores 625B-25 - 625B-27) were taken beyond the APC cores to a final depth of 235.2 m.

Past and Present Work on Site 625B

Site 625B is an ideal core for AAR in foraminiferal tests because of the good geochronological control already placed on the core. The biostratigraphy has been studied by Johnson (1988) and Spotz (1989) at the University of Delaware. Foraminiferal species abundances are available, and a Plio-Pleistocene boundary has been identified to within a half meter at 98 m on the basis of

Table 1.1: Summary of core recovery for Site 625B (from Rabinowitz et al., 1985).

CORES ¹	SUB-BOTTOM DEPTH		TOTAL RECOVERY (m) ²	PERCENT RECOVERED
	TOP(m)	BOTTOM (m)		
1H	0.0	7.9	7.9	100
2H	7.9	17.4	9.9	100
3H	17.4	26.9	7.2	57
4H	26.9	36.4	9.9	100
5H	36.4	40.9	4.7	103
6H	40.9	50.4	9.9	103
7H	50.4	58.5	8.8	108
8H	58.5	67.5	9.5	105
9H	67.5	75.4	8.3	109
10H	75.4	83.6	8.2	100
11H	83.6	92.2	8.5	98
12H	92.2	100.8	8.5	98
13H	100.8	109.5	8.1	92
14H	109.5	118.5	8.9	99
15H	118.5	127.3	8.6	98
16H	127.3	136.6	9.1	98
17H	136.6	145.8	9.2	99
18H	145.8	153.6	7.9	102
19H	153.6	162.1	8.1	95
20H	162.1	170.6	8.5	101
21H	170.6	179.3	8.6	97
22H	179.3	188.0	8.7	100
23H	188.0	197.1	8.9	99
24X	197.1	206.7	6.4	67
25X	206.7	216.3	9.6	100
26X	216.3	225.8	5.3	55
27X	225.8	235.2	5.7	61

Penetration:	235.2 m
Number of cores:	27
Total length of cored section:	235.2 m
Total core recovered:	222.9 m
Core recovery:	94.8 %

From Rabinowitz et al., 1985.

the last appearance datum (LAD) of Discoaster brouweri (Johnson, 1988; Spotz, 1989).

The paleomagnetic record is thought to be accurate through the Brunhes-Matuyama boundary (58 m) and the upper part of the Jaramillo (62 m) at Site 625B (Brad Clement, personal communication to R.E. Martin, 1986). Below approximately 64 m, the paleomagnetic record becomes obscured through the rest of the core, and identification of the Plio-Pleistocene boundary based on the paleomagnetic record is impossible.

Site 625B also provides a long core with high Pleistocene sediment accumulation rates, ranging from 2.6-16.5 cm/1000 yrs (Johnson, 1988). Because of the inverse relationship between sedimentation rates and reworking of sediment, the aminostratigraphy developed in Site 625B will not be altered by significant amounts of biological activity. The reader is referred to the work of Johnson (1988) and Spotz (1989) for a more in-depth discussion of the geologic and oceanographic setting of Site 625B.

Based on seismic data, site 625B is interpreted to represent a "complete" depositional history from the lower Pliocene throughout the Pleistocene (Rabinowitz et al., 1985). The

biostratigraphy of the Pleistocene and Pliocene sections supports this idea (Johnson, 1988; Spatz, 1989, personal communication).

Other studies have been performed on Site 625B. Ed Joyce at Union Oil examined the $\delta^{18}\text{O}$ record preserved in the sediments, but has not yet published the results. The nannofossil biostratigraphy was examined by Stefan Gartner and T.C. Huang at Texas A & M University.

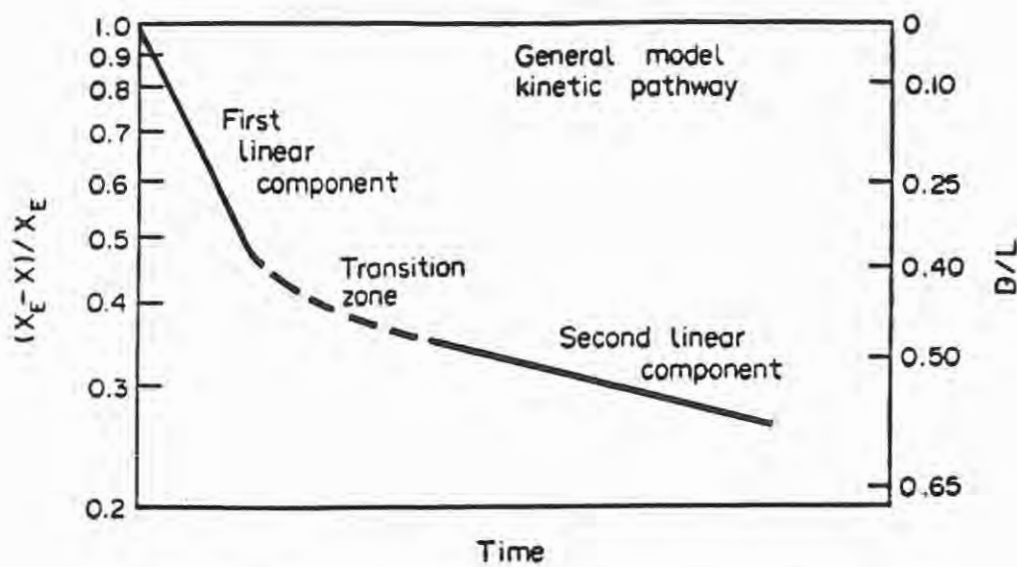
CHAPTER 2

KINETICS OF RACEMIZATION/EPIMERIZATION

Introduction

Amino acid racemization can be a valuable tool for providing age estimates and/or temperature histories of samples assuming the kinetics of racemization are understood. Most studies on the kinetics of racemization are based on observed trends in marine cores, where there is good chronologic control, and temperature variations are minimized (Wehmiller and Hare, 1971; Bada and Schroeder, 1972; Schroeder and Bada, 1976; King and Neville, 1977; Kriausakul and Mitterer, 1978; Katz et al., 1979; and Mueller, 1984). These studies have yielded non-linear kinetic models for racemization/epimerization (Figure 2.1). Wehmiller and Belknap (1978) also support the non-linear model of racemization after comparing it to a linear model in mollusc samples from the Pacific and Atlantic coasts of the United States.

This non-linearity is thought to be due to the complex reactions proteins undergo during diagenesis, including



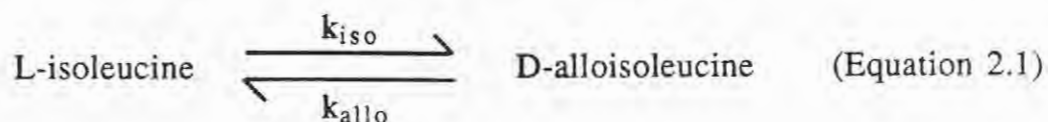
Kinetic model examples, in the logarithmic format of Wehmiller and Hare (1971), $X = D/(D + L)$ at any time T , $X_E = X$ at equilibrium. For most amino acids, $X = 0.50$. $(X_E - X)/X_E$ would be a linear function of time (in this format) if diagenetic racemization followed simple first-order reversible kinetics. Format presented here is mathematically equivalent to similar notations used by other workers, such as $\ln [A_e/(A_e - A_t)]$ or $\ln [(1 + D/L)/(1 - K'(D/L))]$. See articles in Hare *et al.* (1980) for other examples.

Figure 2.1: "Non-linear" kinetic curve of isoleucine epimerization in marine sediments, where $X = (A/A+I)$ at any time, T , and $X_E = X$ at equilibrium (modified from Wehmiller and Hare, 1971; and Wehmiller, 1982). For isoleucine, $X_E = .556$. It is important to note that first-order reversible reactions appear linear on a semilogarithmic plot, and describe the kinetics of the first and third segments of the curve. A "transition zone" exists between the two that implies a "non-linearity" in the kinetics of epimerization over these A/I ratios.

hydrolysis, epimerization, leaching, and decomposition of isoleucine (Wehmiller and Hare, 1971; Mitterer and Kriausakul, 1984; Mueller, 1984; and Wehmiller, 1989, in prep). These factors will be discussed in more detail at the end of this chapter.

First-Order Reversible Kinetics

The non-linear kinetic model is broken down into two linear segments described by first-order reversible kinetics, separated by a transition zone (Figure 2.1). Isoleucine epimerization can be described by reversible first-order kinetics up to A/I ratios of approximately 0.30 ± 0.05 (Wehmiller and Hare, 1971; Bada and Schroeder, 1972; and Schroeder and Bada, 1976). The general reaction is the following:



The forward and reverse rate constants are represented by k_{iso} and k_{allo} , respectively. The equilibrium constant, $k_{\text{eq}} = k_{\text{iso}}/k_{\text{allo}}$, is between 1.25 and 1.40 (Hare and Mitterer, 1967; 1969). Thus, in ideal circumstances, if either the age or temperature history of a sample is known, it becomes possible to determine the other variable, provided the A/I is less than .30.

Age Determinations

Bada and Schroeder (1972) derived the integrated first-order rate equation for the isoleucine epimerization reaction to be the following:

$$\ln \left[\frac{1 + \left(\frac{\text{allo}}{\text{iso}} \right)}{1 - \left(\frac{k_{\text{allo}}}{k_{\text{iso}}} \right) \left(\frac{\text{allo}}{\text{iso}} \right)} \right]_t = \left(1 + \frac{k_{\text{allo}}}{k_{\text{iso}}} \right) k_{\text{iso}} t + C \quad (\text{Equation 2.2})$$

where $\frac{k_{\text{allo}}}{k_{\text{iso}}} = .714$, $t =$ age of fossil (reaction time), and the constant in Equation 2.2 is the following:

$$C = \ln \left[\frac{1 + \left(\frac{\text{allo}}{\text{iso}} \right)}{1 - \left(\frac{k_{\text{allo}}}{k_{\text{iso}}} \right) \left(\frac{\text{allo}}{\text{iso}} \right)} \right]_{t=0}$$

Under ideal circumstances, the amount of alloisoleucine is negligible at $t = 0$; therefore, the value of this constant is zero. In actuality, studies show that racemization/epimerization during hydrolysis of the sample contributes no more than 0.01 to the D/L ratio (Kvenvolden et al., 1970; and Wehmiller, 1971). Thus, a value of 0.00 is usually assigned to the integration constant, C .

Equation 2.2 can be used to extrapolate sample ages when A/I ratios are less than 0.30 (Miller et al., 1983). Inherent assumptions are that first-order reversible kinetics describe epimerization over this A/I range, and that the temperature history of the sample is constant, or is known.

Paleotemperature Estimates

Rates of epimerization increase with increased temperatures. Thus, faster rates of isoleucine epimerization occur during interglacial stages and slower rates occur during glacial stages. Miller and Mangerud (1985) report an approximate doubling of the rate of racemization every 4 °C rise in temperature.

Thus, the effective Quaternary temperature (EQT) that a sample has experienced determines the rate of epimerization. This is important in terrestrial deposits, where changes in temperature during glacial and interglacial stages are significant. In deep-sea cores, however, bottom-water temperature fluctuations between glacial and interglacial stages are generally considered to be less than 1 or 2 °C.

The equation relating temperature and k_{iso} is species-dependent. Bada and Schroeder (1972) found the temperature

dependence of isoleucine epimerization in calcareous marine sediments to be described by the following equation:

$$\text{Log } k_{\text{iso}} (\text{year}^{-1}) = 15.77 - \frac{5939}{T (\text{°K})} \quad (\text{Equation 2.3})$$

Miller and Sejrup (unpublished data from Miller et al., 1983) determined this relationship in the benthic foraminiferal species, Cibicides lobatulus, to be described by the following:

$$\text{Log } k_{\text{iso}} (\text{year}^{-1}) = 16.30 - \frac{6150}{T (\text{°K})} \quad (\text{Equation 2.4})$$

where T = temperature (° Kelvin), and k_{iso} is the forward rate constant of the epimerization reaction in Equations 2.3 and 2.4. The reader is referred to McCoy (1987) for a close examination of the derivation of the paleotemperature equations.

Values of k_{iso} are determined by solving Equation 2.2 for k_{iso} from A/I ratios measured at depths with known absolute ages. Thus, it is possible to assign numerical ages to other parts of the core by using the measured A/I ratio and predetermined k_{iso} at the appropriate temperature. Another approach, taken by Miller et al. (1983), is to substitute Equations 2.3 and 2.4 for k_{iso} into Equation 2.2, and solve for temperature to obtain the EQT of a sample.

Many have estimated Quaternary paleotemperatures from isoleucine epimerization data (Wehmiller, 1977; Bada and Man, 1980; and Miller et al., 1983, 1987). Williams and Smith (1977) and McCoy (1987) present a more critical view and deal with the uncertainties of estimating paleotemperatures from racemization/epimerization data. At any rate, it is important to realize that Equations 2.3 and 2.4 seem to be valid only when the kinetics of epimerization are described by the first-order reversible reaction.

The complicated interaction of the processes proteins undergo during diagenesis seems to account for the non-linearity of the epimerization reaction. A brief explanation of these processes follows.

Diagenetic Reactions Affecting Epimerization

Hydrolysis and Epimerization

Isoleucine (and all other amino acids) can occupy one of the following three positions in a peptide unit: 1) bound into the interior of the protein structure; 2) bound at a terminal position of a protein chain; 3) or, existing as a free amino acid. The position of the amino acid at any one time is determined by the rates of hydrolysis, strength of peptide bonds, and the nature of the surrounding amino acids (Kriausakul and Mitterer, 1978).

Isoleucine in each of these positions epimerizes at different rates where,

$$\text{TERMINAL}_{\text{isoleucine}} \gg \text{INTERIOR}_{\text{isoleucine}} \geq \text{FREE}_{\text{isoleucine}}$$

In apparent conflict to these relative rates, it is usually found that free isoleucine is more extensively epimerized than total isoleucine $[(A/I)_{\text{free}} \gg (A/I)_{\text{total}}]$. [Hare and Hoering (1973), and Kvenvolden et al. (1973) found this trend to be true in the racemization of amino acids other than isoleucine, as well.] This observation is explained as being the result of hydrolysis of extensively epimerized terminal isoleucine to the free form (Kriasakul and Mitterer, 1978).

The lower apparent rate of epimerization seen in the second linear segment of the kinetic curve (see Figure 2.1) is about equal to that for isoleucine epimerization in the free form (Kriausakul and Mitterer, 1978). This observation indicates that after a certain amount of time, the net rate of hydrolysis has declined to a very small value.

Initial rates of hydrolysis are fast, because the easily-cleaved amino acids are removed from the terminal sites, and extensively epimerized isoleucine is released to the free state. As the easily-cleaved amino acids are removed from the protein structure, however, the remaining strongly-bound amino acids

become more resistant to hydrolysis, and rates of hydrolysis decrease. Only the most resistant polypeptides remain, and the overall epimerization reaction becomes controlled by epimerization in the free and interior positions.

Carbonate Dissolution and Leaching

Leaching of material in carbonate samples results in the removal of amino acids from the system. The extent of removal depends upon the degree of carbonate dissolution, as well as the relative stability of the amino acid in the polypeptide structure. Higher rates of carbonate dissolution are accompanied by higher rates of removal. More labile amino acids (particularly those found in the free state) are easier to remove than those bound strongly to other amino acids.

Dissolution leads to progressive removal of the more labile, free amino acids and proteinaceous material in the outermost carbonate structures of the test (Mueller, 1984). It is particularly effective on fragile and thin foraminiferal tests. It can occur syn-depositionally and/or post-depositionally.

Comparisons are made between the epimerization data from Gulf of Mexico Site 625B, mid-Atlantic Core 13519-2 (Mueller, 1984), and Pacific Core V28-238 (King and Neville,

1977) in Chapter 6 of this thesis to better understand the carbonate dissolution processes, and leaching of amino acids.

Decomposition of Amino Acids

The decomposition of isoleucine is relatively insignificant in fossil carbonate samples (Katz and Man, 1980). It is a diagenetic process that does occur in other amino acids, however. For example, serine and threonine, decompose to form the more stable amino acid, alanine (Miller and Hare, 1980).

CHAPTER 3

METHODOLOGY

Introduction

The methodology for preparation and analysis of foraminiferal samples is described in Wehmiller and Hare (1971), King and Hare (1972b), Mueller (1984), Macko and Aksu (1986), and by Brigham-Grette (personal communication, 1987). Each author describes a different set of circumstances that lead to the different methods they employed. The methods developed in this study came from a combination of those already in print, and evolved as the investigation proceeded. Figure 3.1 is a flowsheet outlining the methods developed in this study, and is described in detail in the sections that follow.

Processing and Isolating Foraminifera

Core Sample Processing

The foraminiferal tests used in this study were picked from 115 core samples from the upper 100 m of ODP Site 625B.

PROCEDURES FOR PERFORMING AMINO ACID ANALYSES ON FORAMINIFERAL TESTS

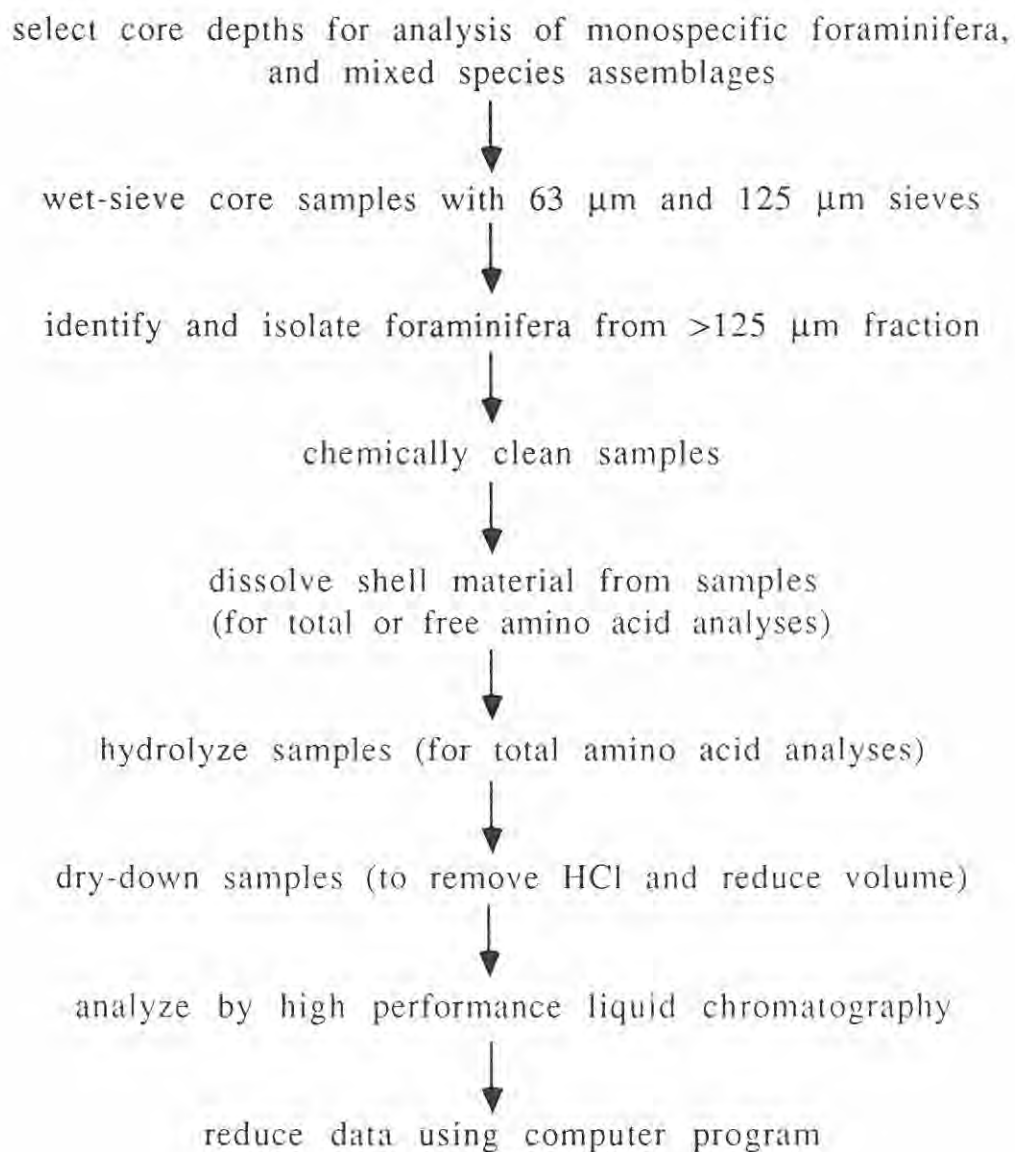


Figure 3.1: Diagram of generalized procedures used for amino acid analysis in foraminiferal tests from ODP Site 625B.

Most of these core samples were wet-sieved through 63 μm and 125 μm -sized meshes using the procedure outlined in Appendix A.

At certain depths in the core it was necessary to pick the foraminiferal tests from core samples previously prepared for the biostratigraphic analyses of Johnson (1988) and Spotz (1989), due to a lack of available material. These core samples were similarly processed, but the wet sediment was placed under an infra-red heat lamp for several minutes to facilitate drying.

It was originally thought that this accelerated drying at high temperatures would increase the degree of isoleucine epimerization and yield higher A/I ratios in the sample. Therefore, new core samples were requested from ODP before this investigation began.

Species Identification

The species chosen for amino acid analysis in this study were highly dependent on the availability through Hole 625B. The high-resolution biostratigraphic work performed by Johnson (1988) and Spotz (1989) revealed the abundances of 30-40 planktonic foraminiferal species. Figures 3.2 a-d show the faunal percent of the species examined in this study down core 625B (from Johnson, 1988; Spotz, 1989). It was also necessary for the

FAUNAL ABUNDANCES OF THE SPINOSE SPECIES
ANALYZED FOR AMINO ACIDS IN ODP SITE 625B

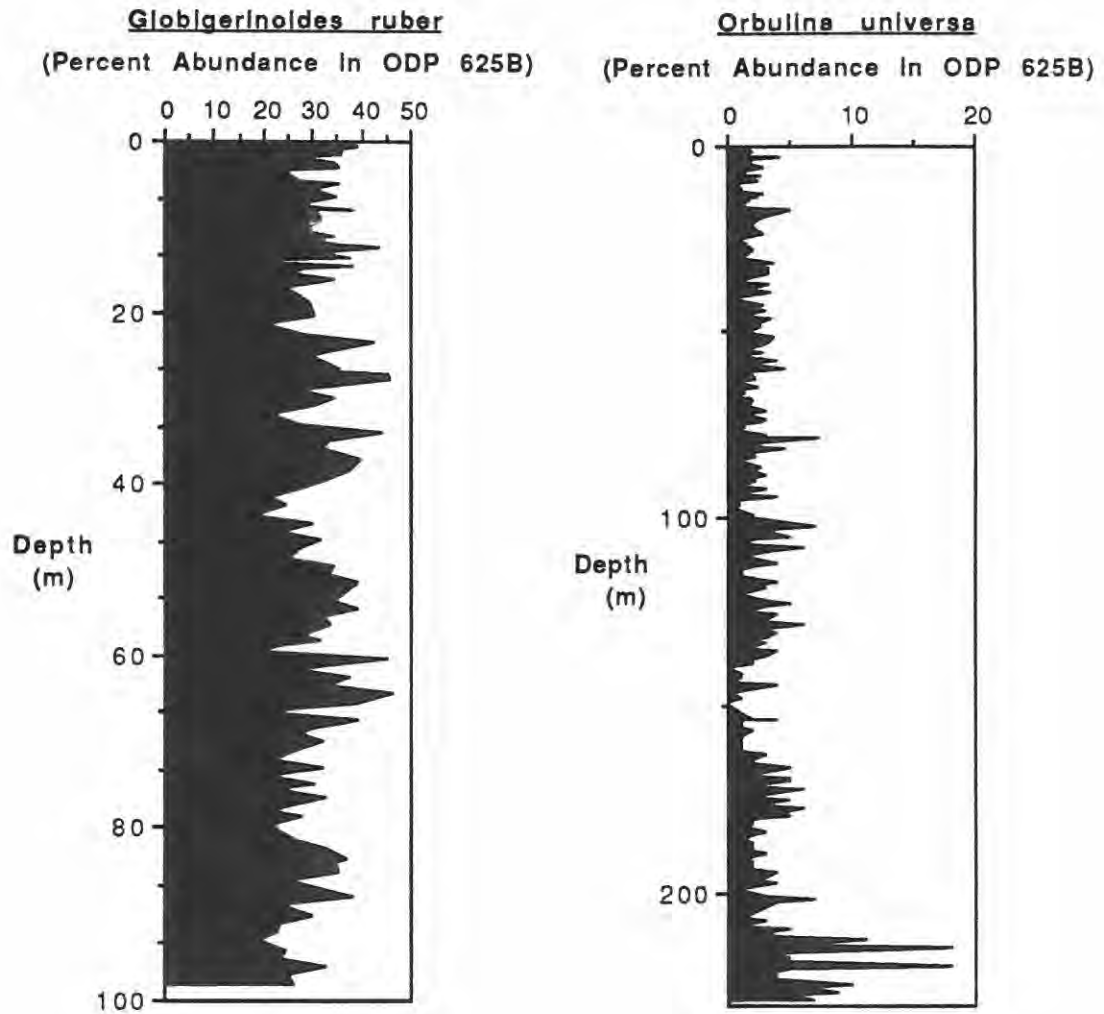


Figure 3.2.a: Percent abundance of Globigerinoides ruber in the upper 100 m of ODP Site 625B (from Johnson, 1988).

Figure 3.2.b: Percent abundance of Orbulina universa in the upper 230 m of ODP Site 625B (from Johnson, 1988; Spatz, 1989).

FAUNAL ABUNDANCES OF THE NON-SPINOSE SPECIES
ANALYZED FOR AMINO ACIDS IN ODP SITE 625B

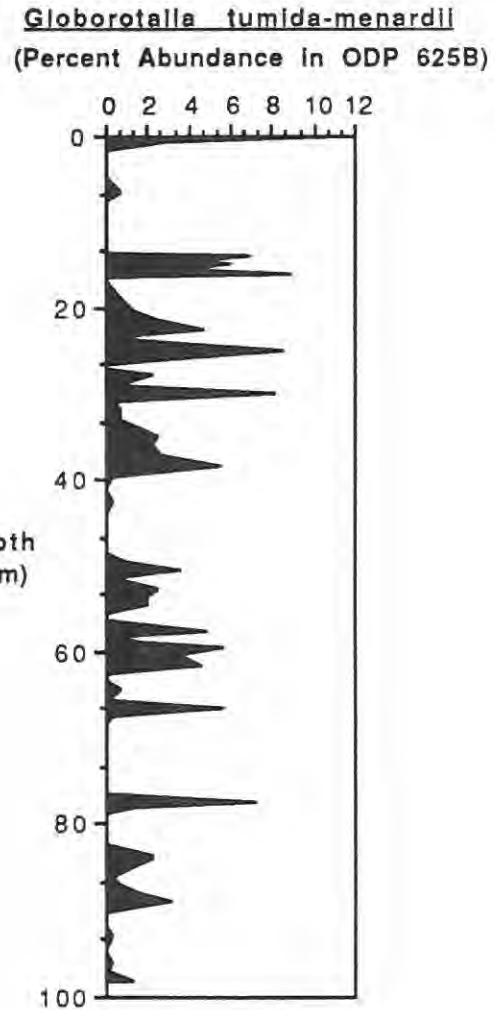
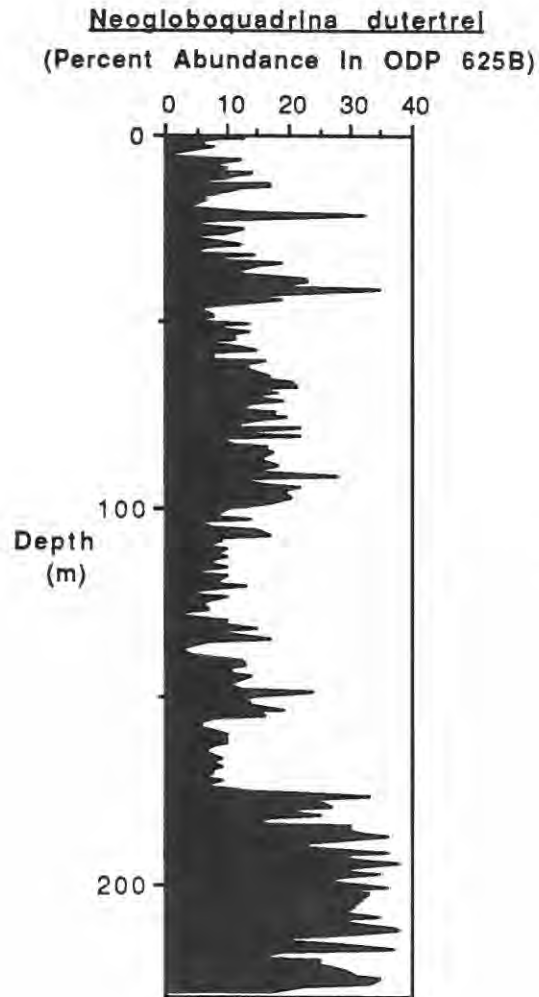


Figure 3.2.c: Percent abundance of Neogloboquadrina dutertrei in the upper 230 m of ODP Site 625B (from Johnson, 1988; Spetz, 1989).

Figure 3.2.d: Percent abundance of the Globorotalia tumida-menardii complex in the upper 100 m of ODP Site 625B (from Johnson, 1988).

species to be relatively easy to recognize by the eyes of a novice micropaleontologist.

Four planktonic foraminiferal species were analysed for amino acid composition at various depths in core 625B. Two of the species analyzed were spinose, and two were non-spinose (Parker, 1962; Bé, 1977).

The two spinose species analyzed, Globigerinoides ruber and Orbulina universa, belong to the same family as the slow racemizer Globigerinoides sacculifer (King and Neville, 1977). The results of this study will allow direct comparisons between three members of the same foraminiferal family.

Globigerinoides ruber was the most abundant species in the Pleistocene portion of Site 625B (Figure 3.2.a), and was sampled approximately every 2 m in the upper 100 m of the core for a total of 58 samples. It was hoped that a high resolution aminostratigraphy of the Pleistocene of Site 625B could be obtained from these data; however, because it was the first species picked and prepared in this study, much of the methodology was worked out on these samples.

Orbulina universa was chosen for analysis because of its availability (Figure 3.2 b), ease in identification, and for direct comparison with the Orbulina universa results of Mueller (1984).

It was sampled approximately every 10 m throughout the Pleistocene and Pliocene of core 625B, for a total of 19 samples.

The two non-spinose species analyzed were Neogloboquadrina dutertrei and the Globorotalia tumida-menardii complex. Neogloboquadrina dutertrei was chosen for analysis because of its availability (Figure 3.2.c). It was sampled approximately every 10 m through the Pliocene and Pleistocene of 625B, for a total of 26 samples.

The Globorotalia tumida-menardii complex was analyzed because of its availability (Figure 3.2.d), and for direct comparison to the Globorotalia tumida-menardii results of Mueller (1984). It was sampled approximately every 15 m through the Pleistocene of 625B, for a total of 11 samples. The Globorotalia tumida-menardii complex, as defined in this study, and in Mueller (1984), includes differing proportions of the following four subspecies: Globorotalia menardii-menardii, Globorotalia tumida-tumida, Globorotalia tumida-flexuosa, and Globorotalia menardii-cultrata. Differences in amino acid composition of these four subspecies are at a minimum (King and Hare, 1972), so they can be grouped as one in the two studies.

Identification to the species and subspecies level was based on the taxonomy of Kennett and Srinivason (1983), Snyder

(1978), and Stainforth et al. (1975). Glenn Johnson and Brenda Spatz helped to verify the accuracy of this author's species identification.

Amino acid analyses were also performed on the bulk sediment (>125 μm fraction) at selected depths of the Pleistocene section of Hole 625B. As over 75% of this size fraction is comprised of planktonic foraminifera (Johnson, 1988), the analysis of this fraction of the total sediment represents a mixed foraminiferal assemblage as defined by King and Neville (1977). Total and free amino acid analyses were performed on the mixed species assemblages taken at the same depth every 10 m through the Pleistocene section of the core, for a total of 20 samples.

A total of 112 monospecific samples, and 10 mixed species assemblage samples were analyzed for total amino acids. The 10 mixed species assemblage samples were also analyzed for free amino acids.

Sample Picking

Roughly 300 individual foraminiferal tests were picked from each sample. It was found in this study that the masses of 300 foraminiferal tests ranged anywhere from 2 mg to 120 mg, depending upon the species picked, and the size of the individual tests.

Foraminiferal tests were isolated from the $>125\ \mu\text{m}$ fraction of the sample. A binocular microscope was used to aid in the identification of the species. The foraminiferal tests were removed by hand from a picking tray with a paintbrush moistened with distilled water. The 300 foraminiferal tests were placed on a new cardboard slide, covered with a clean, glass cover-slide, and stored in a cool, dark place until prepared for analysis by HPLC.

Intra-sample contamination was minimized by wiping the picking tray with Kimwipes®, and by changing the distilled water reservoir between the picking of each sample. Care was taken not to handle, or sneeze, cough, or breathe on the tests to minimize contamination with fresh amino acids.

Methodology of Amino Acid Analyses

Chemical Cleaning

The 300 monospecific foraminiferal tests were placed into pre-weighed sterile test tubes. The total weight of the sample and test tube was recorded. The mixed foraminiferal assemblages were obtained by microsplitting the bulk sediment fraction $>125\ \mu\text{m}$. This material was placed into sterile test tubes, and weighed in the same manner.

Cleaning methods for marine sediment samples have varied through time. Wehmiller and Hare (1971) ultrasonically cleaned and wet sieved the bulk sediment with distilled water to obtain the foraminifera fraction ($>74 \mu\text{m}$) used in their study. Sodium hexametaphosphate (1% by weight) interspersed with distilled water washes, and ultrasonic cleaning on samples of mono-specific foraminiferal tests were used by King and Hare (1972b) and Mueller (1984). Others have used ultrasonic cleaning with interspersed distilled water washes and rinses (Macko and Aksu, 1986; and Brigham-Grette, personal communication, 1987).

Figure 3.3 is a flow sheet depicting the generalized cleaning procedures. Table 3.1 outlines the cleaning agents used, and the time soaked in each. All cleaning agents used were diluted to their respective concentrations with triple-distilled water prepared in the University of Delaware laboratory.

The picked foraminiferal tests were ultrasonically cleaned in a cleaning agent for a maximum of one minute, and then set aside to soak for a specified amount of time. They were then subjected to 3 alternating series of centrifugation for five minutes, siphoning off the supernatant, rinsing with triple distilled water, and ultrasonic cleaning for 30 seconds.

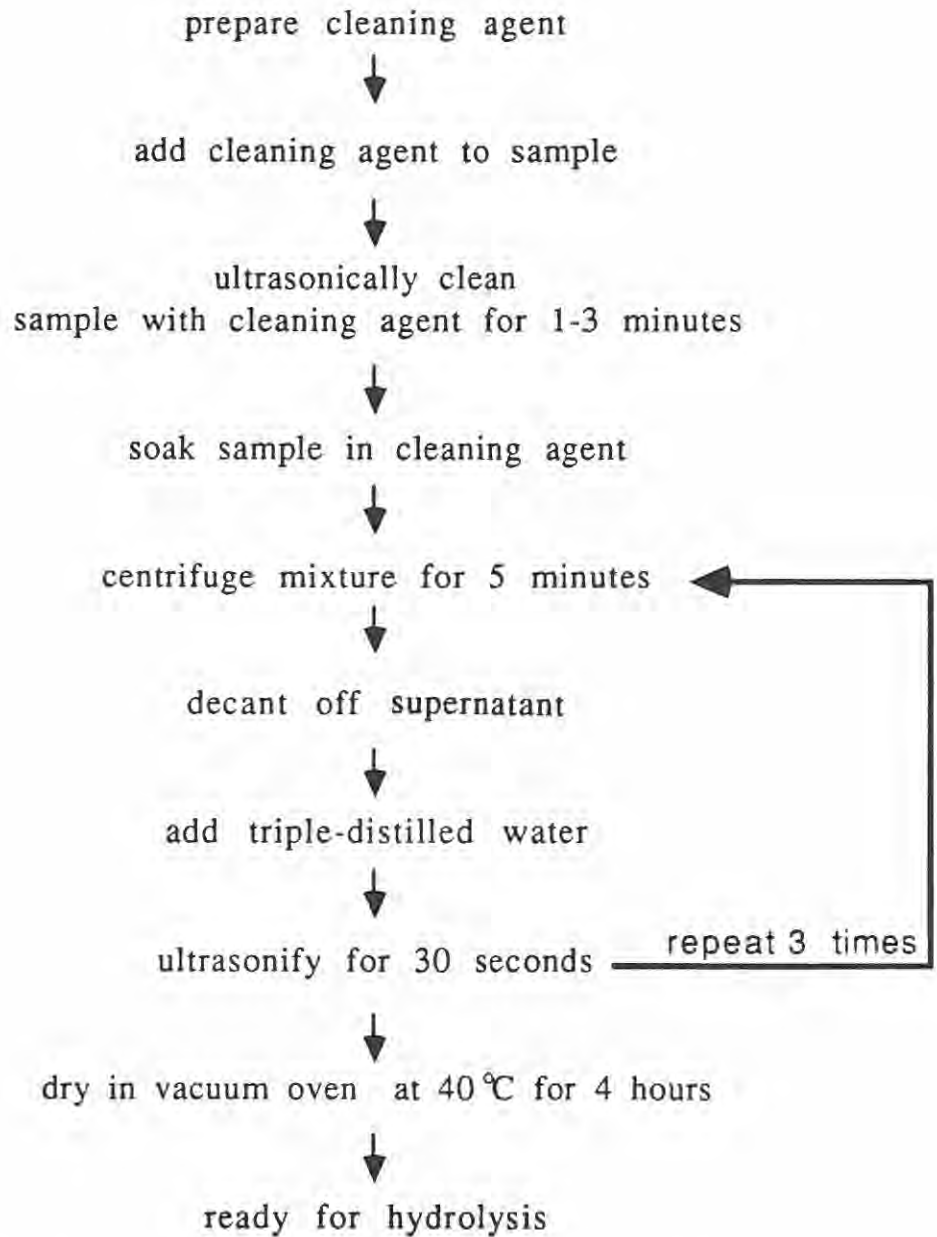
METHODOLOGY OF CHEMICAL CLEANING

Figure 3.3: Diagram of procedures used for cleaning of foraminiferal tests from ODP Site 625B.

Ultrasonic cleaning of foraminiferal tests helps to remove clay particles, with bound amino acids, adhering to the shell surface. Katz and Man (1980) found that ultrasonic cleaning in excess of 30 minutes led to changes in amino acid content, while A/I ratios remained relatively stable. The samples from ODP Site 625B were ultrasonically cleaned for a maximum of 5.5 minutes keeping them relatively safe from alteration.

These steps were repeated three times for each sample. Samples were dried in an oven at 40 °C for a few hours after rinsing. They were then ready for dissolution and hydrolysis and/or analysis by HPLC.

Dissolution, Hydrolysis, and Drying-Down of Samples

The hydrolysis step allows for break-down of the peptide bonds, and subsequent analysis of the total fraction of isoleucine preserved in the shell structure. This includes those that were originally bound (in the interior, or terminal positions) into the polypeptide structure, and those that were originally found in the free state. Omission of the hydrolysis step allows for analysis of amino acids in the free state.

Dissolution of the carbonate material for analysis of epimerization in the total isoleucine fraction took place at room

temperature. The carbonate matrix of the foraminiferal tests were dissolved, and brought to a concentration of 6N HCl. The samples were then sealed under a stream of nitrogen, and placed in a heating block for 22 hours at 110 °C, where hydrolysis took place.

Dissolution of the carbonate material for analysis of epimerization in free isoleucine took place in an ice bath. (Presumably, the reduced temperature keeps natural epimerization and hydrolysis from occurring). Triple distilled water was added to the sample so that the tests were barely covered with liquid. A few drops of concentrated HCl were then added to the sample to dissolve the carbonate material. The final concentration of HCl was approximately 1 N; thus, there was little danger of destruction of the polypeptide from interaction with this mild acid.

At this point the amino acid residues from both the total and free analyses were dried under a stream of nitrogen while at least three 0.1 ml aliquots of triple distilled water were added to reduce the acidity of the sample. The residue was taken up in an HCl buffer solution, at a pH of 2, and stored frozen prior to analysis on the HPLC.

High Performance Liquid Chromatography (HPLC)

The St. John Model 2000 Amino Acid Analyzer includes many of the current innovations in HPLC mentioned by Hare et al. (1985), and was used for all quantitative amino acid analyses in this study. This system utilizes a single ion exchange column packed with 5 micron-sized resin, a step-gradient elution system, and a post-column amino acid derivatization by ortho-phthalaldehyde (OPA) coupled with fluorescence detection.

Samples were centrifuged prior to injection onto the HPLC. 50 μ l of material were injected onto the sample loop by the Micromeritics automated injector, or manually using a stainless steel syringe. The syringe was rinsed with dilute HCl between injections to minimize cross contamination. Availability of sample material was clearly the factor determining the type of injection utilized.

In all cases of automatic injection, two runs of each sample were performed. In most cases of manual injection, two runs of each sample were also performed. Column temperatures and flow rates were adjusted until optimum resolution of chromatographic peaks was maintained. Machine settings were then held constant for groups of injections taking place over several days.

Because Mueller (1984) found between 5-10% variation in duplicate analysis of foraminifera, the results of single injections in this study are compared to those of double injections. Those samples analyzed only once are differentiated in the appendices mentioned below, and should be treated with a little more caution than others.

Appendices C, D, E, and F list the mean absolute abundances of the 13 amino acids resolved for each sample, according to the species analyzed, and the cleaning method used. Appendices G and H list the same information for the mixed species assemblages and the interlaboratory comparison (ILC) powders analyzed. [The reader is referred to Wehmiller (1984) for a discussion on the use of ILC powders.] These appendices include other information, such as the number assigned the sample in the Delaware laboratory, the core sample the specimens were recovered from, the number of injections of each sample on the HPLC, the method of drying (heat or air) during processing of the raw material, and the depths and ages of each sample (from Johnson, 1988; and Spatz, 1989).

Chromatographic peaks were integrated electronically by a Hewlett Packard 3390a integrator. Samples of chromatograms from analyses of foraminiferal tests are shown in Figures 3.4 and 3.5. Each peak corresponds to the amino acid shown. Again, it is

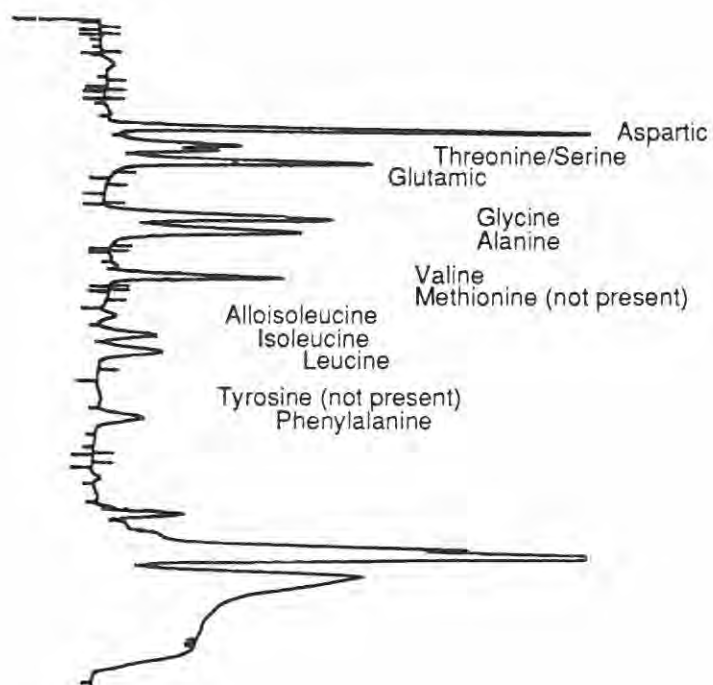


Figure 3.4: Sample chromatogram of *Neogloboquadrina dutertrei* taken from ODP 625B core sample 3/4: 53-55 cm (22.5 m sub-bottom depth).

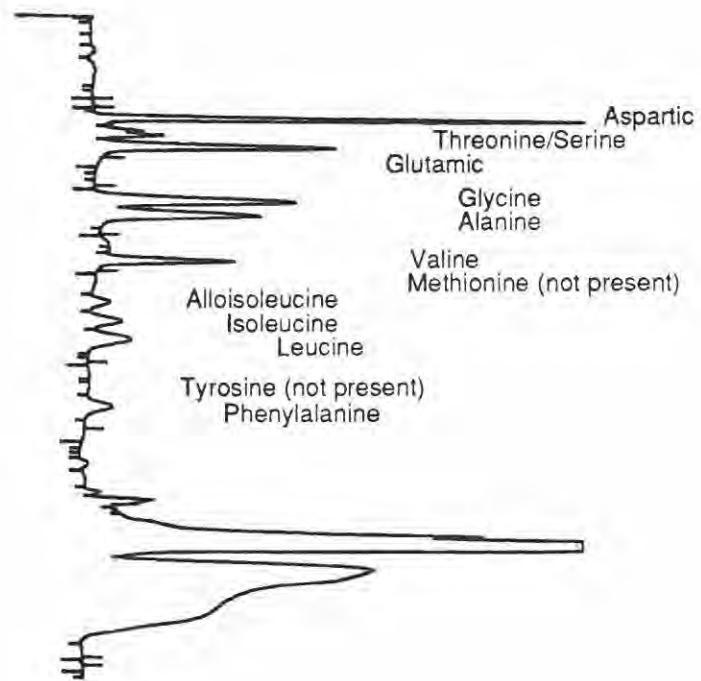


Figure 3.5: Sample chromatogram of the *Globorotalia tumidamenardii* complex taken from ODP 625B core sample 12/6: 0-2 cm (99.5 m sub-bottom depth).

important to realize that all peaks, with the exception of D-alloisoleucine and L-isoleucine, represent the combined D- and L-forms for each amino acid. A chromatogram from a quantitative standard is shown in Figure 3.6.

Data Reduction

The integrated areas of 12 amino acids were entered manually into a Microsoft Works spreadsheet program on the MacIntosh computer. The amino acids include aspartic acid, threonine, serine, glutamic acid, glycine, alanine, valine, methionine, alloisoleucine, isoleucine, leucine, tyrosine, and phenylalanine. Area/height ratios for alloisoleucine and isoleucine, original sample weight, volume injected onto the column, volume of buffer added, and volume of HCl added for dissolution and hydrolysis were also entered. A calculations program written by John Wehmiller was then used to determine the A/I values, and the absolute abundances of the 13 amino acids for each sample. A sample calculation can be found in Appendix B.

These calculated amino acid abundances should be used with some degree of caution. Often, because the resolution between threonine and serine is so poor, these peaks are integrated as one by the automatic integrator. In such cases, the

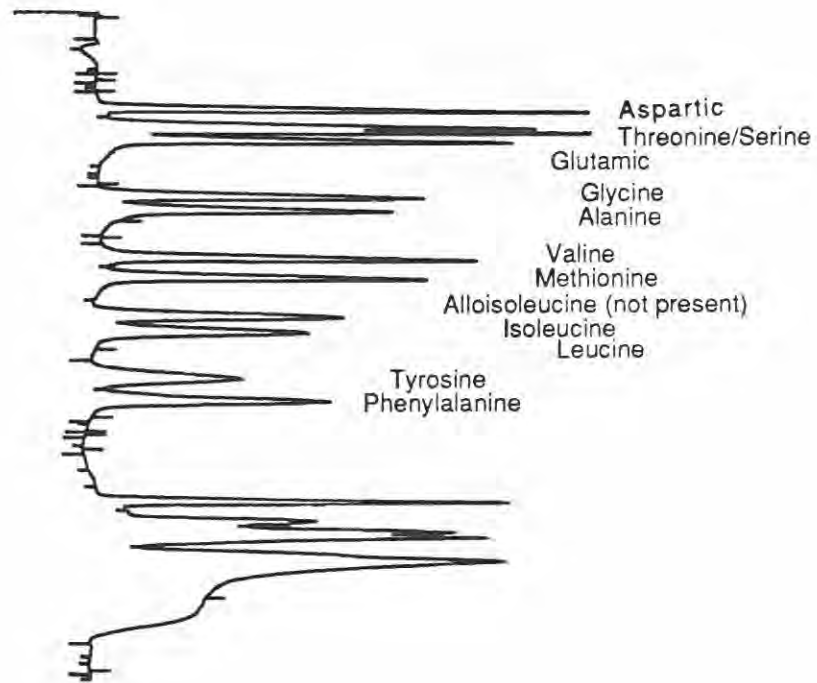


Figure 3.6: Sample chromatogram of the quantitative standard.

peak area is split evenly, and divided between threonine and serine. Also, amino acids such as methionine and tyrosine usually are present in such small amounts that their peaks are not integrated very accurately. In any case, a closer examination of chromatograms with seemingly anomalous amino acid results will reveal those peaks not integrated properly (often indicated by area/height ratios greater than 0.80).

Ratios of amino acid abundances are used more effectively for discerning down-core trends than are the calculated amino acid abundances. Abundances of amino acids reflect loss or gain of material from the carbonate system as a whole. Ratios, however, help to identify the presence of contaminant amino acids, as well as those amino acids selectively removed during degradation, or other diagenetic processes.

Precautions Used Against Contamination

Several precautions were taken to aid against contaminant amino acids entering the sample during the wet lab procedures. Samples were handled only while wearing disposable PVC gloves. The chemical reagents used in the lab were prepared by bubbling HCl and NH₄OH gases through triple-distilled water. Blanks of these reagents were periodically analyzed to check for reagent contamination.

Precautions were also taken to detect possible mistakes in the preparatory techniques themselves. An interlaboratory comparison powder was prepared with each batch of samples prepared to ensure consistency of preparatory techniques throughout the study. A quantitative standard was run on the HPLC every 4-6 samples to ensure consistency in instrument operation throughout the study, and to normalize unknown concentrations of amino acids in samples to known concentrations.

Glassware used for reagents was recycled by soaking in 25% HCl for at least 36 hours, repeated rinsing with triple-distilled water, and storing in a high temperature oven for a minimum of 48 hours. Test tubes used for containment of the foraminiferal samples were never recycled. New ones were acid rinsed and stored at 300 °C for a minimum of 48 hours. These sterile test tubes were the site for the chemical cleaning, the dissolution, the hydrolysis, and the drying-down of the sample. The test tube and the sample were stored in a freezer, and the sample was withdrawn directly from the test tube for injection onto the HPLC. Consequently, the foraminifera extract was never transferred from the original test-tube in which the sample was dissolved.

Numerical Age Assignment

Numerical ages are assigned to the Quaternary section of Site 625B, based on the work of Johnson (1988). He established a high-resolution biostratigraphic framework, and correlated it to the work of others in the mid-Atlantic Ocean and the northeast Gulf of Mexico (Ericson and Wollin, 1968; Neff, 1985, respectively). He assigned ages to certain depths in the core based on the correlation of his last appearance datums (LAD) and first appearance datums (FAD), to corresponding time-restricted zones established by Ericson and Wollin (1968) and Neff (1985), and to the paleomagnetic record of the Quaternary in Site 625B established by Clement [personal communication to R.E. Martin (1986)].

Numerical ages are assigned to the Pliocene of Site 625B based on the work of Spotz (1989). As the paleomagnetic record is disturbed in this section of Site 625B, only biostratigraphic markers are used to assign numerical ages at certain depths. Spotz (1989) uses planktonic datums established by Berrgren et al. (1985). Gartner [personal communication to R.E. Martin (1986)] provided the depths of the nannofossil datums. An average sediment accumulation rate was determined for the whole Pliocene to be 3.4 cm/1000 years (Spotz, 1989).

Table 3.2 shows the sub-bottom depths and corresponding ages of the Neogene of Hole 625B as they are interpolated from the sedimentation rates determined by Johnson (1988) and Spotz (1989). The reader is referred to these papers for more detail on the datums used.

Data Presentation

Logarithmic regressions are best fit to some of the data using the Logarithmic Curve Fit command available on version 1.2 of Cricketgraph. Values of R^2 are also calculated by this software package and are included on these curves the first time they are presented in this thesis.

Generalizations made in the text about other figures are based solely on visual observations. Hand-drawn lines are made on some of the figures, as they are seen to best-fit the data. Because the sampling density is not great enough, a formal statistical analysis was not performed.

Table 3.2: Numerical ages assigned to the Neogene of Core 625B, as determined by Johnson (1988) and Spotz (1989).

<u>Depth in Core (m)</u>	<u>Age (ka)</u>
1.25	11
14.25	90
16.25	128
18.00	195
39.50	485
49.00	610
67.50	990
77.00	1300
89.50	1650
97.50	1860
223.00	5600

CHAPTER 4

RESULTS-CLEANING EXPERIMENTS

Introduction

The majority of the cleaning experiments were performed on Globigerinoides ruber. As the study progressed, the cleaning techniques were modified in response to the data obtained from the analyses of Globigerinoides ruber. Eventually, the two most effective cleaning methods found from the experiments on the Globigerinoides ruber samples were compared in samples of Orbulina universa, and Neogloboquadrina dutertrei. Finally, the most effective cleaning method determined from this study was used on the remaining samples, including the Globorotalia tumida-menardii complex and mixed foraminiferal species assemblage.

Appendices C, D, E, F, G and H list the amino acid concentrations for the different cleaning methods used for Globigerinoides ruber, Orbulina universa, Neogloboquadrina dutertrei, the Globorotalia tumida-menardii complex, the mixed

foraminiferal species assemblage, and the ILC powders, respectively. Some of the A/I ratios reported were determined from measuring the relative peak-heights of alloisoleucine and isoleucine directly off the chromatogram. Because the concentrations in the appendices are determined directly from the integrated peak-areas on the chromatograms relative to a quantitative standard, the reported A/I values may differ slightly from the ratio of the concentrations of alloisoleucine to isoleucine.

All cleaning methods follow the same general procedures outlined in the flow chart in Figure 3.3. The differences between the procedures are the cleaning agents used, and the times soaked in each (see Table 3.1).

Criteria For Determining Sample Cleanliness

Contamination of foraminiferal samples can occur in a number of different ways. Natural contamination can occur if relatively "old" or "young" organic material adsorbs onto, or is incorporated into the foraminiferal tests during diagenesis. Laboratory contamination can also occur if the sample is exposed to fresh amino acids in dust or fingerprints, for example.

While it not easy to determine the source of contamination in a foraminiferal sample, certain down-core trends of amino acid ratios can be used to evaluate the quality of

cleaning in the samples. (Ratios of amino acids are examined because they are less variable over time than the absolute abundances.)

The trends expected to be seen in well-cleaned samples are presented in this section. Each trend can be used as a criterion for determining which samples may be contaminated. Each criterion should be used in conjunction with the others, and not as a means for identifying poorly cleaned samples alone.

Ideally, serine/leucine ratios decrease with time. In well-cleaned samples, the more unstable amino acid, serine, decomposes faster than the more stable amino acid, leucine. Anomalously high values in this ratio reveal samples contaminated with serine.

Ideally, glycine/alanine should remain relatively constant with time. Both amino acids are relatively stable (Hare, 1962, 1963). While neither amino acid is directly indicative of contamination, suspect samples may be identified by anomalous variations in this ratio.

Ideally, A/I ratios increase with time. Anomalously low values in this ratio reveal samples with high L-isoleucine concentrations due to a lack of extensive epimerization, or due to an excess of contaminant amino acids.

Trends of total isoleucine (alloisoleucine + isoleucine) concentrations used in conjunction with trends of A/I ratios, can aid in recognizing those samples with "low" A/I values that might be contaminated (increased total isoleucine) or leached (decreased total isoleucine). Some of these results are discussed here, and some are discussed in Chapter 6.

However, trends of amino acid abundances with time should be used with a certain degree of caution. Diagenetic processes such as leaching of amino acids, or contamination of amino acids may not be revealed by amino acid concentrations alone.

It is important to note that the presence of β -alanine and γ -aminobutyric acids implies insufficient cleaning in foraminifera (Schroeder, 1975). However, for analytical reasons, an attempt was not made to look at these amino acids in this study. Thus, the cleaning methods employed in this project will be presented in the order of which they were tried, unless otherwise mentioned, and the trends mentioned in the above paragraphs will be examined in the samples analyzed to help detect possible contamination.

Hydrogen Peroxide

The cleaning agent first examined was hydrogen peroxide. It was diluted with triple-distilled water to proportions of 1:3. Samples were originally soaked in this cleaning agent for 15 minutes.

The first samples cleaned using hydrogen peroxide were taken from those species first picked from core 625B. At the time of this experiment, only Globigerinoides ruber had been isolated from depths lower than 70.5 m. Thus, selected Globigerinoides ruber samples from below 70.5 m in ODP 625B were the first to be cleaned and analyzed.

The A/I ratios of this cleaning experiment are plotted against core depth in Figure 4.1. A/I values range from between 0.056 and 0.363 over a spread of 25 m. The high variability and unexpectedly low A/I ratios were attributed to contamination of the sample during the original picking procedure.

Originally, the picking water and tray were not cleaned between samples, and were left uncovered for weeks at a time, thereby creating a source for contaminant amino acids into the system. All Globigerinoides ruber samples below 70.5 m were picked using this unclean procedure. (It is interesting to note the

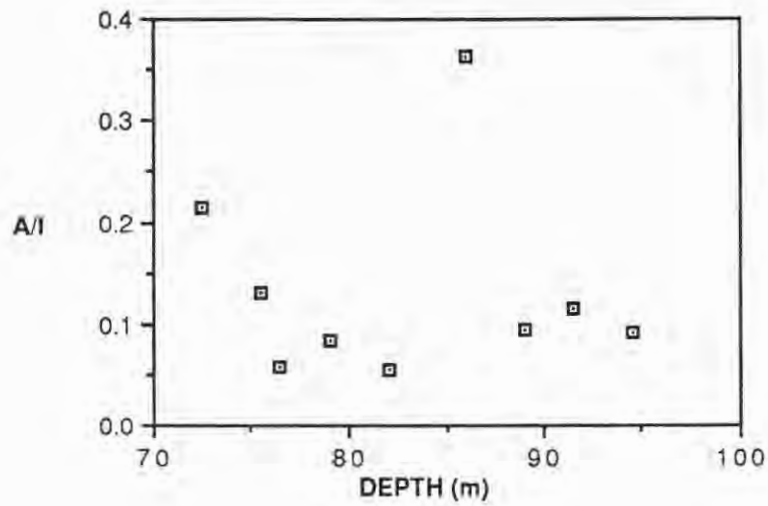


Figure 4.1: A/I ratios in samples of *Globigerinoides ruber* found at depths greater than 70.5 m in ODP Site 625B. Samples were cleaned in hydrogen peroxide for 15 minutes. External contamination may have affected the A/I ratios below 70.5 m.

coincidence of these anomalous results with the beginning of the obscured paleomagnetic record in Hole 625B.)

After the discovery of this presumed error, more precautions were taken to minimize contamination of samples from the picking procedure. Picking waters and the picking tray were cleaned between samples, and stored in isolated areas. All other samples analyzed in this study, including Globigerinoides ruber samples above 70.5 m were isolated from the core with considerably more caution.

Seven Globigerinoides ruber samples from 68.00 to 70.25 m were the next to be cleaned for 15 minutes in dilute hydrogen peroxide and analyzed. Figure 4.2 shows A/I ratios between these 2.25 m of sediment to range between 0.073 and 0.281. This high variability in ratios was reason enough to explore extending soak-times to 60 minutes in dilute hydrogen peroxide.

A brief experiment to try to understand the degree of contamination introduced by the revised picking procedure was performed next. Chips of a crushed mollusc of known A/I value, ILC-C (Wehmiller, 1984), were picked as a foraminiferal sample would be, including spreading the sample material onto a picking tray, and removing individual shell fragments with a paintbrush moistened with distilled water. This "picked" material, along with

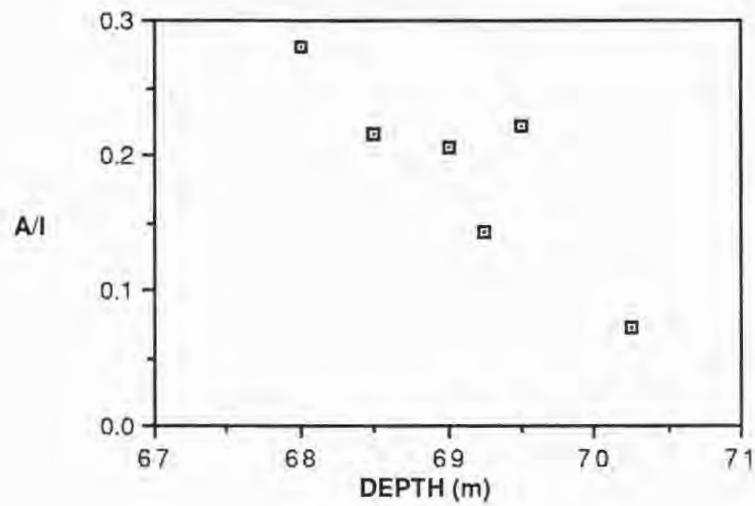


Figure 4.2: A/I ratios in samples of *Globigerinoides ruber* found at depths between 68.00 and 70.25 m in ODP Site 625B. Samples were cleaned in hydrogen peroxide for 15 minutes.

an ILC-C control were cleaned in dilute hydrogen peroxide for 60 minutes.

Table 4.1 summarizes the results for the two ILC-C powders. (Recall that Appendix H lists the amino acid abundances for all of the ILC powders examined in this study). A lower A/I ratio, a higher serine/leucine ratio, and a higher amino acid concentration were found in the ILC-C powder treated like a foraminiferal sample, than in the control sample. Though it is impossible to quantify how much contamination is present on the basis of this experiment involving only two samples, these general trends support a need for determining a "cleaner" way to isolate foraminifera.

The next set of cleaning experiments entailed soaking foraminiferal samples in dilute hydrogen peroxide for 60 minutes. These experiments were performed on 13 samples of Globigerinoides ruber found above 70.5 m (picked carefully), and 3 samples of Globigerinoides ruber found below 70.5 m (picked not so carefully). Figure 4.3 demonstrates the A/I ratios plotted against core depth in these samples.

A/I ratios in the samples below 70.5 m are generally lower than those above 70.5 m. This is to be expected because of the careless way in which these older Globigerinoides ruber

Table 4.1: Summary of epimerization results for two ILC-C powders handled differently before chemical cleaning. The second sample was treated similarly to a foraminiferal sample, in that chips of the shell material were isolated ("picked") with a paintbrush moistened with distilled water before chemical cleaning. The first sample was chemically cleaned directly from the sample container, and excluded the intermediate "picking" step.

	ILC-C (Control Sample)	ILC-C ("Picked" Sample)
A / I	.936	.836
Serine/Leucine	.261	1.106
Total amino acids (nmoles/gram)	1866	2107

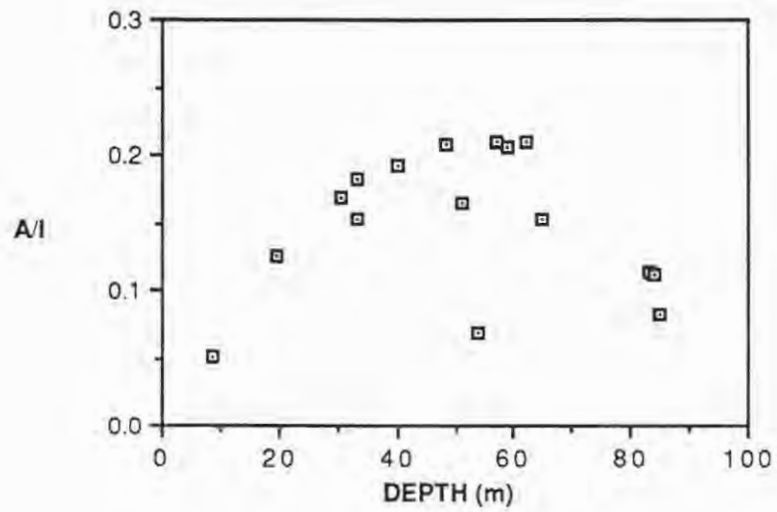


Figure 4.3: A/I ratios in samples of *Globigerinoides ruber* from ODP Site 625B. Samples were cleaned in hydrogen peroxide for 60 minutes. External contamination may have affected the A/I ratios below 70.5 m.

samples may have been picked.

A/I ratios above 70.5 m show a general increase with depth. While there is more variability in ratios from samples soaked for 15 minutes than in those soaked for 60 minutes, the variability in those soaked for 60 minutes is still significant, and reason enough to explore the effects of a different cleaning agent on foraminiferal samples.

Ammonium Hydroxide

Ammonium hydroxide was diluted with triple-distilled water in proportions of 1:3. It was used as a secondary soak, after the initial soak in hydrogen peroxide for 60 minutes, to try to remove the remaining contamination present.

The first samples examined using this combined cleaning agent technique were Globigerinoides ruber through the upper 100 m of ODP 625B. Figures 4.4.a-e demonstrate various amino acid trends with depth in these samples.

All plots show evidence for external contamination at depths below 70.5 m, as is expected from the results presented in the preceding section. However, the samples analyzed from depths above 70.5 m show amino acid trends that begin to mimic those expected from well-cleaned samples.

Figures 4.4.a-4.4.e: Various amino acid trends in samples of Globigerinoides ruber from ODP Site 625B. All samples illustrated in these figures were cleaned in hydrogen peroxide for 60 minutes, followed by a secondary cleaning in ammonium hydroxide for 36 hours.

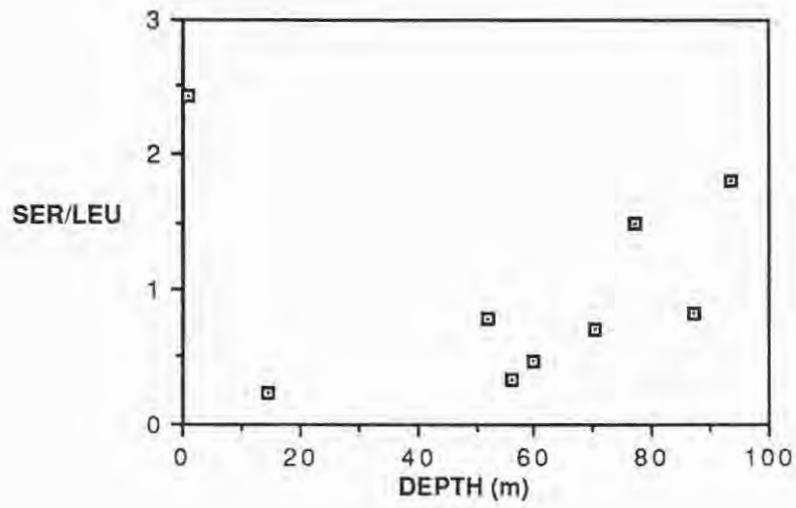


Figure 4.4.a: Serine/Leucine ratios in samples of Globigerinoides ruber from ODP Site 625B.

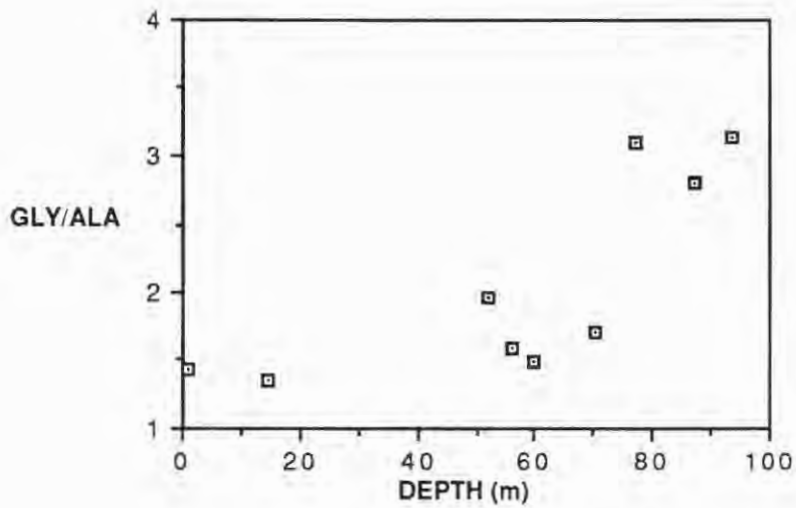


Figure 4.4.b: Glycine/Alanine ratios in samples of Globigerinoides ruber from ODP Site 625B.

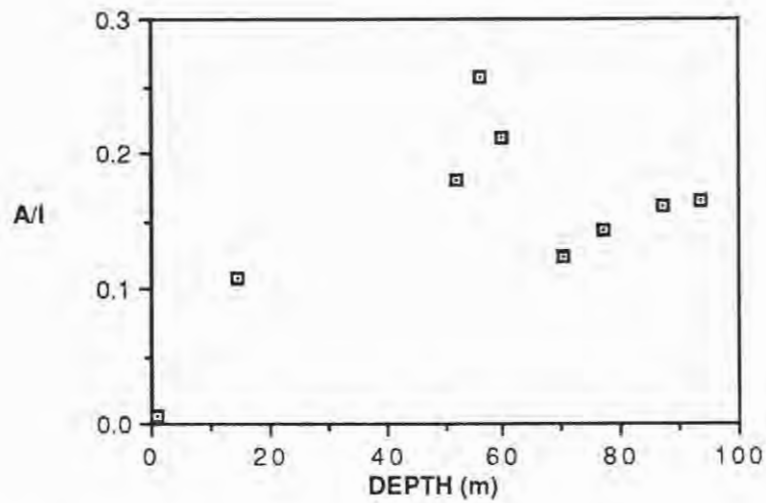


Figure 4.4.c: A/I ratios in samples of Globigerinoides ruber from ODP Site 625B.

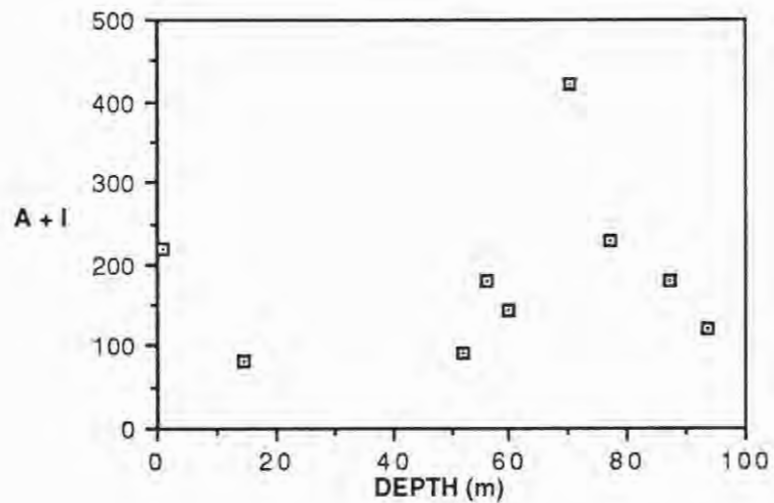


Figure 4.4.d: Total isoleucine concentrations (alloisoleucine + isoleucine) in samples of Globigerinoides ruber from ODP Site 625B.

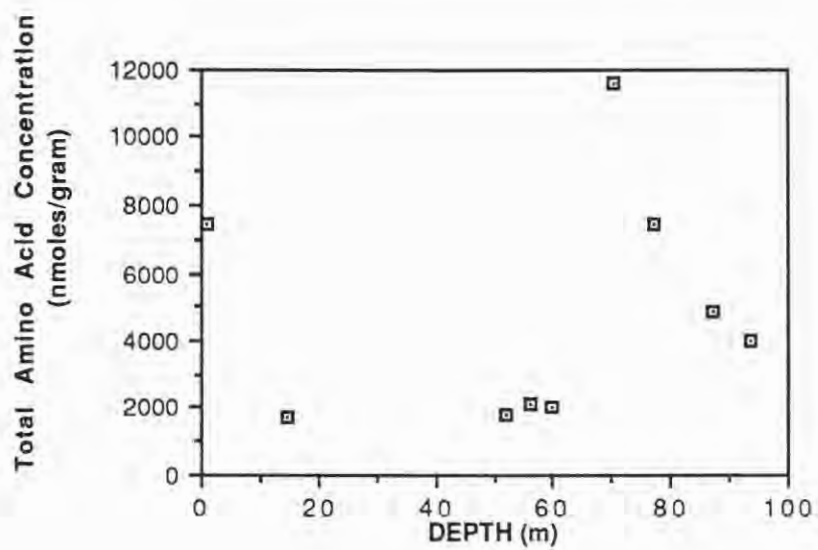


Figure 4.4.e: Total amino acid concentrations in samples of *Globigerinoides ruber* from ODP Site 625B.

Figure 4.4.a reveals initially high serine/leucine ratios, followed by a rapid decrease with depth, as serine becomes depleted relative to leucine. Figure 4.4.b shows relatively consistent glycine/alanine ratios with depth, until contamination becomes prevalent below 70.5 m. A/I ratios increase from 0.005 to 0.256 over the upper 70.5 m (see Figure 4.4.c), after which they decrease to values of 0.123 to 0.164. Total isoleucine (alloisoleucine + isoleucine) concentrations, and total amino acid concentrations show marked increases in samples below 70.5 m (see Figures 4.4.d and 4.4.e, respectively).

The effect of the primary cleaning with hydrogen peroxide used in conjunction with the secondary cleaning agent, ammonium hydroxide, was examined in samples of Globigerinoides ruber from between 50 and 65 m. Three samples were soaked in hydrogen peroxide for 60 minutes, followed by a soak in ammonium hydroxide for 36 hours, and showed A/I values between 0.180 and 0.256. Three samples were soaked once in ammonium hydroxide for 36 hours, and showed A/I values between 0.041 and 0.276. Three samples were soaked once in ammonium hydroxide for 7 days, and showed A/I values between 0.194 and 0.276. (See Figure 4.5 for the A/I ratios of these samples plotted against depth.)

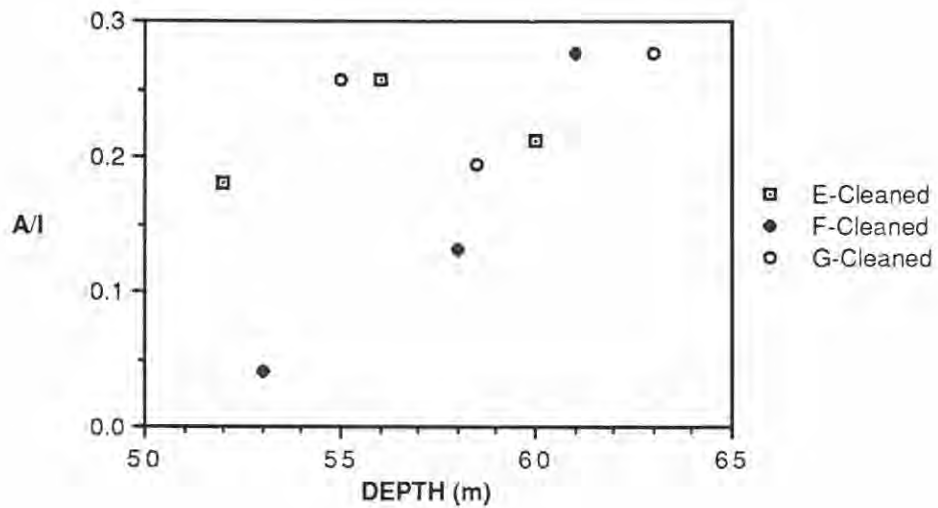


Figure 4.5: A/I ratios in samples of *Globigerinoides ruber* found at depths between 50.0 and 65.0 m in ODP Site 625B. Samples were cleaned in one of three methods: 1) E-cleaned = primary soak in hydrogen peroxide for 60 minutes, followed by a secondary soak in ammonium hydroxide for 36 hours; 2) F-cleaned = one soak in ammonium hydroxide for 36 hours; and 3) G-cleaned = one soak in ammonium hydroxide for one week.

Because more variability is seen in those samples soaked only in ammonium hydroxide for 36 hours, one might infer the necessity of the hydrogen peroxide soak prior to the ammonium hydroxide soak. However, results for those samples soaked in ammonium hydroxide for 7 days are comparable to those soaked in both cleaning agents. Thus, it appears that extended lengths of soaking the sample in ammonium hydroxide has the same effects as double soaking it in hydrogen peroxide and ammonium hydroxide for shorter time periods. Once again, it is important to realize that this is only a pilot study, and many more experiments should be performed before any hard conclusions are drawn.

Two Cleaning Methods Compared In Foraminiferal Samples

The next set of experiments entailed a comparison of samples soaked in hydrogen peroxide for 60 minutes to samples soaked in hydrogen peroxide for 60 minutes, followed by ammonium hydroxide for 36 hours. These cleaning experiments were performed on samples of Orbulina universa and Neogloboquadrina dutertrei

Figures 4.6.a-d compare various amino acid trends in Orbulina universa samples cleaned by a single soak in hydrogen peroxide to samples of the same species soaked in both hydrogen peroxide and ammonium hydroxide.

Figures 4.6.a-4.6.d: Various amino acid trends in samples of Orbulina universa from ODP Site 625B cleaned using one of two methods: 1) E-cleaned = primary soak in hydrogen peroxide for 60 minutes, followed by a secondary soak in ammonium hydroxide for 36 hours; and 2) D60-cleaned = one soak in hydrogen peroxide for 60 minutes. Circled points represent samples cleaned differently, but yielding similar results.

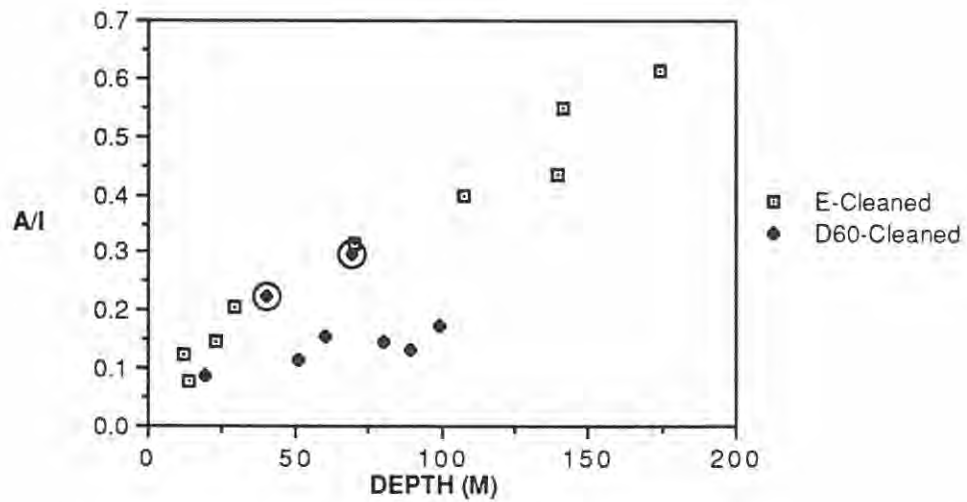


Figure 4.6.a: A/I ratios in samples of *Orbulina universa* cleaned using one of two methods (see preceding page) from ODP Site 625B.

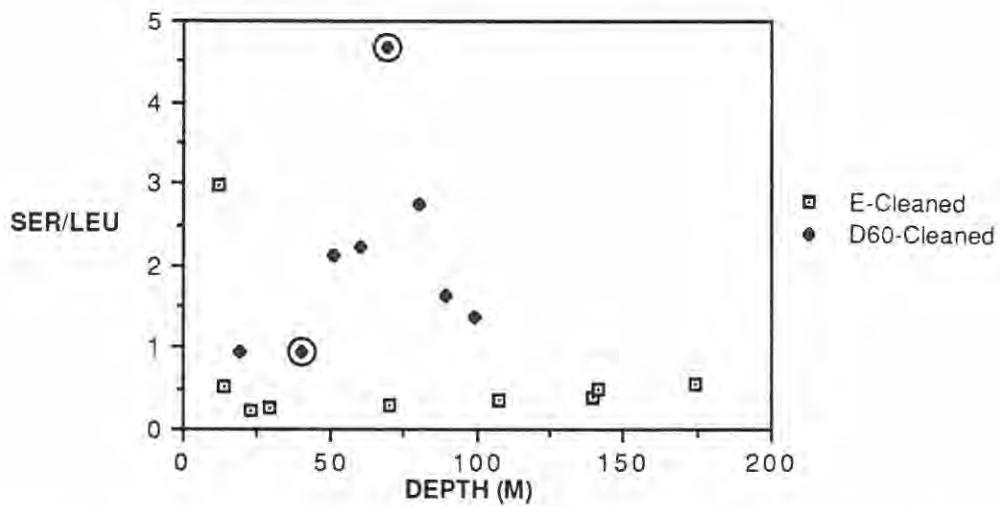


Figure 4.6.b: Serine/Leucine ratios in samples of *Orbulina universa* cleaned using one of two methods (see preceding page) from ODP Site 625B.

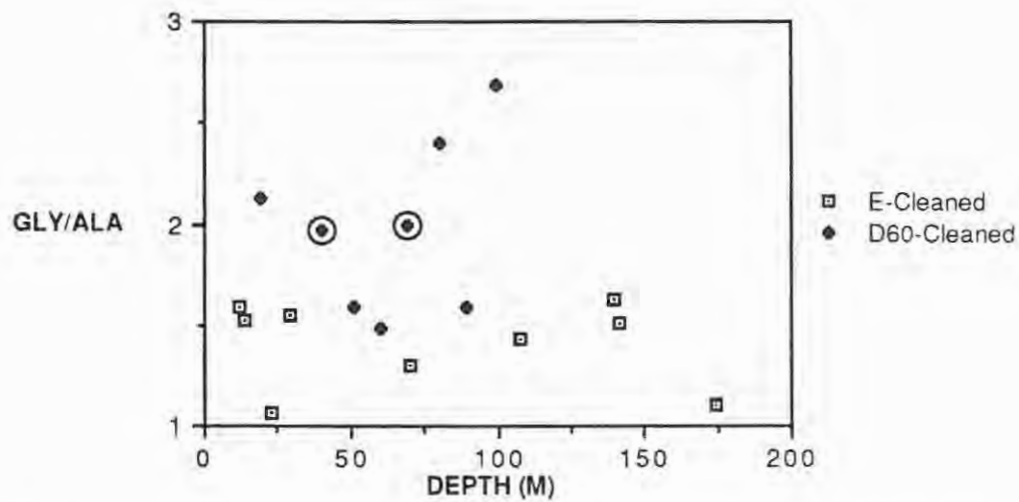


Figure 4.6.c: Glycine/Alanine ratios in samples of *Orbulina universa* cleaned using one of two methods (see second page preceding this one) from ODP Site 625B.

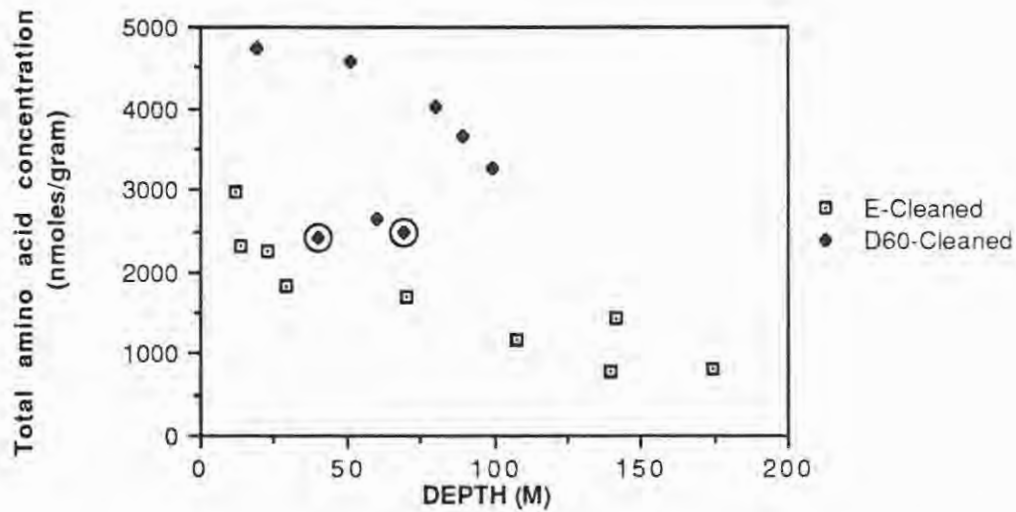


Figure 4.6.d: Total amino acid concentrations in samples of *Orbulina universa* cleaned using one of two methods (see second page preceding this one) from ODP Site 625B.

peroxide and ammonium hydroxide.

Figure 4.6.a shows A/I trends in samples of Orbulina universa subjected to the two cleaning methods. Most of the A/I ratios are lower and show higher degrees of variation in samples soaked only in hydrogen peroxide. Significant differences in A/I ratios between the two cleaning methods begin at approximately 19.5 m, and continue through the rest of the core.

Two samples cleaned only in hydrogen peroxide, represented by circled points in figures 4.6.a-d at 40.00 m and 69.00 m, have A/I ratios that mimic those samples cleaned with both cleaning agents. Further examination of amino acid trends in these samples of Orbulina universa, however, reveal that the similarities of the results between the two cleaning methods stop here.

Figure 4.6.b shows the serine/leucine trends in samples of Orbulina universa subjected to the two cleaning methods. Those samples soaked in both cleaning agents show significantly lower ratios, and less variation below 12 to 13 m, than those soaked only in hydrogen peroxide.

Figure 4.6.c shows the glycine/alanine trends in samples of Orbulina universa subjected to the two cleaning methods. Less variability, and lower ratios are seen in those samples cleaned by

both agents.

Figure 4.6.d shows the total amino acid concentrations in samples of Orbulina universa subjected to the two cleaning methods. Significantly lower, and less variable concentrations are seen in samples cleaned with both hydrogen peroxide and ammonium hydroxide, than in samples cleaned with only with hydrogen peroxide.

Thus, it appears that the double cleaning method used on samples of Orbulina universa leads to more consistent and reliable results reflecting less contamination than those Orbulina universa samples cleaned only with hydrogen peroxide. The effects of the double cleaning method, however, are not as pronounced on samples of Neogloboquadrina dutertrei, as is illustrated in Figures 4.7.a-d.

Figure 4.7.a shows A/I trends in samples of Neogloboquadrina dutertrei subjected to both cleaning methods. Similar results are seen in samples of Orbulina universa (see Figure 4.6.a). Higher A/I ratios are seen in samples cleaned with both agents compared to those cleaned only with hydrogen peroxide. Ratios begin to diverge below approximately 19.5 m, and continue to do so through out the rest of the core.

The two points circled in Figure 4.7.a represent samples

Figures 4.7a-4.7d: Various amino acid trends in samples of Neogloboquadrina dutertrei from ODP Site 625B cleaned in one of two methods: 1) E-cleaned = primary soak in hydrogen peroxide for 60 minutes, followed by a secondary soak in ammonium hydroxide for 36 hours; and 2) D60-cleaned = one soak in hydrogen peroxide for 60 minutes. Circled points represent similarities between samples cleaned differently.

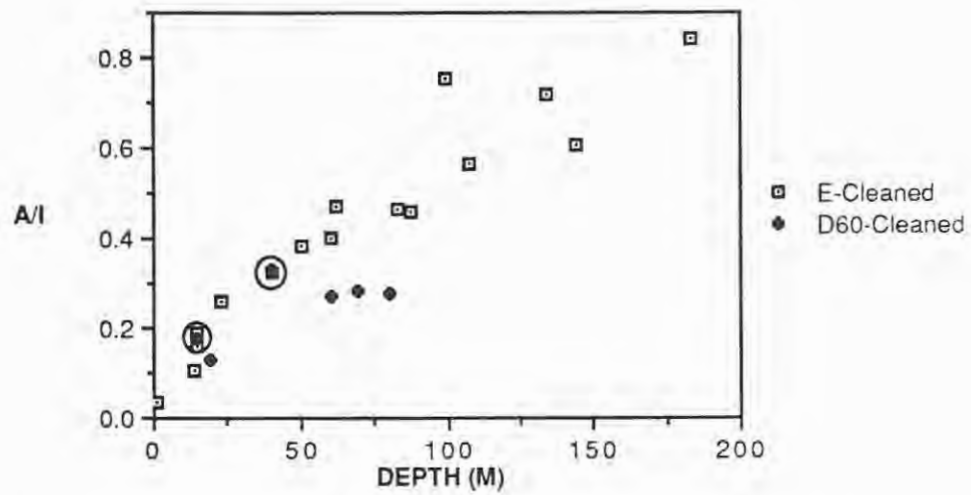


Figure 4.7.a: A/I ratios in samples of *Neogloboquadrina dutertrei* cleaned using one of two methods (see preceding page) from ODP Site 625B.

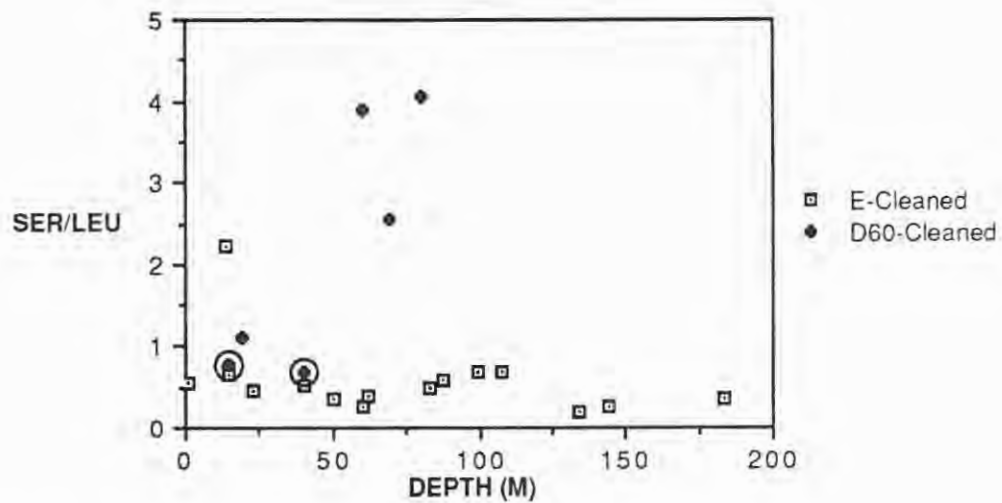


Figure 4.7.b: Serine/Leucine ratios in samples of *Neogloboquadrina dutertrei* cleaned using one of two methods (see preceding page) from ODP Site 625B.

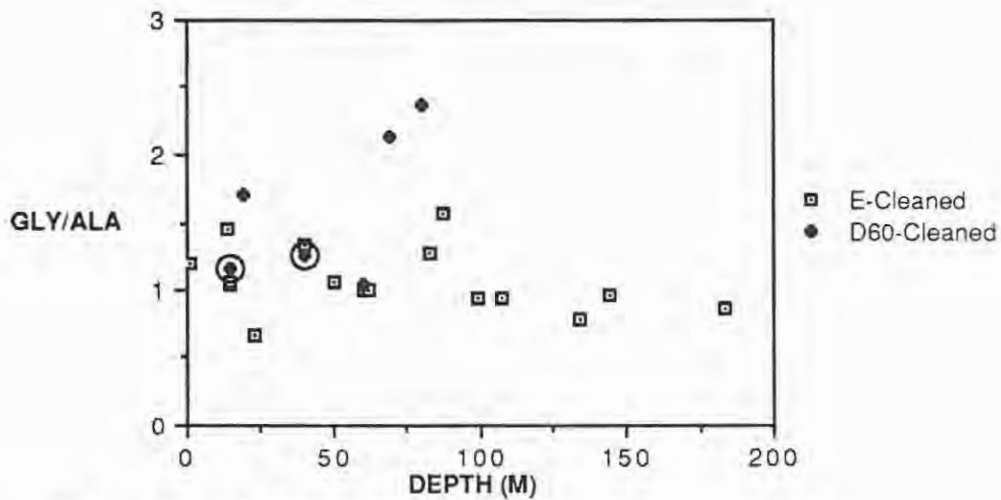


Figure 4.7.c: Glycine/Alanine ratios in samples of *Neogloboquadrina dutertrei* cleaned using one of two methods (see second page preceding this one) from ODP Site 625B.

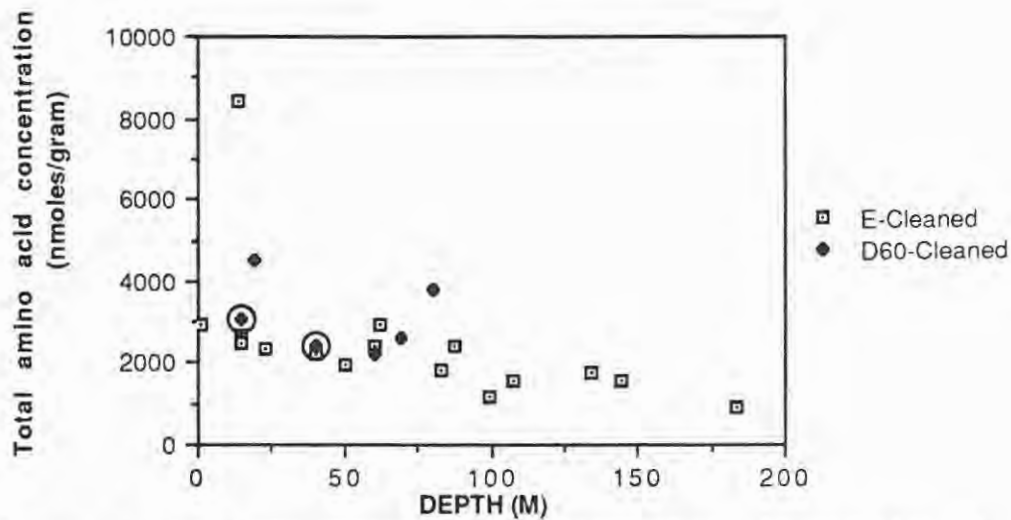


Figure 4.7.d: Total amino acid concentrations in samples of *Neogloboquadrina dutertrei* cleaned using one of two methods (see second page preceding this one) from ODP Site 625B.

cleaned only with hydrogen peroxide that show similar A/I ratios to samples cleaned in both hydrogen peroxide and ammonium hydroxide. Note that the two circled points at 14.44 m and 40.00 m consistently mimic those samples cleaned with both cleaning agents. A close examination of chromatograms of these samples reveal that they are very similar to those chromatograms of samples cleaned by the double cleaning method.

One of the circled samples just mentioned corresponds to the same depth (40.00 m) as one of the circled samples in the Orbulina universa samples. This may be entirely coincidental, or it may be evidence of some significant geochemical phenomenon affecting these two species equally at the time of deposition, and making them less-susceptible to contamination, or easier to clean.

Figure 4.7.b shows serine/leucine trends in samples of Neogloboquadrina dutertrei subjected to both cleaning methods. Higher ratios are seen in samples from the lower portion of the core cleaned only with hydrogen peroxide. Ratios in those samples soaked in both cleaning agents are lower and less variable than those soaked only in hydrogen peroxide.

Figure 4.7.c shows glycine/alanine trends in samples of Neogloboquadrina dutertrei subjected to both cleaning methods. Variation of ratios in samples cleaned with both agents is slightly

less than the variation of ratios in samples cleaned only with hydrogen peroxide.

Figure 4.7.d shows total amino acid concentration trends in samples of Neogloboquadrina dutertrei subjected to both cleaning methods. Samples cleaned in both hydrogen peroxide and ammonium hydroxide show slightly less variation than those cleaned in a single soak of hydrogen peroxide.

It appears that the double cleaning method is more effective in Orbulina universa, Neogloboquadrina dutertrei and Globigerinoides ruber, compared to those samples soaked only in one agent. This double cleaning method is more effective in samples of Orbulina universa than in the samples of Neogloboquadrina dutertrei.

This observation may reflect a difference in susceptibilities to contamination of the two species due to their differences in dissolution vulnerabilities. Orbulina universa is more susceptible to dissolution than Neogloboquadrina dutertrei (Berger, 1968). Spinose species (in this case, Orbulina universa) have "spiny" tests that have more surface area exposed to corrosive bottom waters than do non-spinose tests (in this case, Neogloboquadrina dutertrei). Thus, the spinose species are less resistant to dissolution than are the non-spinose.

A highly dissolved Orbulina universa test will have more surface area exposed to the cleaning agents than a less dissolved Neogloboquadrina dutertrei test. This may result in easier removal of contaminant amino acids trapped in the pore spaces in the Orbulina universa.

An ILC powder was cleaned and run with every seven foraminiferal samples analyzed. This procedure helped to ensure consistency in the preparatory analyses of the samples throughout the extent of the study. The powders and the foraminifera samples were chemically cleaned in the same way. Consequently, the epimerization results of the ILC powders can be used as a control to be sure that the double cleaning method did not affect A/I ratios by "raising" them.

Figure 4.8 is a plot of the A/I ratios measured in the ILC-B powders cleaned by three different techniques. These values cluster about an A/I value of 0.454 with a standard deviation of 0.041. There appears to be little variation in A/I ratios among the three different cleaning methods employed on the ILC-B powders analyzed in this study. This mean and standard deviation are in agreement with results obtained for ILC-B powders without any cleaning (University of Delaware, unpublished results). These results imply that the cleaning methods used in this study do not raise the A/I value significantly.

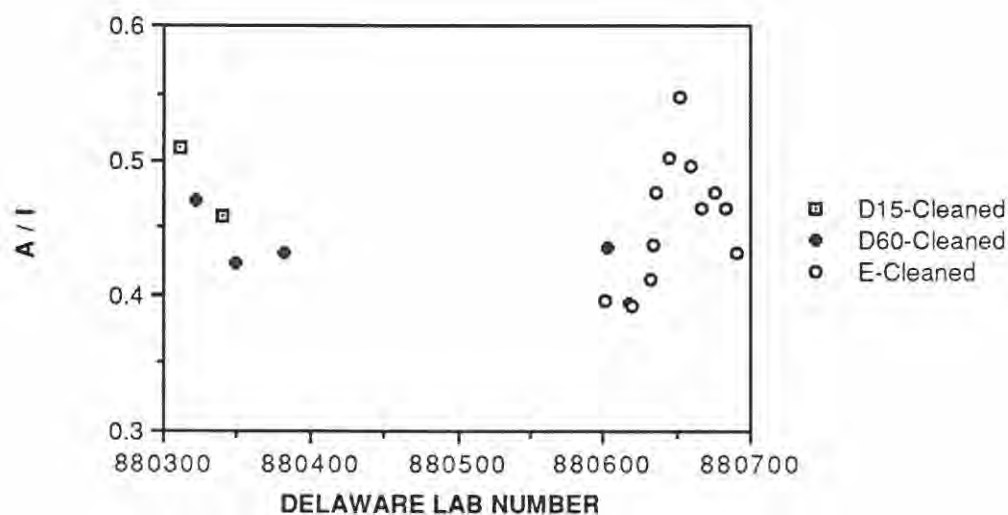


Figure 4.8: A/I ratios in ILC-B samples cleaned using one of three methods listed: 1) D15-Cleaned = one soak in hydrogen peroxide for 15 minutes; 2) D60-Cleaned = one soak in hydrogen peroxide for 60 minutes; and 3) E-cleaned = primary soak in hydrogen peroxide for 60 minutes followed by a secondary soak in ammonium hydroxide for 36 hours. Delaware lab numbers are the numbers assigned the samples according to the order in which they were processed for amino acid analysis.

Cleaning of foraminiferal samples in hydrogen peroxide, followed by ammonium hydroxide seems to lead to increased removal of contaminants with low A/I values. It may be that humic acids adsorbed onto the carbonate surface are extracted with the ammonium hydroxide. If these humic acids contain amino acids with low D/L (A/I) values, their removal by ammonium hydroxide would have the effect of raising the measured D/L (A/I) value in the total sample hydrolyzate.

The following chapter presents the aminostratigraphic results obtained from this study. All samples discussed through the rest of this paper were cleaned by the same method- a primary soak in hydrogen peroxide for 60 minutes, followed by a secondary soak in ammonium hydroxide for 36 hours.

CHAPTER 5

RESULTS-AMINOSTRATIGRAPHY OF ODP HOLE 625B

Epimerization Results of the Total Fraction

Epimerization results for Orbulina universa, Neogloboquadrina dutertrei, the Globorotalia tumida-menardii complex, and the mixed foraminiferal species assemblage can be found in Appendices D, E, F, and G. All those monospecific samples listed were analyzed for epimerization in the total isoleucine fraction, the results of which will be discussed in this section. Analysis of epimerization in the free and bound fractions of the mixed foraminiferal species assemblage will be examined in the following section.

Orbulina universa

Plots of A/I verses age for Orbulina universa are found in Figures 5.1.a-5.1.b. Figure 5.1.a shows the actual data, and Figure 5.1.b shows a logarithmic curve best fit to the data generated by Version 1.2 of Cricket Graph on the MacIntosh. (All subsequent

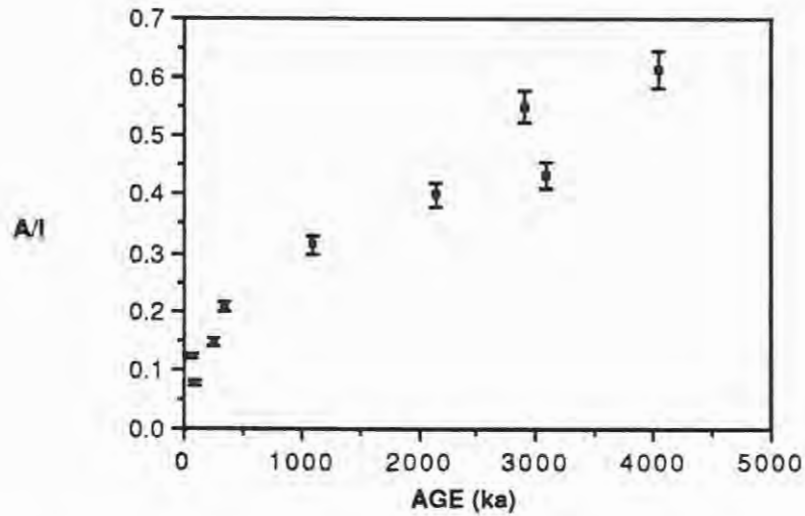


Figure 5.1.a: A/I ratios plotted against age in samples of Orbulina universa through the Pleistocene and Pliocene of ODP Site 625B.

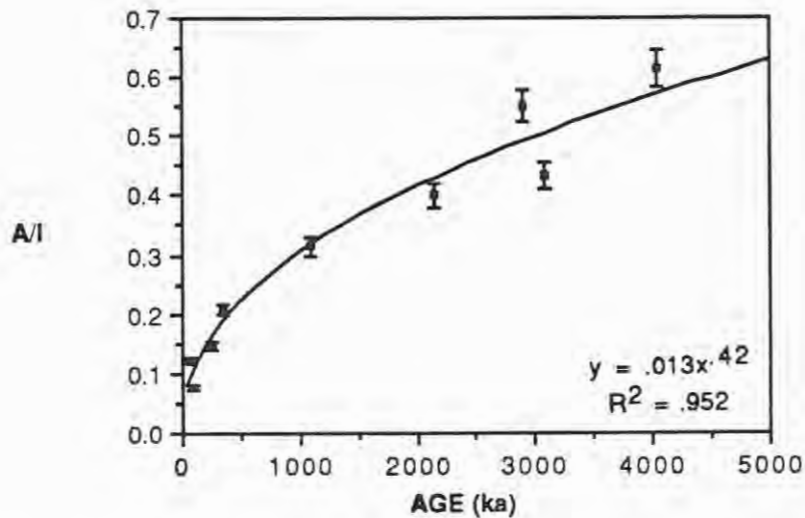


Figure 5.1.b: A/I ratios plotted against age in samples of Orbulina universa through the Pleistocene and Pliocene of ODP Site 625B. A computer-generated logarithmic curve is best fit to the data.

computer-generated curves are a result of this feature in Cricket Graph.)

The kinetic curve may be logarithmic (Figure 5.1.b). These data demonstrate initially rapid apparent epimerization rates, until A/I ratios of 0.23-0.25 are reached, and 400-700 ka have passed. After this time, apparent epimerization rates slow by an order of magnitude. At the base of the Pliocene, A/I ratios in Orbulina universa are approximately 0.60.

Neogloboquadrina dutertrei

Plots of A/I versus age are found in Figures 5.2.a-5.2.b. Again the kinetic curve can be described as logarithmic (Figure 5.2.b). Apparent rate constants decrease by an order of magnitude when A/I ratios of 0.25-0.33 are reached, and 400-600 ka have passed. In the early Pliocene, ratios in Neogloboquadrina dutertrei are close to 0.90.

Globorotalia tumida-menardii Complex

Plots of A/I versus age for the Globorotalia tumida-menardii complex are found in Figures 5.3.a-5.3.b. Figure 5.3.b illustrates the computer generated logarithmic curve that best fits the data. Consistent with the other two species examined, the kinetic curve demonstrates a significant decrease in apparent

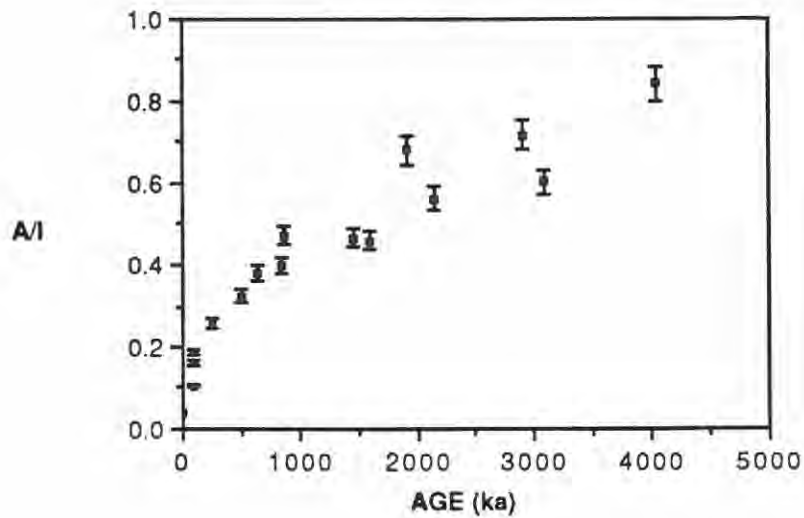


Figure 5.2.a: A/I ratios plotted against age in samples of Neogloboquadrina dutertrei through the Pleistocene and Pliocene of ODP Site 625B.

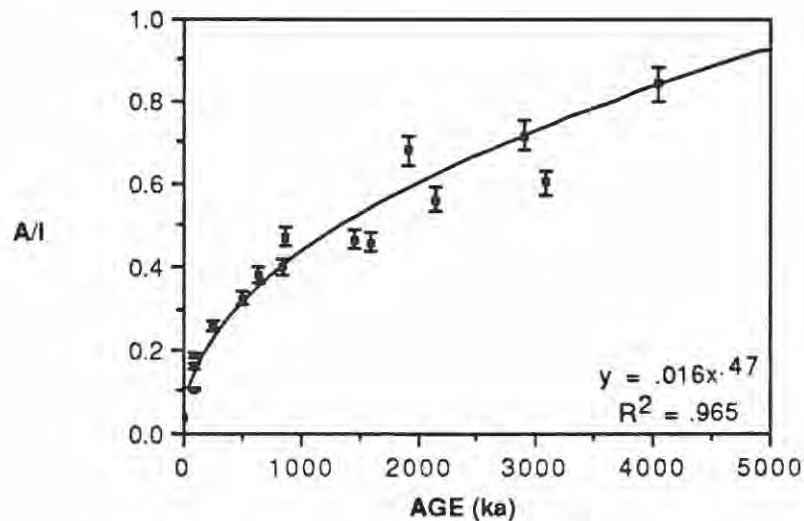


Figure 5.2.b: A/I ratios plotted against age in samples of Neogloboquadrina dutertrei through the Pleistocene and Pliocene of ODP Site 625B. A computer-generated logarithmic curve is best fit to the data.

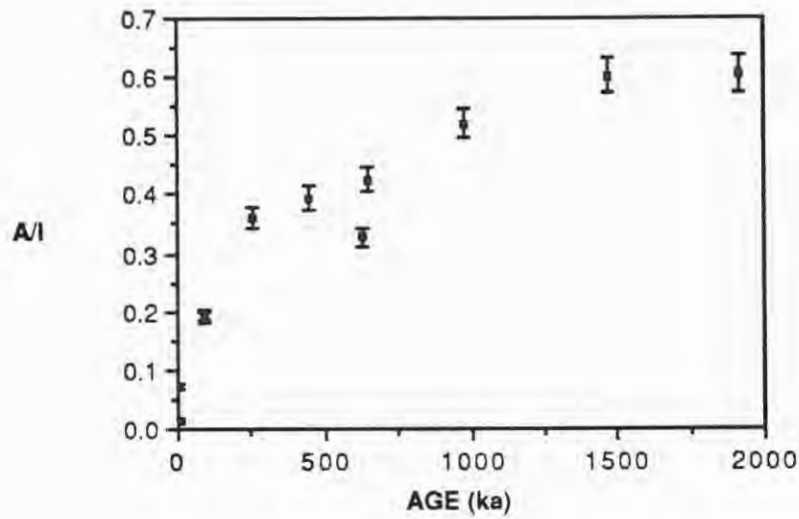


Figure 5.3.a: A/I ratios plotted against age in samples of the Globorotalia tumida-menardii complex through the Pleistocene of ODP Site 625B.

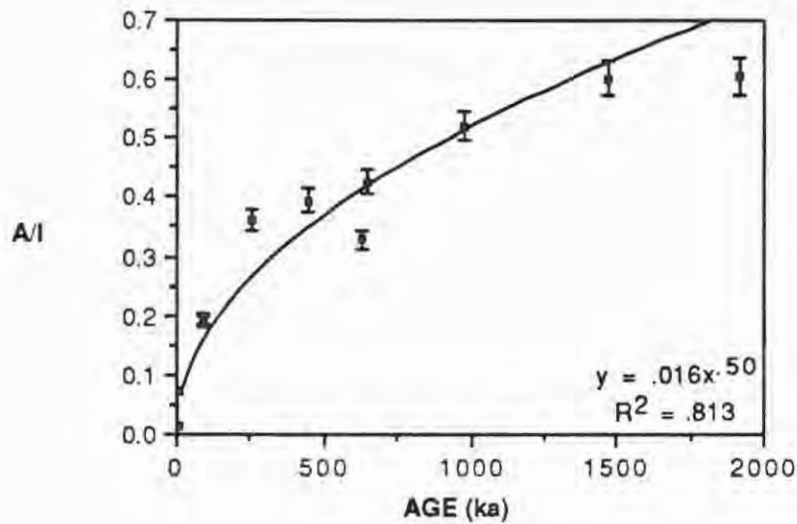


Figure 5.3.b: A/I ratios plotted against age in samples of the Globorotalia tumida-menardii complex through the Pleistocene of ODP Site 625B. A computer-generated logarithmic curve is best fit to the data.

epimerization rates after A/I ratios reach 0.28-0.35 and 250-400 ka have passed. There appears to be a second decrease in apparent epimerization rates at 1500 ka, corresponding to A/I ratios of 0.55-0.58.

The anomalously low A/I ratio (0.366) at 630 ka is probably due to contamination with L-isoleucine during the laboratory preparation procedures (see Figure 6.3 for the total isoleucine concentration in this sample). Otherwise, similarly low A/I ratios would be expected from the same ages in the other species.

Monospecific Species Comparison

The monospecific aminostratigraphic curves are superimposed in Figure 5.4.a. It is important to recall that the Globorotalia tumida-menardii complex was analyzed only through the Pleistocene section of Site 625B, while Orbulina universa, and Neogloboquadrina dutertrei were analyzed through the Pliocene and Pleistocene section.

There is a noticeable difference in total A/I ratios measured between species. Logarithmic fits to the data reveal highest A/I ratios in the Globorotalia tumida-menardii complex, and the lowest A/I ratios in Orbulina universa. A/I ratios of Neogloboquadrina dutertrei fall between the limits delineated by

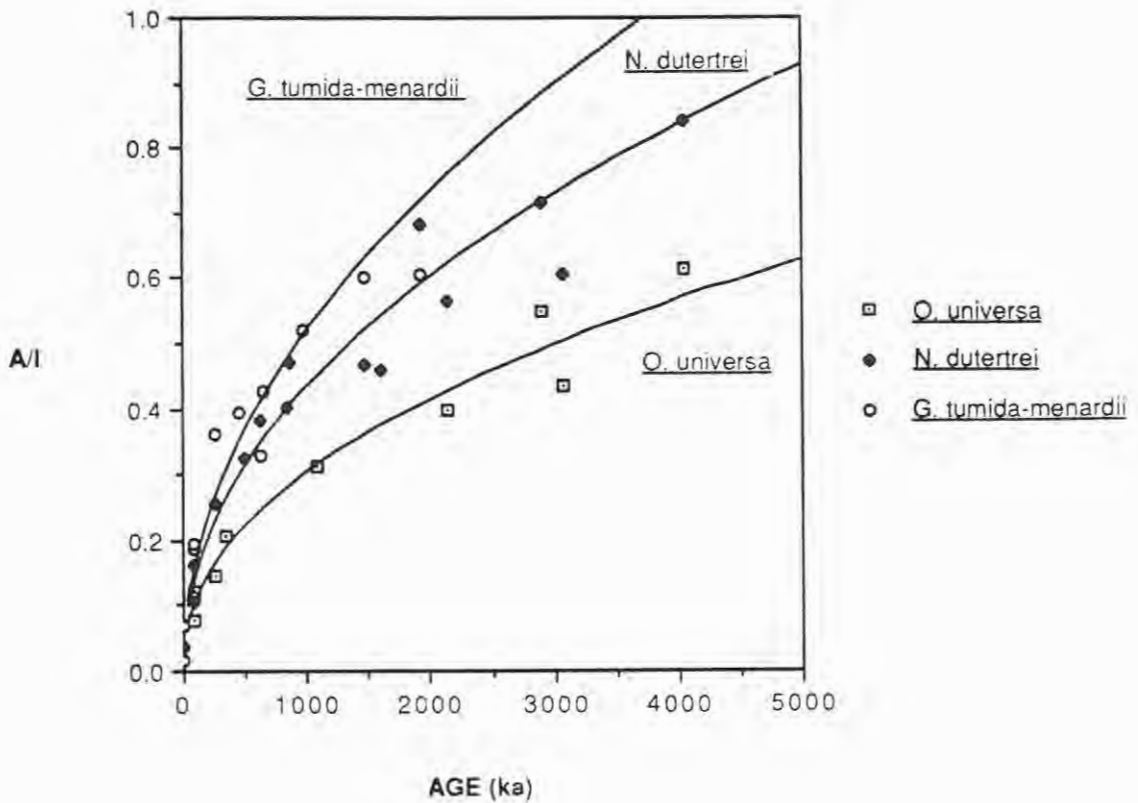


Figure 5.4.a: A/I ratios plotted against age in samples of *Orbulina universa*, *Neogloboquadrina dutertrei*, and the *Globorotalia tumida-menardii* complex through ODP Site 625B. Computer-generated logarithmic curves are best fit to the data.

the other two. This observation supports the work of others who find a dependence on epimerization rates at the genus level (King and Neville, 1977; Mueller, 1984).

It is important to note that greater precision of A/I values is found in the upper parts of the core. More variability of A/I ratios is seen in older samples found deeper in the core for all genera studied.

Figure 5.4.a reveals higher A/I ratios in the non-spinose forms analyzed (Globorotalia tumida-menardii complex, and Neogloboquadrina dutertrei) than in the spinose form analyzed (Orbulina universa). This is in agreement with the work of King and Hare (1972a, b) and King and Neville (1977) who correlated foraminiferal test morphologies to relative rates of epimerization. They predicted greater observed A/I ratios in non-spinose species than in spinose. The results from Site 625B denote a difference in epimerization rates even among the non-spinose forms.

A closer examination of the A/I trends in the uppermost sections of 625B is seen in Figure 5.4.b. Initial apparent epimerization rates are similar and nearly parallel in Globorotalia tumida-menardii, and Neogloboquadrina dutertrei, and are 2-3 times greater than in Orbulina universa. It appears that a species effect between spinose and non-spinose foraminifera takes place

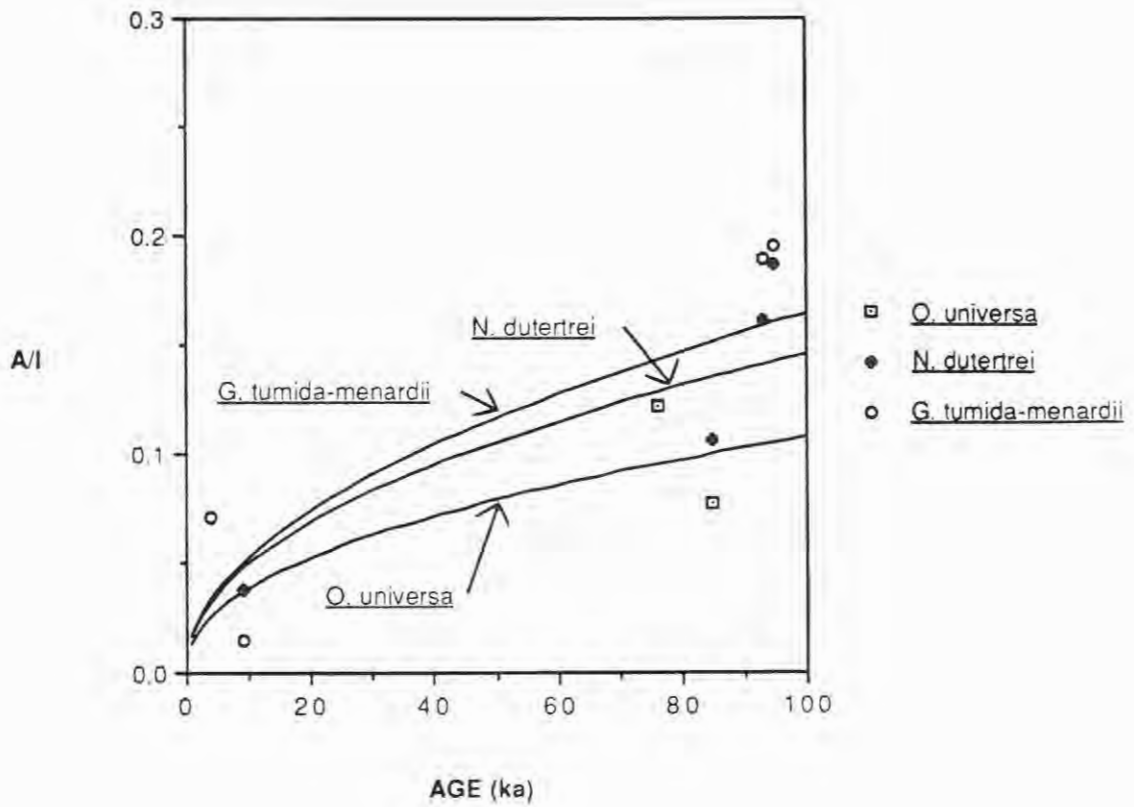


Figure 5.4.b: A/I ratios plotted against age in samples of *Orbulina universa*, *Neogloboquadrina dutertrei*, and the *Globorotalia tumida-menardii* complex over the first 100 ka (14.5 m). These curves are derived from Figure 5.4.a.

in the youngest of samples. (The species effect between the non-spinose samples, however, does not become significant until approximately 90 ka.)

Mixed Foraminiferal Species Assemblage

Epimerization trends in the total fraction of the bulk sediment, (mixed foraminiferal species assemblage) are seen in Figure 5.5.a. A logarithmic fit to these data is superimposed on the monospecific curves in Figure 5.5.b. The mixed foraminiferal species assemblage curve falls between the limits delineated by the Globorotalia tumida-menardii and Orbulina universa curves, and crosses each of the monospecific curves. This may result from different mixtures of spinose and non-spinose species found at different depths in the core.

The A/I ratios of the mixed foraminiferal species assemblage more closely parallel those of the non-spinose species Globorotalia tumida-menardii than the spinose species Orbulina universa. It is interesting to note that the biostratigraphic analyses of the Pleistocene section of ODP Site 625B indicate a dominance of spinose foraminiferal species throughout most of the core (Johnson, 1988). Thus, it appears that epimerization in non-spinose species provides a stronger signal in the Gulf of Mexico than epimerization in spinose species.

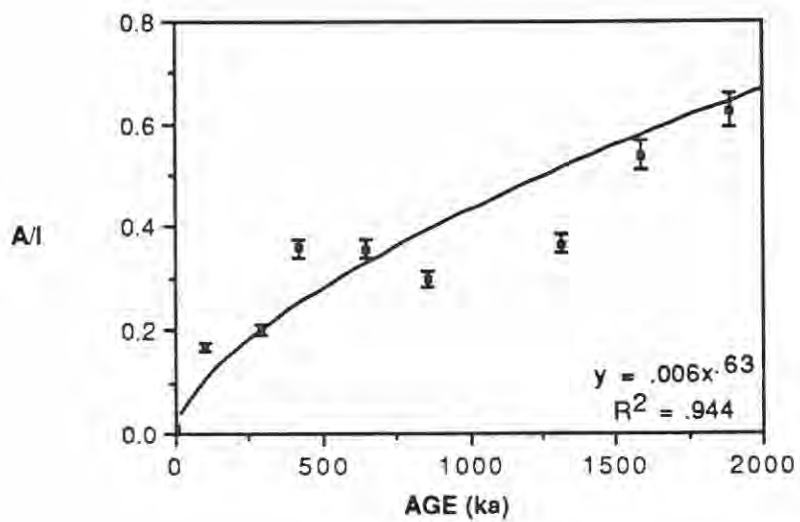


Figure 5.5.a: A/I ratios plotted against age in samples of the mixed foraminiferal species assemblage through ODP Site 625B. A computer-generated logarithmic curve is best fit to the data.

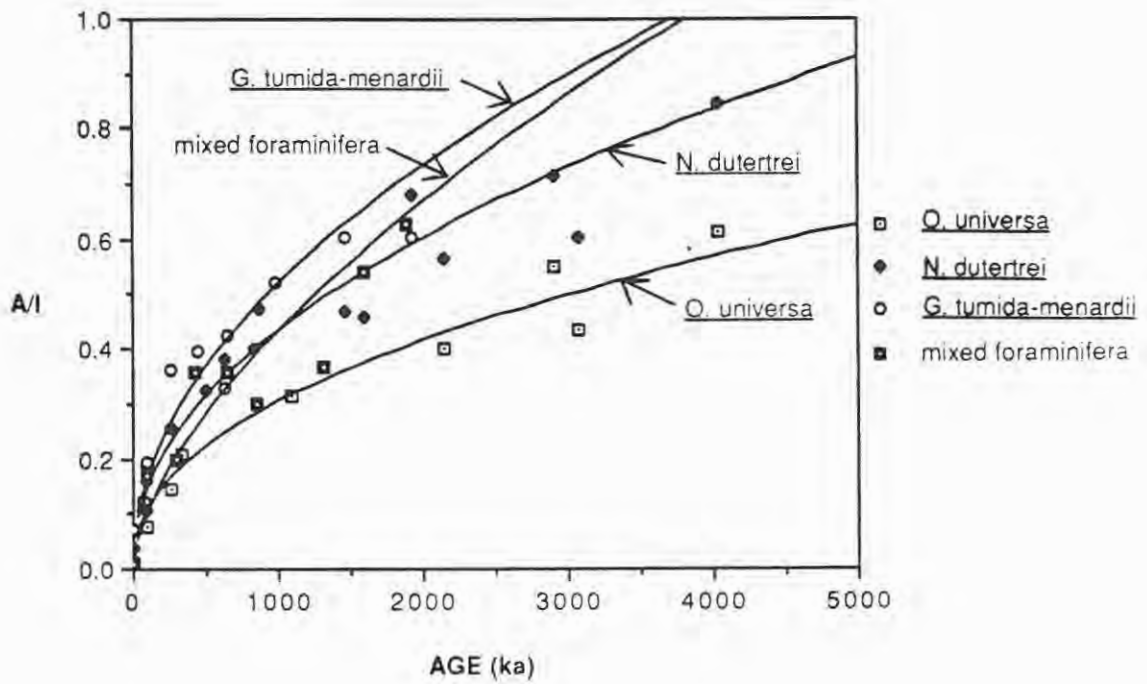


Figure 5.5.b: A composite aminostratigraphy of ODP Site 625B, including the A/I ratios measured in the monospecific samples, as well as those ratios measured in the mixed foraminiferal species assemblages.

Epimerization Results of the Free and Bound Fractions

Free Fraction

Analyses of epimerization in the free isoleucine fraction were performed on the mixed foraminiferal species assemblage. Figure 5.6.a demonstrates the relationship between A/I values in the free and total isoleucine fractions of the samples.

Free isoleucine consistently exhibits a much higher degree of epimerization than does total isoleucine. The initial apparent rate of epimerization in free isoleucine is higher than that of total isoleucine. The apparent epimerization rate of the free fraction decreases by an order of magnitude, and becomes somewhat parallel to the rate in the total fraction in samples older than about 100 ka.

Bound Fraction

Epimerization ratios in the bound fraction were not measured directly. They can be calculated by subtracting the abundances of the amino acids in the free fraction from those in the total fraction, and then dividing the bound (by difference) isoleucine abundance into the bound alloisoleucine abundance.

Figure 5.6.b shows the A/I trends in the total, free, and bound (by difference) fractions with increasing age. At two depths, there are negative values for the A/I ratios in the bound fraction. These negative values occur because measured abundances of alloisoleucine or isoleucine in the free fraction appear to be greater than those in the total fraction. This seeming contradiction may reflect a different amino acid composition of the bulk sediment at the same depth, and/or uncertainties in the quantitative analysis of small peaks. This problem may be avoided in the future by extracting a portion of the sample for analysis of the free fraction, before hydrolysis. With this observation in mind, all that can be said about the degree of epimerization of bound isoleucine is that it is quite low relative to the degree of epimerization in the total and/or free isoleucine fraction.

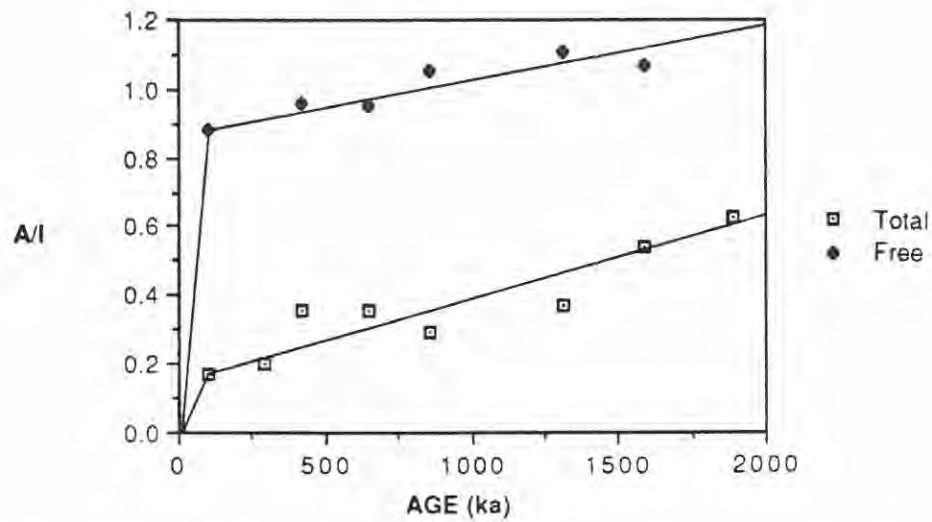


Figure 5.6.a: A/I ratios of the total and free fraction of isoleucine plotted against age in samples of the mixed foraminiferal species assemblages from ODP Site 625B. Lines are hand-drawn as best seen to fit the data.

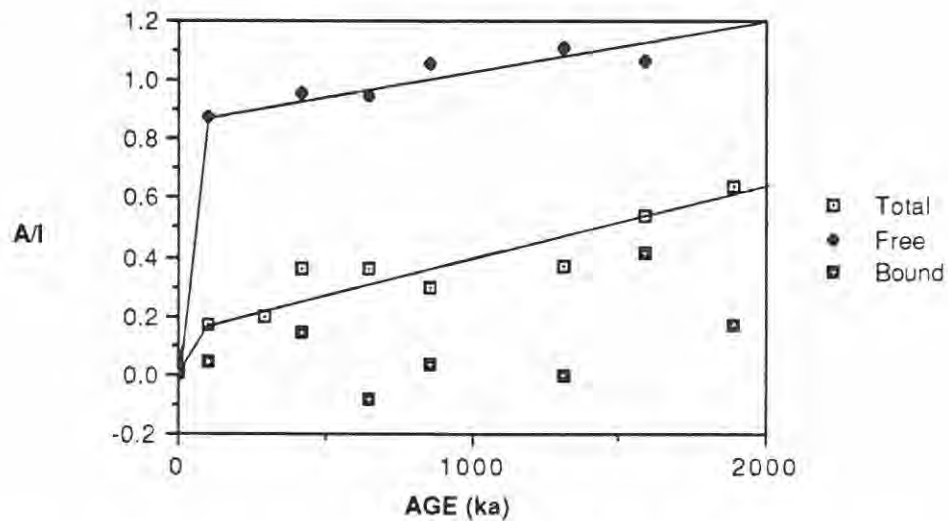


Figure 5.6.b: A/I ratios of the total, free and bound (total - free) fractions of isoleucine plotted against age in samples of the mixed foraminiferal species assemblages from ODP Site 625B. Lines are hand-drawn as best seen to fit the data.

CHAPTER 6

DISCUSSION

Intercore Correlations Between Gulf of Mexico Core 625B, Mid-Atlantic Core 13519-2, and Equatorial Pacific Core V28-238

Introduction

The location of Core 13519-2 is in the mid-Atlantic, on the Sierra Leone rise at a latitude/longitude of 5°40'N/19°51'W. It was taken at a water depth of 2862 m (during R.V. "Meteor" cruise 51/1979), and was terminated at about 1050 cm, just below the Matuyama/Jaramillo geomagnetic reversal. Calcium carbonate content ranges from between 30-90% dry weight, as reported by Mueller (1984).

The Brunhes/Matuyama boundary is found in Core 13519-2 at 990 cm sub-bottom depth. The average sedimentation rate through the upper 990 cm of the core is 1.36 cm/1000 yrs. The Matuyama/Jaramillo reversal is found just 60 cm below the Brunhes/Matuyama boundary. The average

sedimentation rate over the lowest 60 cm of the core is 0.41 cm/1000 yrs. This drastic reduction in sediment accumulation rates may indicate a break in deposition at 990 cm; however, there is no apparent sedimentologic evidence to support this. The reader is referred to Mueller (1984), and the references therein for a more detailed description of Site 13519-2.

The location of Core V28-238 is in the western equatorial Pacific, at a latitude/longitude of 01°01'N/160°29'E. It was taken at a depth of 3120 m and covers approximately the same time-span as Core 13519-2. The Brunhes/Matuyama geomagnetic reversal is found at 1200 cm in Core V28-238. The average sedimentation rate through the core is 1.71 cm/1000 yrs. The reader is referred to King and Neville (1977), Mueller (1984), and the references therein, as well as Shackleton and Opdyke (1973) for a more detailed description of Core V28-238.

It is important to realize that different time intervals and sampling densities are represented by the data obtained from Site 625B, and Cores 13519-2 and V28-238. Site 625B represents the last 5 million years, and was sampled approximately every 2-10 m. (Samples are taken between approximately every 44 and 222 ka.) Core 13519-2 represents the last 0.9 million years, and was sampled by Mueller (1984) approximately every 0.20 m.

(Samples are taken approximately every 18 ka). Core V28-238 represents the last 0.7 million years, and was sampled approximately every 0.10 m. (Samples are taken approximately every 60 ka). Thus, the results from the analysis of Site 625B represent more general trends in deep-sea sediments over longer periods of time than those of Cores 13519-2 and V28-238.

Epimerization Trends In All Three Cores

Comparison plots of epimerization trends in monospecific samples from northeast Gulf of Mexico Site 625B, mid-Atlantic Core 13519-2, and Pacific Core V28-238 are shown in Figures 6.1. and 6.2.a-b. The slowly epimerizing species (*Orbulina universa* from Site 625B and Core 13519-2, and *Globigerinoides sacculifer* from Core V28-238) are presented in Figure 6.1. Both of these spinose species are of the same family, *Globigerinoides*. The quickly epimerizing species (the *Globorotalia tumida-menardii* complex) from all three cores are presented in Figure 6.2.a-b.

It should be noted that epimerization trends in core 13519-2 are described by three linear segments decreasing in slope with time (Mueller, 1984). Because Site 625B and Core V28-238 were sampled on a coarser time scale than Core 13519-2, it is not possible to fit the data from 625B and V28-238 to a three-linear-segment model. Instead, logarithmic regressions are fit to

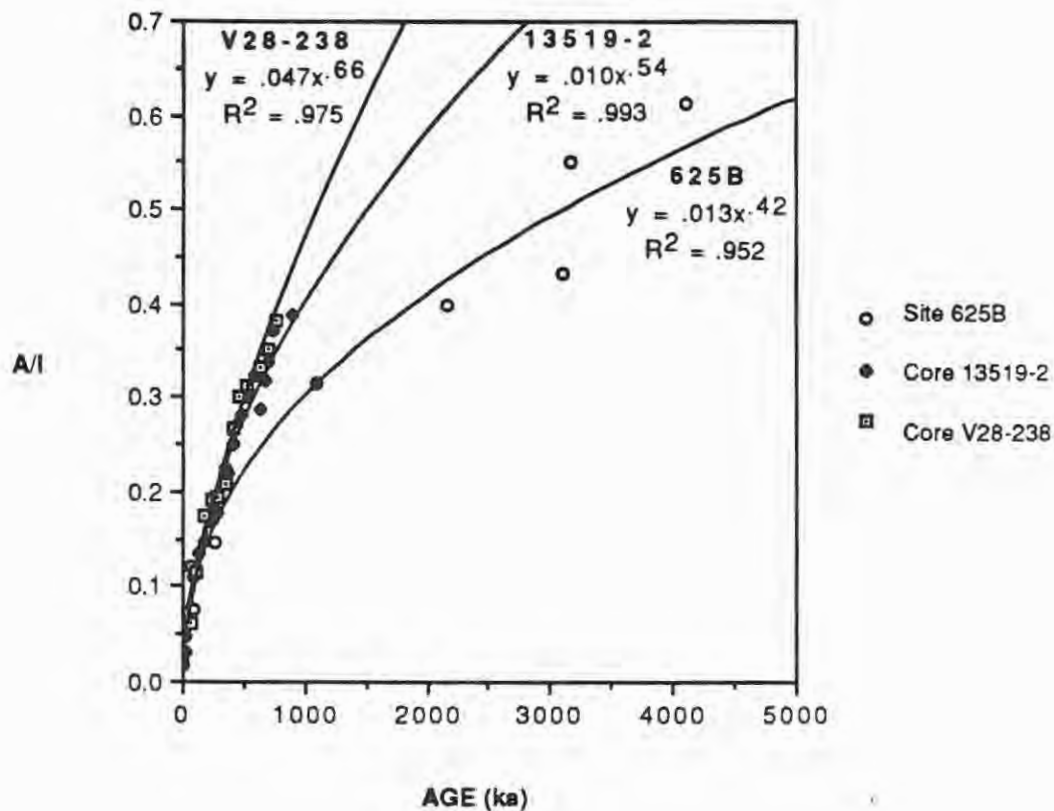


Figure 6.1: A/I ratios in samples of 2 spinose species of the same family, Globigernioides compared in three ocean basins. Orbulina universa analyzed in the Gulf of Mexico Site 625B, and in the mid-Atlantic Core 13519-2 (from Mueller, 1984). Globigerinoides sacculifer analyzed in Pacific Core V28-238 (from King and Neville, 1977). Horizontal scale extends from the present to 5000 ka before present. Equations describe a logarithmic fit to the data.

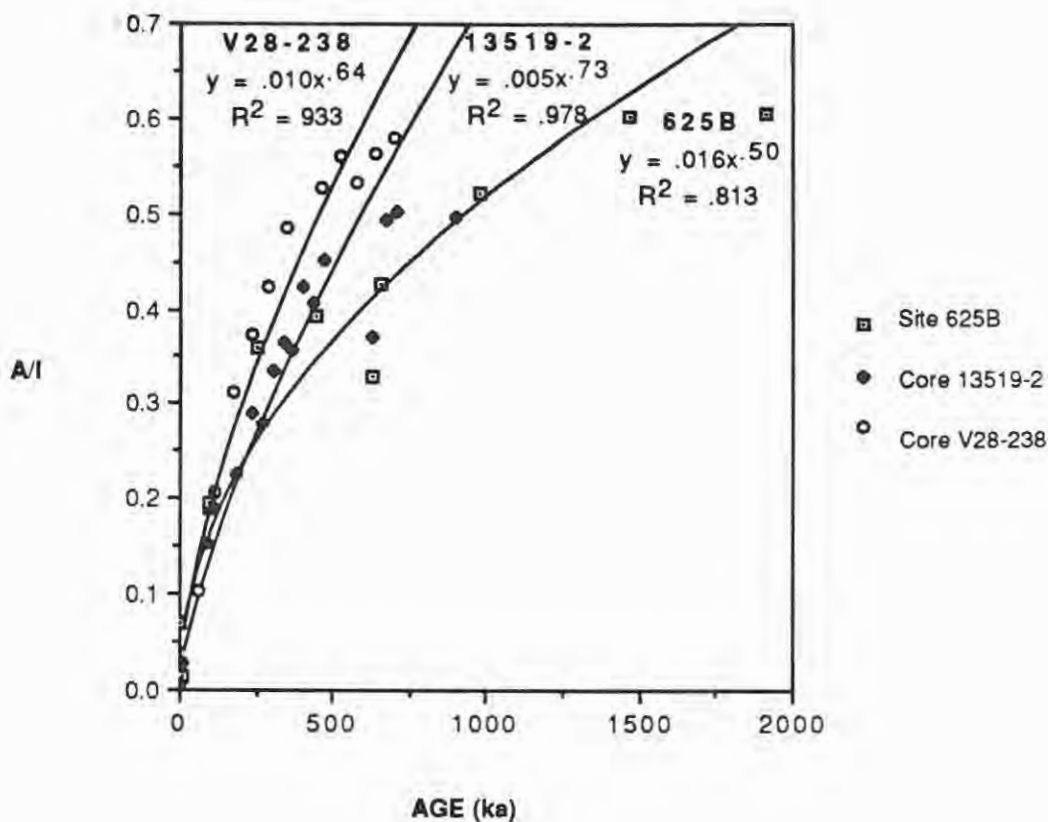


Figure 6.2.a: A/I ratios in samples of the non-spinose species *Globorotalia tumida-menardii* from Gulf of Mexico Site 625B, mid-Atlantic Core 13519-2 (from Mueller, 1984), and Pacific Core V28-238 (from King and Neville, 1977). Horizontal scale extends from the present to 2000 ka before present. Equations describe a logarithmic fit to the data.

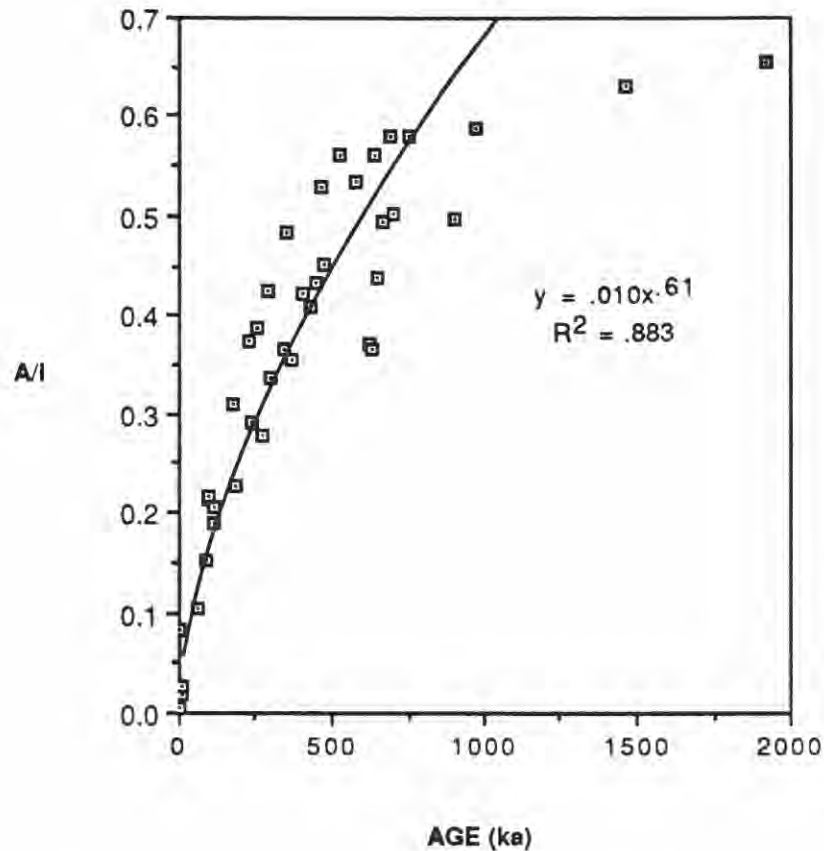


Figure 6.2.b: A/I ratios in samples of the Globorotalia tumida-menardii complex from Gulf of Mexico Site 625B, mid-Atlantic Core 13519-2 (from Mueller, 1984), and Pacific Core V28-238 (from King and Neville, 1977) plotted against age. One logarithmic regression is fit to all of the data to demonstrate that the differences in the data sets from the three sites graphed in Figure 6.2.a is significant. The horizontal scale extends from the present to 2000 ka before present.

the data presented. This approach allows for direct comparisons between the three cores.

Initially, apparent epimerization rates between the three cores are very similar (Figures 6.1 and 6.2.a-b). Between 300-500 ka, epimerization curves for the spinose and non-spinose species diverge between Cores 13519-2 and V28-238, and Site 625B. A/I ratios in the mid-Atlantic and Pacific sites are similar and are higher than in the Gulf of Mexico. (Figure 6.2.b reveals the logarithmic regression fit to the Globorotalia tumida-menardii complex data from all three sites. The lower R^2 value for this combined data set implies a significant difference between the three sets of data does exist.)

In samples between 350 and 1000 ka, the highest A/I ratios are seen in both species from Pacific Core V28-238. Mueller (1984) relates the difference in A/I ratios between the cores to different rates of hydrolysis and to different degrees of carbonate dissolution at the sites. This, in turn, results in different leaching characteristics at the sites.

A close examination of epimerization data from deep-sea cores allows for the differentiation of a syn-depositional dissolution effect (process occurring at, or near the sediment-water-interface) and a post-depositional dissolution effect

(process occurring at some depth in the core). Epimerization results from the Globorotalia tumida-menardii complex from Site 625B, Core 13519-2 and Core V28-238 will be examined in the following two sections to illustrate this point.

Syn-Depositional Dissolution In All Three Sites

The following relative relationships were found to exist among the epimerization data from samples of Globorotalia tumida-menardii for a given age analyzed in Gulf of Mexico Site 625B, mid-Atlantic Core 13519-2 (Mueller, 1984), and Pacific Core V28-238 (King and Neville, 1977):

$$\text{Allo})_{\text{Gulf}} = \text{Allo})_{\text{Atlantic}} = \text{Allo})_{\text{Pacific}}$$

$$\text{Allo} + \text{Iso})_{\text{Gulf}} > \text{Allo} + \text{Iso})_{\text{Atlantic}} > \text{Allo} + \text{Iso})_{\text{Pacific}}$$

These relationships are represented graphically in Figure 6.3.

King (1980) found an inverse relationship between the concentration of amino acids in foraminiferal tests and the degree of dissolution. (Presumably, higher degrees of dissolution correspond to a greater amount of amino acids leached from the system.)

Assuming that King (1980) was correct, and that dissolution is the predominant process responsible for the loss of

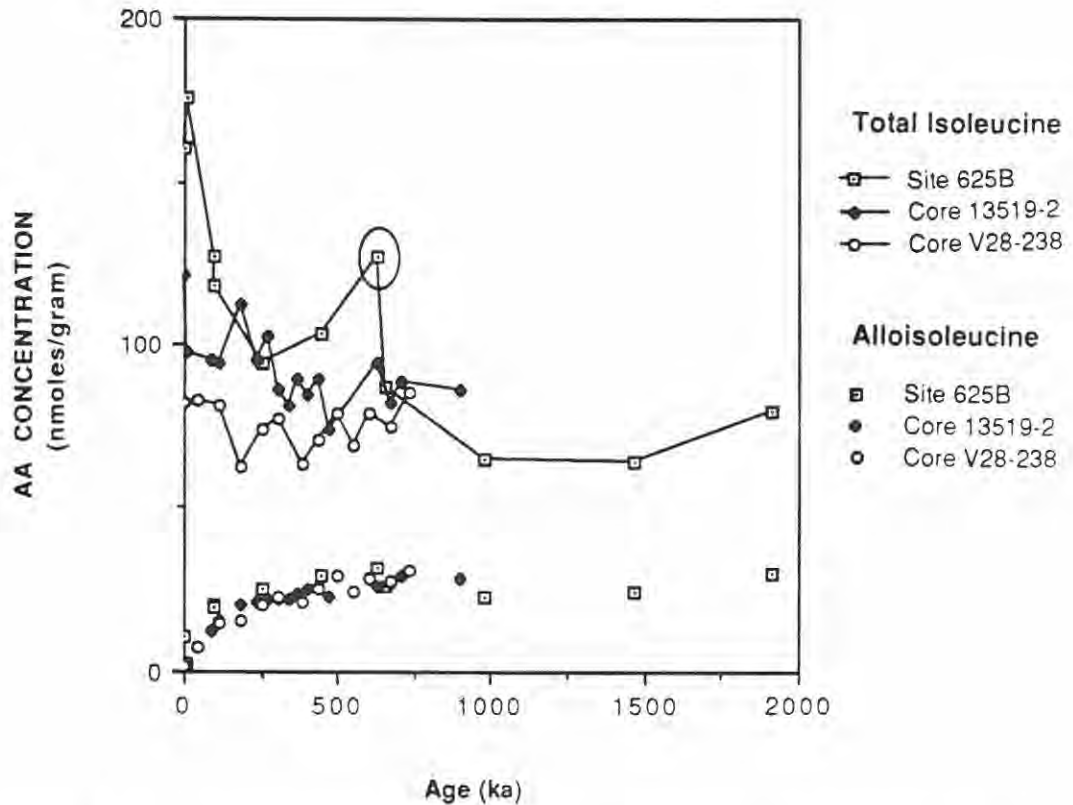


Figure 6.3: Alloisoleucine and total isoleucine (alloisoleucine + isoleucine) concentrations in samples of the *Globorotalia tumida-menardii* complex from Gulf of Mexico Site 625B, mid-Atlantic Core 13519-2 (from Mueller, 1984) and Pacific Core V28-238 (from King and Neville, 1977) plotted against age. Circled point represents sample from this study thought to have been contaminated with isoleucine during laboratory preparation procedures.

amino acids, the relative amino acid abundances at the three core-tops should reveal the relationships of dissolution that has occurred at the sediment-water-interface (syn-depositionally). Thus, syn-depositional dissolution appears to be greater in the Pacific, followed by the Atlantic, followed by the Gulf.

Post-Depositional Dissolution In All Three Sites

Recall the following relationships mentioned and graphed earlier in this chapter (Figure 6.2.a):

$$A/I)_{\text{Gulf}} < A/I)_{\text{Atlantic}} < A/I)_{\text{Pacific}}$$

Based on the data from the Atlantic and Pacific, Mueller (1984) attributed this to preferential leaching of free alloisoleucine in the outer layers of the carbonate structure, after the tests had been deposited. Presumably, this material would already have been removed if the tests were deposited in more corrosive waters.

Mueller (1984) reasoned that A/I ratios in tests deposited in more corrosive waters reflected epimerization in the interior, more stable and resistant polypeptides not removed by dissolution, thereby representing a relatively closed system, post-depositionally. Tests deposited in less corrosive waters, however, appeared to be more effected by post-depositional dissolution

processes, and reflected a more open system than those deposited in less-corrosive waters.

Another approach to examining this post-depositional leaching process may be to look at the rate of production and removal of alloisoleucine as a function of the amount of isoleucine present in each core. This, in turn, may be described by first-order sequential radioactive decay.

The following equations describe the growth of an unstable daughter (D) relative to the decay of a parent (P) in radioactive decay:

$$\frac{dD}{dt} = \lambda_1 P - \lambda_2 D \quad (\text{Equation 6.1})$$

where λ_1 = the decay constant for the parent, and λ_2 = the decay constant for the unstable daughter. If the amount of parent initially present = P_0 , and the amount of daughter initially present = 0, then the amount of daughter at any time, t , is described by:

$$D = \frac{\lambda_1}{\lambda_2 - \lambda_1} P_0 (e^{-\lambda_1 t} - e^{-\lambda_2 t}) \quad (\text{Equation 6.2})$$

Alloisoleucine accumulation may be described by first-order sequential decay by making some substitutions into equations 6.1 and 6.2 to obtain the following equations:

$$\frac{dA}{dt} = k_E I - k_L A \quad (\text{Equation 6.3})$$

$$A = \frac{k_E}{k_L - k_E} I_0 (e^{-k_E t} - e^{-k_L t}) \quad (\text{Equation 6.4})$$

where, A = alloisoleucine, I = isoleucine, k_E = the rate constant describing the accumulation of alloisoleucine due to the epimerization of isoleucine, k_L = the rate constant describing the loss of alloisoleucine presumably caused by diffusion of free alloisoleucine (in response to syn- and post-depositional dissolution) from the system, and I_0 = the amount of isoleucine present initially.

A closer look at the relationship between the rate constants and the amount of initial isoleucine present leads to a better understanding of post-depositional dissolution and how it varies in different ocean basins through time. Because the measured abundance of alloisoleucine is constant at any time, t , an inverse relationship must exist between

$$I_0 \text{ and } \left[\left(\frac{k_E}{k_L - k_E} \right) (e^{-k_E t} - e^{-k_L t}) \right].$$

And, if k_E is held constant, an inverse relationship must exist between

$$k_L \text{ and } \left[\left(\frac{k_E}{k_L - k_E} \right) (e^{-k_E t} - e^{-k_L t}) \right].$$

Thus, if k_E remains constant, I_0 and k_L will vary proportionally.

In other words, if initial amounts of isoleucine are high (corresponding to smaller amounts of syn-depositional dissolution), the rate of post-depositional removal will be high, as well. These relationships and those shown in Figures 6.2.a and 6.3 lead one to conclude that because the largest abundance of isoleucine is found in the Gulf of Mexico, the rate of post-depositional alloisoleucine loss must be highest there, as well, followed by the Atlantic, followed by the Pacific.

There are two assumptions necessary to support this logic. The first one is that the rate constant describing alloisoleucine accumulation does not vary between ocean basins. The temperature difference between the bottom waters of the three ocean basins used in this study are assumed to contribute to negligible differences in rates of alloisoleucine accumulation.

The second assumption is that the amount of isoleucine present at the top of the core reflects the amount that should be present at time = 0, and that none of the record is missing. A high precision radiocarbon date would help to determine how much of the record had been removed (by current winnowing, or during coring procedures, for example).

As was mentioned earlier, Mueller (1984) suggests that preservation (i.e., low carbonate dissolution) of the outer-most peptides results in relatively rapid rates of hydrolysis and subsequent leaching of extensively epimerized amino acids, post-depositionally. He finds less-corrosive waters in the Atlantic reflecting more "open" systems post-depositionally than in the Pacific. Comparisons of total isoleucine in the Gulf of Mexico and in the Atlantic are made to further illustrate that the Gulf is less-corrosive and reflects an even more "open" system post-depositionally than the Atlantic.

Figures 6.4.a-b present semilogarithmic plots of total isoleucine loss in Orbulina universa at Core 13519-2 and Site 625B, and total isoleucine loss in the Globorotalia tumida-menardii complex at Core 13519-2 and Site 625B, respectively. (It is important to realize that the time-scales for comparison of Orbulina universa and the Globorotalia tumida-menardii complex are not the same through Site 625B.)

Figure 6.4.a shows the initial loss of total isoleucine in Orbulina universa to be negligible. However, total isoleucine concentrations decrease at a relatively steady rate through the Pliocene, beginning at approximately 500 ka. (The data could also be interpreted as one linear trend decreasing at a steady rate with time.) The carbonate structure in tests of Orbulina universa

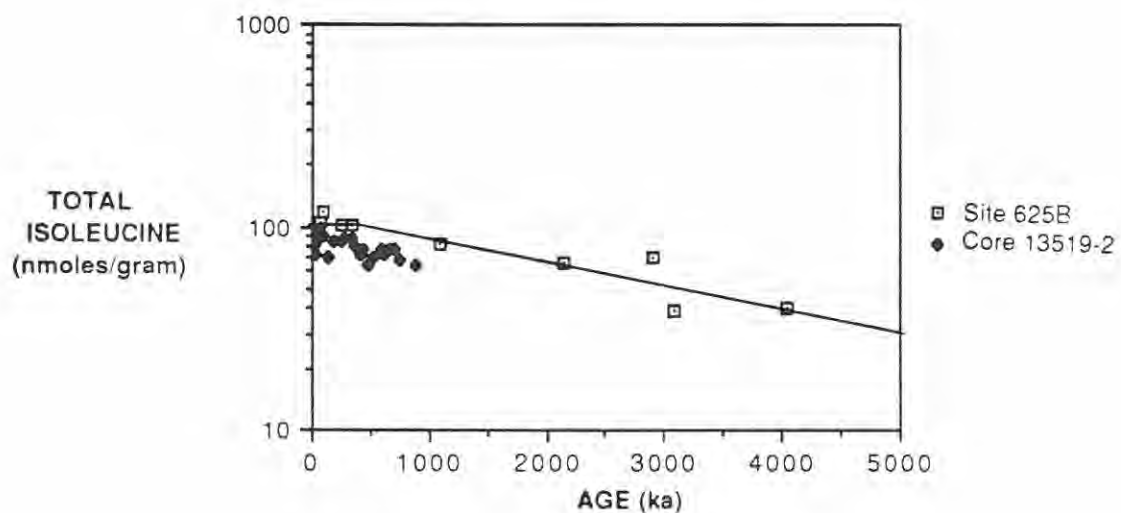


Figure 6.4.a: Total isoleucine (alloisoleucine + isoleucine) concentrations in samples of *Orbulina universa* from Gulf of Mexico Site 625B and mid-Atlantic Core 13519-2 (from Mueller, 1984) plotted against age on a semilogarithmic graph.

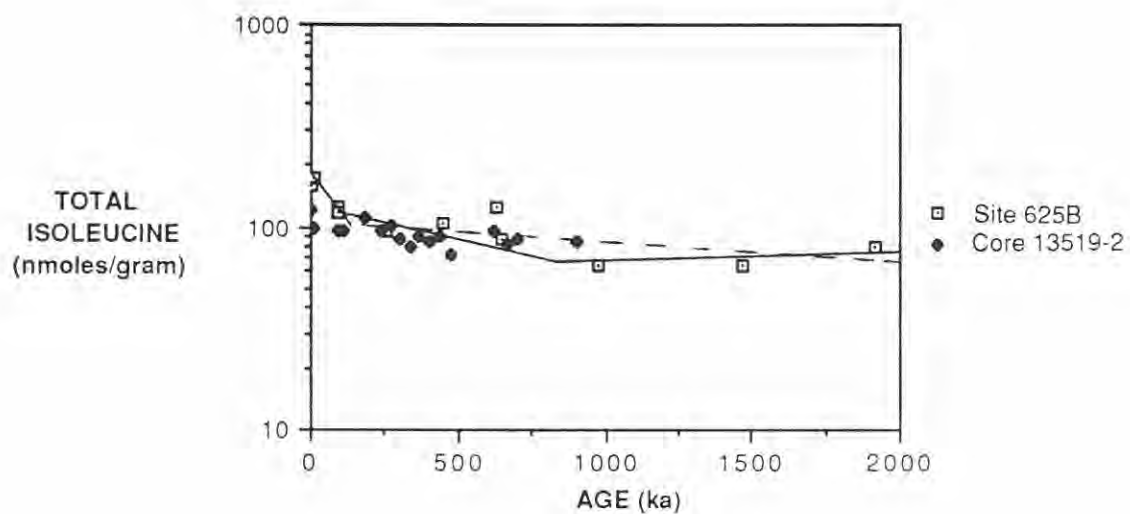


Figure 6.4.b: Total isoleucine (alloisoleucine + isoleucine) concentrations in samples of the *Globorotalia tumida-menardii* complex from Gulf of Mexico Site 625B and mid-Atlantic Core 13519-2 (from Mueller, 1984) plotted against age on a semilogarithmic graph.

represents an "open" system, where hydrolysis and subsequent removal of isoleucine are continuing post-depositional processes.

Figure 6.4.b shows the isoleucine loss in the Globorotalia tumida-menardii complex to be a little more difficult to interpret. The initial loss of isoleucine is extremely rapid in both cores. At approximately 175 ka, loss of isoleucine slows significantly, and at 750-1000 ka loss of isoleucine becomes negligible (note solid line in Figure 6.4.b); or, at approximately 200 ka, isoleucine loss slows, and proceeds at a steady, slow rate through the rest of the Pleistocene (note dashed line in Figure 6.4.b). The carbonate structure in tests of Globorotalia tumida-menardii represents a "closed" system, where hydrolysis and subsequent removal of isoleucine becomes insignificant after a certain amount of time.

The different patterns of post-depositional dissolution (and subsequent removal of amino acids) seen in the same ocean basin seem to reflect differences in morphologies of the two species examined (Mueller, 1984). Over the same period of time in the Gulf, amino acids in the fragile and spinose tests continue to be removed; whereas, the thicker and non-spinose species reach a threshold value, beyond which little or no amino acid material is removed.

Quantification of Dissolution Using Amino Acid Data

It is difficult to quantify objectively degrees of dissolution in foraminifera down a core. The reader is referred to Johnson (1988), who examines five micropaleontological parameters used to quantify the degree of dissolution in Site 625B. A systematic study of isoleucine loss may reveal the utility of this geochemical parameter as an objective quantifier of dissolution in foraminifera tests.

Site 625B

Preliminary paleontological work done on Site 625B by Martin et al. (1987), revealed negligible carbonate dissolution in the Pleistocene beyond the initial stage, based on the abundance of Globigerinoides ruber. A closer look at Site 625B showed possible evidence of minor dissolution at eight levels in the core (Johnson, 1988). The total isoleucine concentrations measured near these depths, however, showed no evidence of significant syn-depositional dissolution, and subsequent removal of amino acids.

Table 6.1 lists the depths at which Johnson (1988) found evidence for carbonate dissolution. Three species are listed from left to right in decreasing susceptibility to dissolution (Berger,

Table 6.1: Sub-bottom depths corresponding to samples thought to have undergone some dissolution (from Johnson, 1988), and depths corresponding to samples analyzed for total isoleucine concentrations.

Evidence of Dissolution Seen at the Following Depth (m) from Johnson (1988)	Depths (m) at Which the Following Species Were Analyzed		
	<i>Orbulina universa</i>	<i>Neoglobo- quadrina dutertrei</i>	<i>Globorotalia tumida- menardii</i>
6.5			
7.5			
21.5	22.5	22.5	22.5
25.0	28.5		
35.0			36.5
41.5		40.0	
50.5		50.0	50.0
			51.0
77.5	70.5		

1968), along with the depths at which they are analyzed for total isoleucine concentration. It is important to emphasize that none of the species was analyzed for amino acids at the exact depths Johnson (1988) sampled.

Figures 6.5.a-c show the total isoleucine concentration of the monospecific samples through the Pleistocene on a semilogarithmic plot. The boxed data points represent the isoleucine concentrations at approximately the same depths where partial dissolution occurred (Johnson, 1988).

The expected decrease in isoleucine concentrations at depths associated with possible syn-depositional dissolution are not seen. It is possible that the dissolution Johnson (1988) recognizes occurs post-depositionally, or simply that the sample came from a different depth reflecting different ocean-water chemistries.

If the expected decreases in alloisoleucine concentrations associated with post-depositional dissolution are not seen in the samples in question, the following may provide explanations for the observed dissolution by Johnson (1988): 1) the samples were analyzed for amino acid content at slightly different depths than those mentioned by Johnson (1988), and are not subjected to recognizable degrees of dissolution; or 2) the degree of dissolution,

Figures 6.5.a-6.5.c: Total isoleucine (alloisoleucine + isoleucine) concentrations in the three monospecific samples of Orbulina universa, Neogloboquadrina dutertrei, and the Globorotalia tumida-menardii complex, from Gulf of Mexico Site 625B plotted against age on a semilogarithmic graph. Boxed data points represent samples taken from ages approximating those recognized by Johnson (1988) to have undergone the most dissolution.

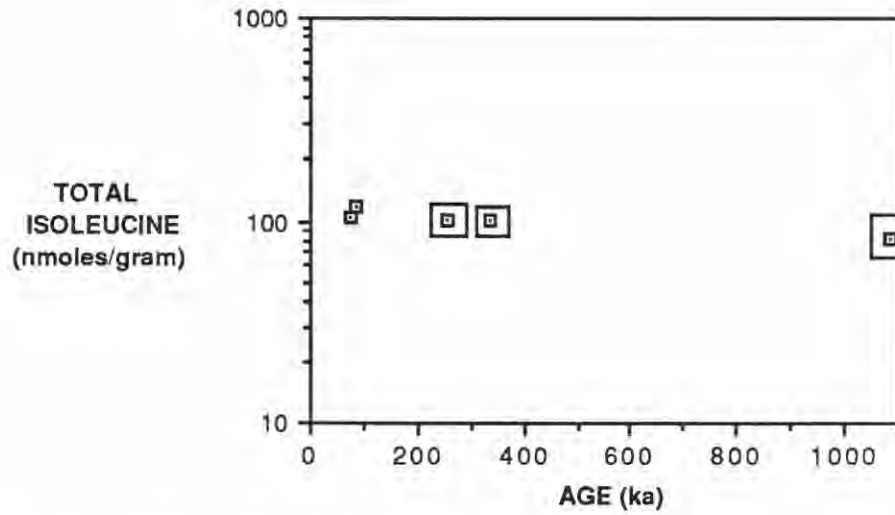


Figure 6.5.a: Total isoleucine (alloisoleucine + isoleucine) concentrations in samples of *Orbulina universa* from Gulf of Mexico Site 625B.

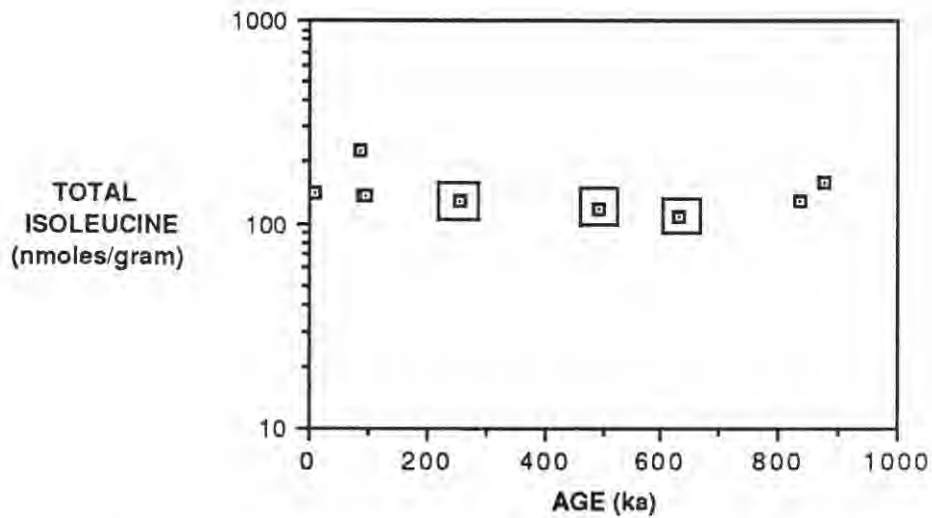


Figure 6.5.b: Total isoleucine (alloisoleucine + isoleucine) concentrations in samples of *Neogloboquadrina dutertrei* from Gulf of Mexico Site 625B.

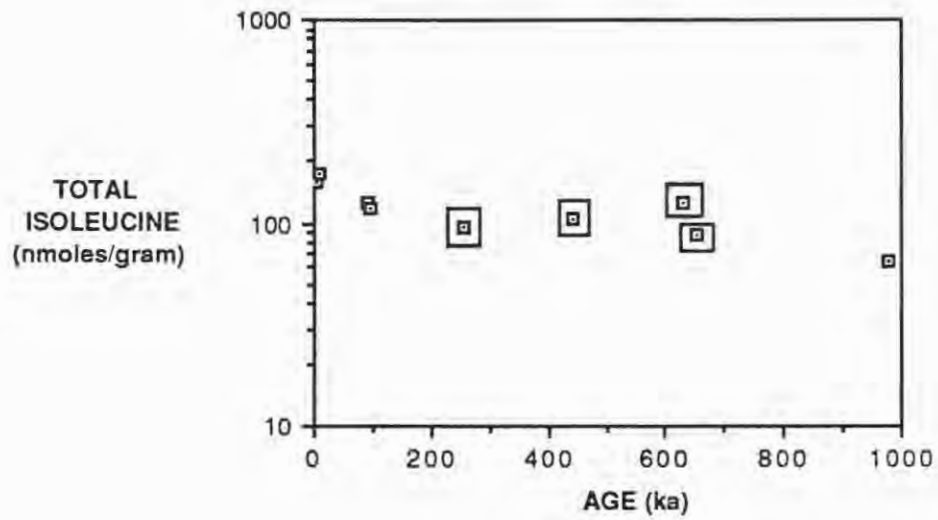


Figure 6.5.c: Total isoleucine (alloisoleucine + isoleucine) concentrations in samples of the *Globorotalia tumida-menardii* complex from Gulf of Mexico Site 625B.

and subsequent amount of amino acids lost are negligible, or are undetectable.

Core 13519-2

No micropaleontological study on dissolution is presently available for Core 13519-2. However, dissolution studies have been performed on Core V28-188, which is located at a similar water depth, and close to Core 13519-2 (Gardner, 1975). Gardner (1975) notices no significant dissolution in Core V28-188. Mueller (1984) uses these results to qualify his dissolution interpretations based on measured isoleucine concentrations down neighboring Core 13519-2.

Mueller (1984), however, finds anomalously low concentrations of isoleucine measured in Orbulina universa and the Globorotalia tumida-menardii complex during glacial stages 2, 6, and 12 down Core 13519-2. The circled points in Figures 6.6.a-b reveal these low values, and presumably represent a syn-depositional loss of isoleucine due to more corrosive glacial-stage water.

The decreased isoleucine abundances in Orbulina universa correlate to all three glacial stages aforementioned. The decreased isoleucine abundances in the Globorotalia tumida-

Figure 6.6.a-b: Total isoleucine (alloisoleucine + isoleucine) concentrations in the two monospecific samples Orbulina universa, and the Globorotalia tumida-menardii complex from mid-Atlantic Core 13519-2 plotted against age on a semilogarithmic graph. Circled points represent those samples thought to have undergone dissolution from glacial stages 2, 6, and 12.

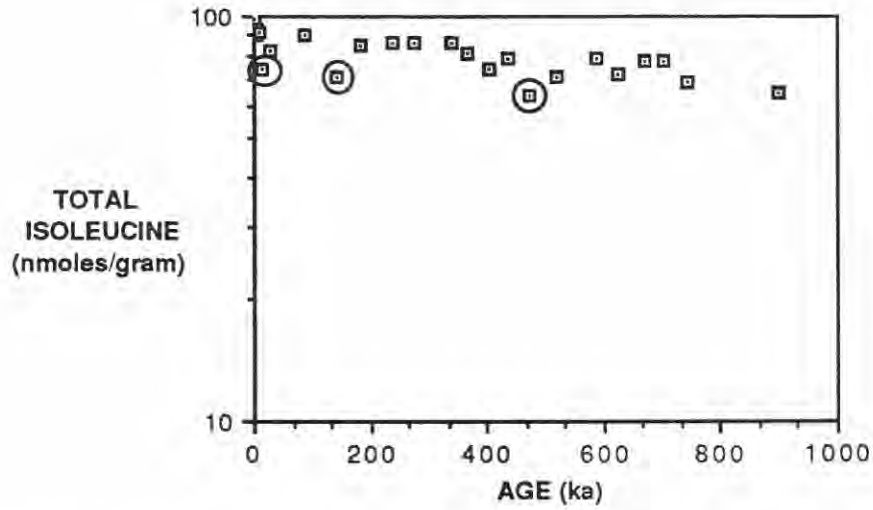


Figure 6.6.a: Total isoleucine (alloisoleucine + isoleucine) concentrations in samples of *Orbulina universa* from mid-Atlantic Core 13519-2.

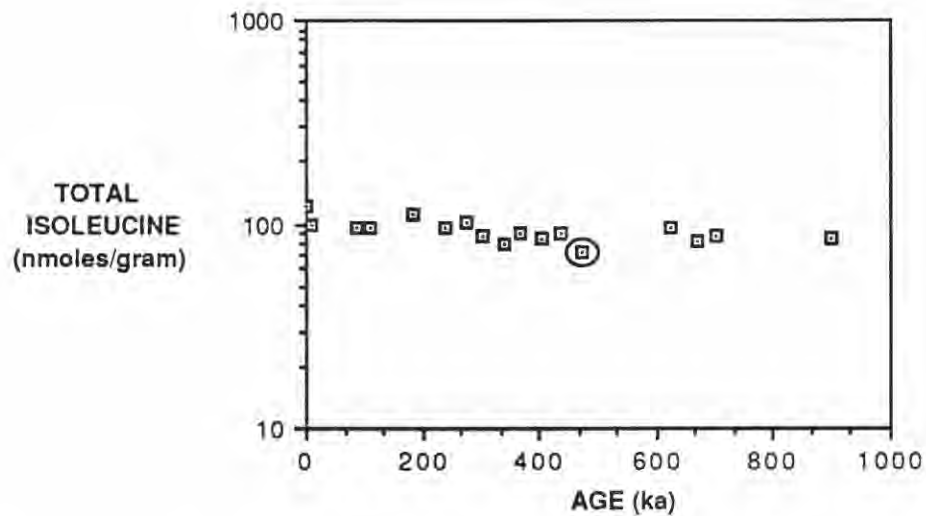


Figure 6.6.b: Total isoleucine (alloisoleucine + isoleucine) concentrations in samples of the *Globorotalia tumidamenardii* complex from mid-Atlantic Core 13519-2.

menardii complex only correlate to glacial stage 12. Because the latter species is more resistant to dissolution than the former (Berger, 1968), it may be that glacial stage 12 was more severe, or longer lasting than stages 2 and 6.

Because Quaternary climatic effects are only seen in the amino acid record preserved in the mid-Atlantic core, it appears that the deep Atlantic is more influenced than the Gulf of Mexico by global climatic change. It is expected that more extreme changes in salinity, ice cover, etc. occur in the Atlantic during the Quaternary and, consequently, result in more sensitive chemical effects in the deeper Atlantic (2862 m) than in the shallow Gulf of Mexico (980 m).

Constant Bottom Water Temperature?

One of the important assumptions in this study is that epimerization rates measured in the Gulf of Mexico have not been significantly affected by small bottom water temperature changes during the Pleistocene. This assumption is considered generally valid, because glacial "pulses" seen in the mid-Atlantic (Mueller, 1984) are not seen in the Gulf of Mexico, and the effects, if real, are quite small compared to normal analytical ranges of results.

It is important to recognize the increasing evidence

suggesting that during the Pleistocene the Atlantic was more sensitive to temperature changes than was the Pacific (Mueller, 1984, and references therein). Mueller (1984) proposes a fluctuation of 1.2 °C in bottom-water temperatures of the Atlantic during glacial stages of the Pleistocene. Inherent assumptions in his work are that bottom-water temperatures in the Pacific remained constant through the Pleistocene, and that rates of epimerization are the same in both ocean basins.

Intergeneric Comparisons

Intergeneric comparisons of A/I ratios are useful for evaluating the quality of amino acid data. Figure 6.7 is a plot of A/I ratios in Neogloboquadrina dutertrei against A/I ratios in Orbulina universa. A linear regression was fit to the data, yielding an R² value of 0.992. This equation provides a quantitative means of comparing A/I ratios between the species, and becomes useful when multiple genera are not available for analyses at a site.

Amino Acids in the Clay Fraction

The highly porous, thin, and fragile structure of the Orbulina universa test would seem to make it an efficient repository for clay particles. Indeed, it was noted during the picking procedure, that many of the Orbulina universa tests had a dirty appearance, and contained sediment. (Tests of the other

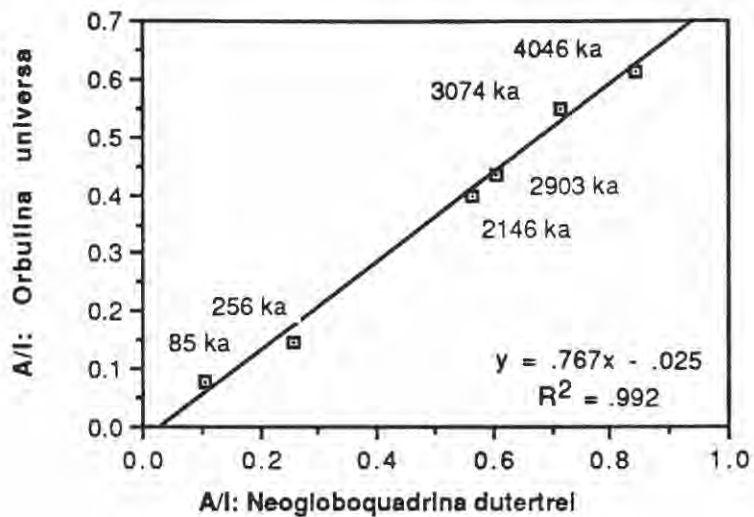


Figure 6.7: A/I ratios in samples of *Neogloboquadrina dutertrei* and *Orbulina universa* from Core 625B plotted against each other. Each point represents A/I ratios measured in samples of the same age. This type of plot reveals inter-generic epimerization relationships. A linear regression is best-fit to the data.

species analyzed are not as porous, and are structurally stronger than those of Orbulina universa, and were not observed to contain any sediment.)

In turn, the hydrolyzate residues from the mixed species assemblage, and the Orbulina universa samples were noticeably "dirtier" than those of the other monospecific samples. Presumably, this is due to a relatively high terrigenous sediment content in both sets of samples.

Total epimerization results yield similar A/I ratios between the mixed foraminifera samples and the cleaner species, Globorotalia tumida-menardii. Because parallel trends are not seen between the mixed foraminifera samples and the Orbulina universa samples, the amount of non-carbonate clay present in the Orbulina universa samples from 625B does not seem to significantly alter the trend of isoleucine epimerization with time in this species.

CHAPTER 7

CONCLUSIONS

Cleaning Methods

Several cleaning methods of foraminiferal tests for amino acid analysis were examined in this study. Epimerization results from tests of Globigerinoides ruber, Orbulina universa, Neogloboquadrina dutertrei, and the Globorotalia tumida-menardii complex reveal the most effective method entails a primary soak of the tests in hydrogen peroxide for 1 hour, followed by a secondary soak in concentrated ammonium hydroxide for 36 hours.

This combined cleaning method appears to remove organic matter with low A/I ratios from the foraminiferal tests. It is possible that this contaminant originates during the coring procedures, or the sample preparation. The contaminant may also come from humic acids bound to the clay fraction of the sediment. A systematic study of the amino acid content of the clay fraction

surrounding and within the foraminiferal tests would help to quantify the importance of the latter hypothesis for the origin of the contamination. Analyses of the free and total fraction of isoleucine in interlaboratory comparison powders cleaned with ammonium hydroxide would further aid in understanding the combined cleaning method proposed in this study.

Carbonate Dissolution

Two types of amino acid loss (presumably due mainly to leaching and removal of material during dissolution) are recognized in the epimerization data from foraminifera tests. A syn-depositional dissolution process is recognized by examining total isoleucine concentrations in foraminifera species. Low total isoleucine abundances imply high degrees of syn-depositional dissolution. A post-depositional dissolution process may be recognized by examining alloisoleucine abundances in foraminifera species. High rates of removal of alloisoleucine imply high degrees of post-depositional dissolution.

The results of this study compared to the work of King and Neville (1977) and Mueller (1984) reveal an inverse relationship between syn-depositional and post-depositional processes. (Inherent assumptions are that rates of epimerization are constant in the deep-sea sites in question.) The lowest rates

of syn-depositional dissolution occur in the Gulf of Mexico, followed by the mid-Atlantic, followed by the equatorial Pacific. The highest rates of post-depositional dissolution occur in the Gulf of Mexico, followed by the mid-Atlantic, followed by the equatorial Pacific.

The observed inverse relationship between the two dissolution processes is explained by the timing of the removal of the outer and more easily dissolved layers of the carbonate tests. If the outer layers are not removed prior to burial (syn-depositionally), they will be removed during the early stages of diagenesis (post-depositionally). Conversely, if they are removed syn-depositionally, post-depositional dissolution of the more resistant layers of the test will be minimized. A comparison of dissolution in spinose versus non-spinose species may help to explain the degree to which certain test morphologies are preferentially preserved in the geologic record.

Changes in ocean-water corrosivities (resulting in different degrees of dissolution) may be quantified by examining isoleucine concentrations accompanying known climatic fluctuations. After initial examination of epimerization results from Site 625B, it appears that there is no detectable change in ocean-water corrosivity during the Pleistocene, or that the sampling density for this part of the study was too coarse to

conclude anything. Further study is needed to determine if varying isoleucine abundances are, in fact, reliable indicators of climatic fluctuations. This may eventually lead to accurate predictions of ocean water chemistries in the geologic past.

The Record Preserved at Site 625B

At the onset of this study, it was thought that the record preserved in Hole 625B represented a complete section through the upper Miocene and that internally consistent down-core trends could be successfully examined. Any variations in trends would be due to contamination during coring or laboratory procedures, or due to geochemical effects in the core.

Recent evidence indicates that an unconformity representing a complete cycle of the $\delta^{18}\text{O}$ record exists in Site 625B at approximately 67 m (R.E. Martin, personal communication, 1989). Presumably, no more than 1 m of the sedimentary record is missing. (This interpretation of the data should be regarded with some degree of caution, however, because of complications associated with the use and meaning of the $\delta^{18}\text{O}$ record in deep-sea cores.)

Ideally, an unconformity in a deep-sea curve would be evidenced by higher A/I ratios than expected, or an offset in the A/I curve. Unfortunately, the resolution of the present

aminostratigraphy of Site 625B is too low to detect the presence or absence of this unconformity. A detailed analysis of foraminiferal tests taken every 10-20 cm from 65 m to 70 m sub-bottom depth would help to verify the utility of amino acid analysis as a tool for recognizing unconformities in a hole. This is a highly recommended direction for future research in this field.

It is important to realize that the unconformity in the $\delta^{18}\text{O}$ record at 67 m, and the highly variable A/I ratios in Globigerinoides ruber (initially attributed to poor isolation and cleaning of the foraminiferal tests) below 70.5 m, and the indistinguishable paleomagnetic record below 67 m may not be coincidental. The possibility that ODP Site 625B has been altered in the lower two-thirds of the core should not be excluded from any interpretations of data obtained from the site.

However, if pre-Brunhes alteration has occurred, it is not seen in the aminostratigraphic record of the well-cleaned and more robust foraminiferal species. If Site 625B proves to be a complete section with some minor geochemical alteration below 67 m it is hoped that the aminostratigraphic record of the well-cleaned and hearty species will be the reference section for future aminostratigraphic studies in the Gulf of Mexico.

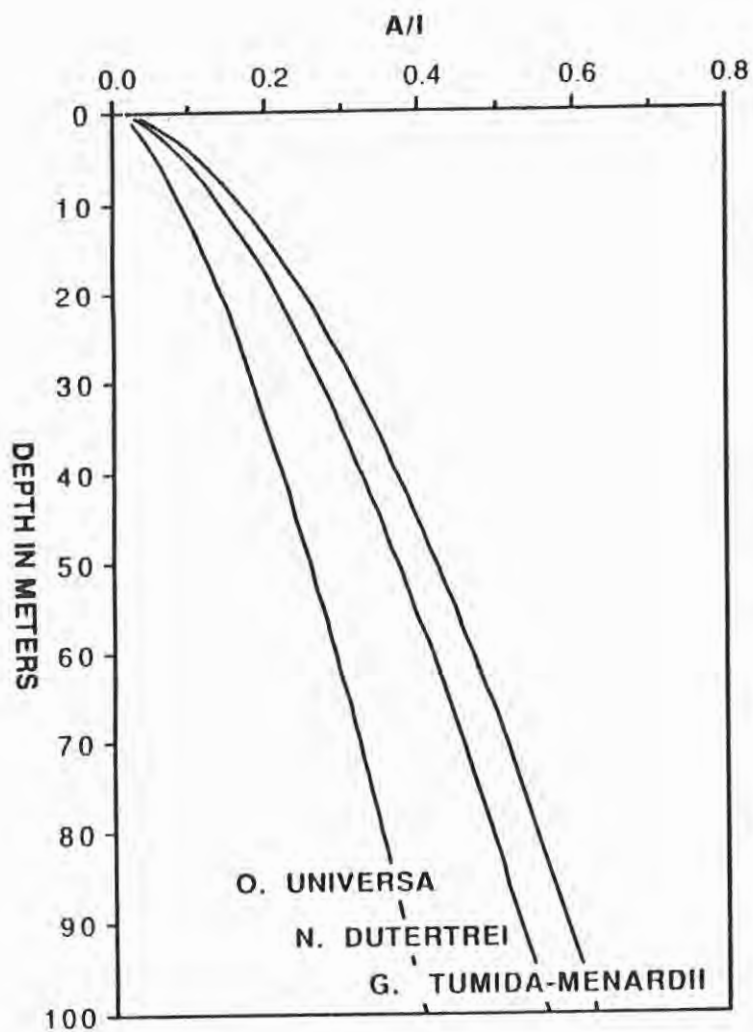
Aminostratigraphy of Site 625B

A composite stratigraphy of the Pleistocene section of Site 625B is presented in Figure 7.1. Included in this diagram are the aminostratigraphy determined in this study, the biostratigraphic zonation as determined by Johnson (1988), the magnetostratigraphy as determined by Clement (personal communication to R.E. Martin, 1986), and important nannofossil datums as determined by Gartner and Huang (1986) and Gartner (personal communication to G.W. Johnson, 1988).

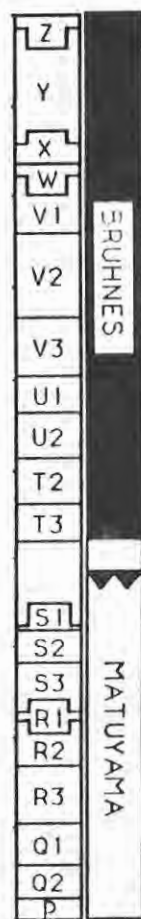
The aminostratigraphic record demonstrates a marked decrease in apparent rates of epimerization in all three species with increased time. Higher apparent rates of epimerization are found in the non-spinose foraminifera species Neoglobobquadrina dutertrei, and the Globorotalia tumida-menardii complex. Lower apparent rates of epimerization are found in the spinose foraminifera species Orbulina universa. Thus, non-spinose species are more useful for resolving the aminostratigraphy of a site over younger sediments, and spinose species are more useful for resolving the aminostratigraphy of a site over older sediments.

A 5% analytical uncertainty in measured A/I ratios in younger sediments results in low variabilities in the

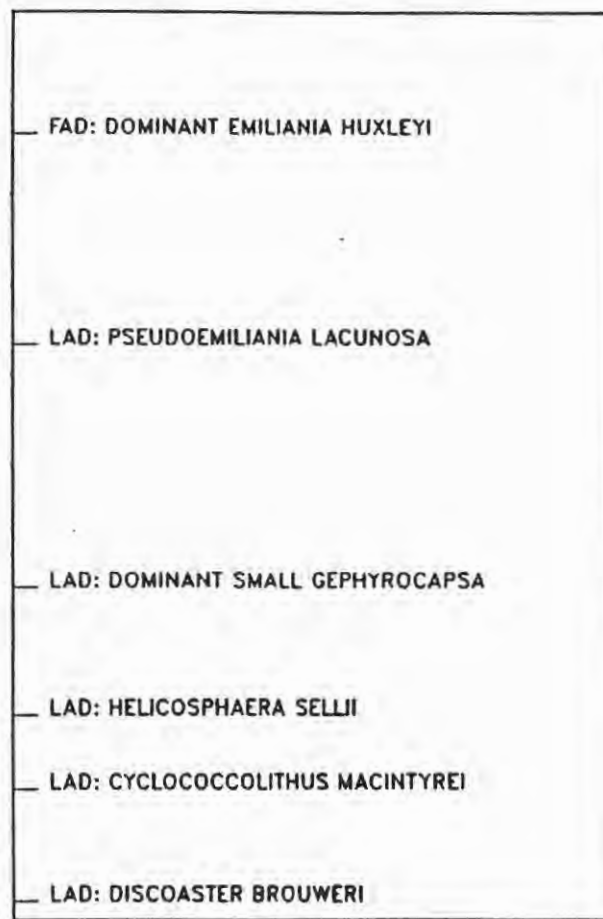
Figure 7.1: Composite stratigraphy of ODP Site 625B (modified from Johnson, 1988). Aminostratigraphy (A) from this study, biostratigraphic zonation (B) from Johnson (1988), magnetostratigraphy (C) from Brad Clement (personal communication to R.E. Martin, 1986), and nannofossil data (D) from Gartner and Huang (1986) and Gartner (personal communication to G.W. Johnson, 1988). The logarithmic equations for the aminostratigraphic curves are presented in Figures 5.1, 5.2, and 5.3.



A



B C



D

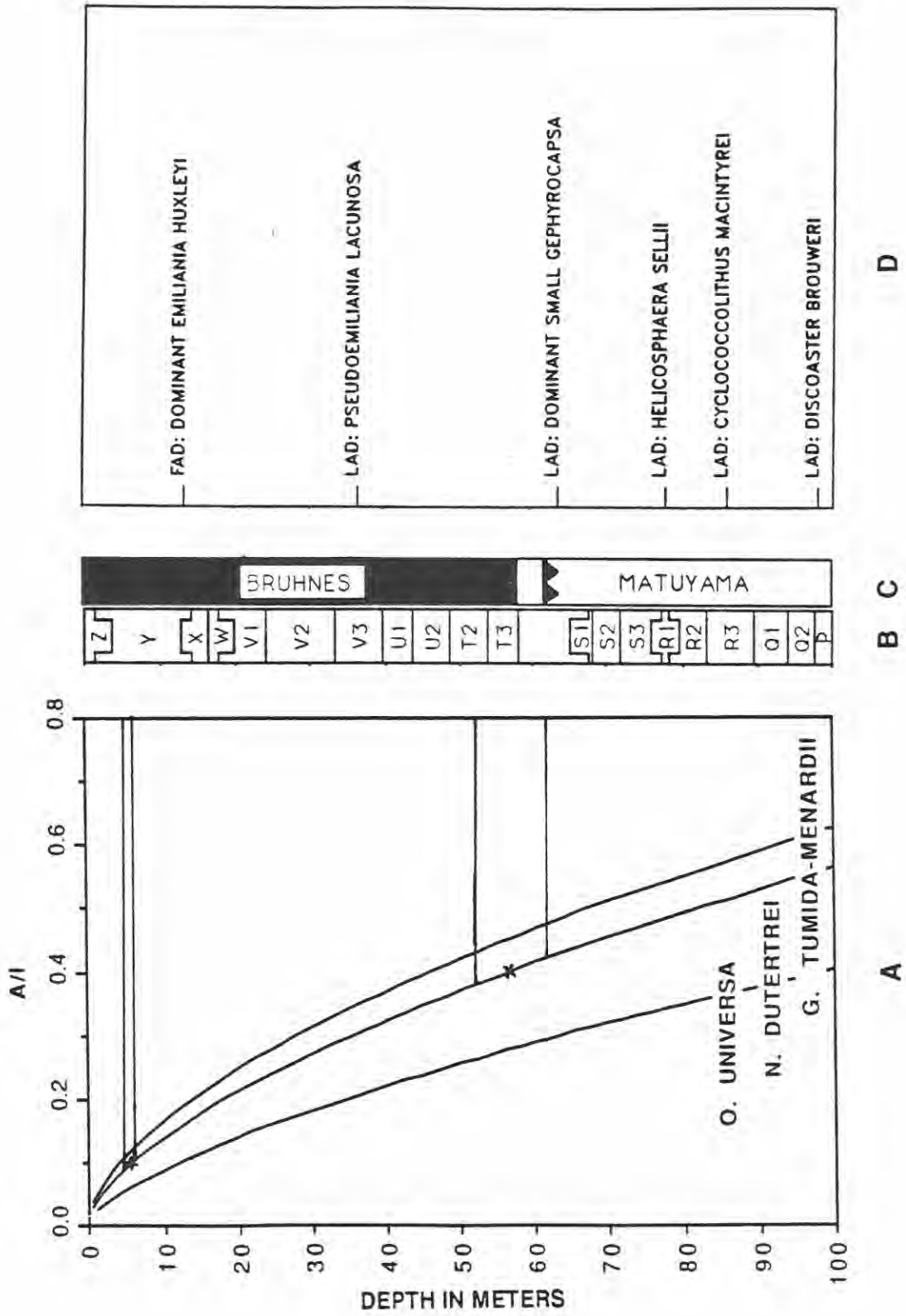
corresponding age estimates. This same uncertainty in older sediments, however, results in larger variabilities in the corresponding age estimates (Figure 7.2). Thus, with increasing time, A/I ratios lose precision as a stratigraphic tool.

Recall that epimeric equilibrium is not reached until the A/I ratio approximates 1.4. At the base of Site 625B (presumably, the upper Miocene), the highest ratios measured in samples of Neogloboquadrina dutertrei approximate 0.80. Potentially, because epimeric equilibrium has not yet been reached, A/I ratios may be used to date sediments far back into the Miocene in Site 625B.

The stratigraphic and relative age-dating potential of amino acid racemization in deep-sea sediments is best illustrated by examining the measured A/I ratios of several genera. For example, a sample has A/I ratios of Orbulina universa, Neogloboquadrina dutertrei and the Globorotalia tumida-menardii complex that are 0.19, 0.28 and 0.32, respectively. All of these ratios plot at approximately the same depth in the core, and clearly represent the same age (Figure 7.3.a).

However, a sample whose A/I ratios are 0.15, 0.28 and 0.45 plot at very different depths in the core (Figure 7.3.b). These data either do not represent the same age, indicate contamination

Figure 7.2: Composite stratigraphy of ODP Site 625B (modified from Johnson, 1988), including variabilities in predicted ages associated with a 5% analytical error in measured A/I ratios. It is important to note the increased variability of ages in the older samples. Aminostratigraphy (A) from this study, biostratigraphic zonation (B) from Johnson (1988), magnetostratigraphy (C) from Brad Clement (personal communication to R.E. Martin, 1986), and nannofossil data (D) from Gartner and Huang (1986) and Gartner (personal communication to G.W. Johnson, 1988). The logarithmic equations for the aminostratigraphic curves are found in Figures 5.1, 5.2, and 5.3.



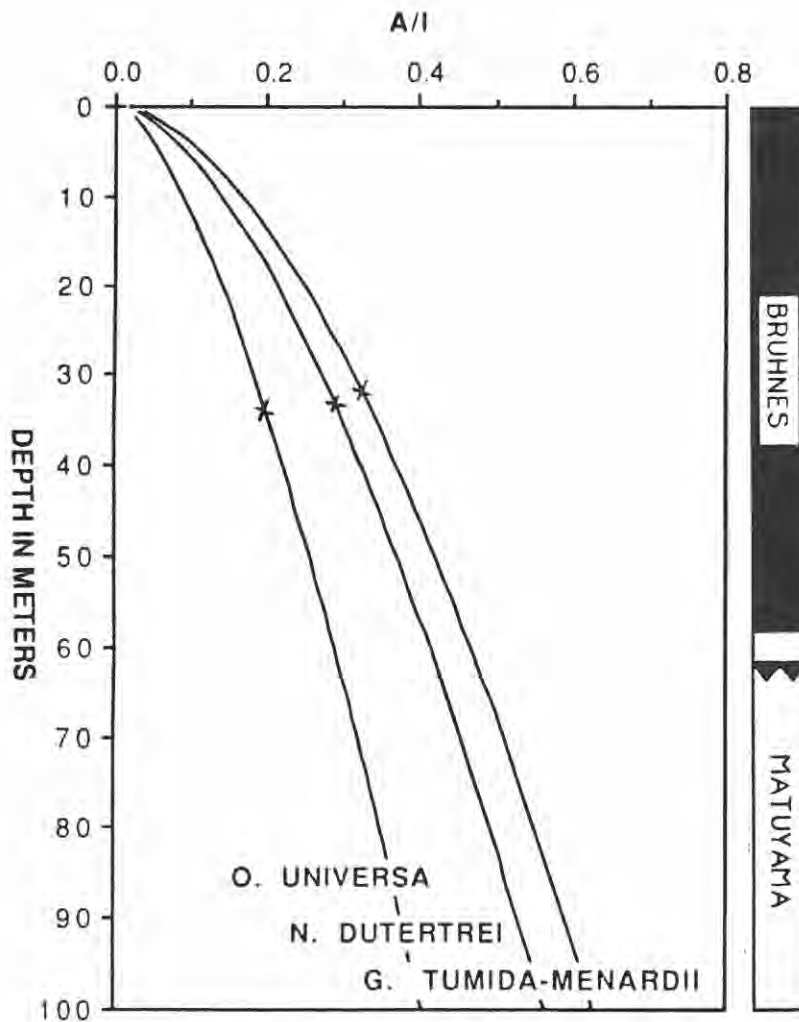


Figure 7.3.a: Concurrent A/I ratios of three species (where *Orbulina universa* = 0.19, *Neogloboquadrina dutertrei* = 0.28, and the *Globorotalia tumida-menardii* complex = 0.32) plotted on the epimerization curves predetermined for ODP Site 625B. These ratios are found at approximately the same depth in the core and represent the same age.

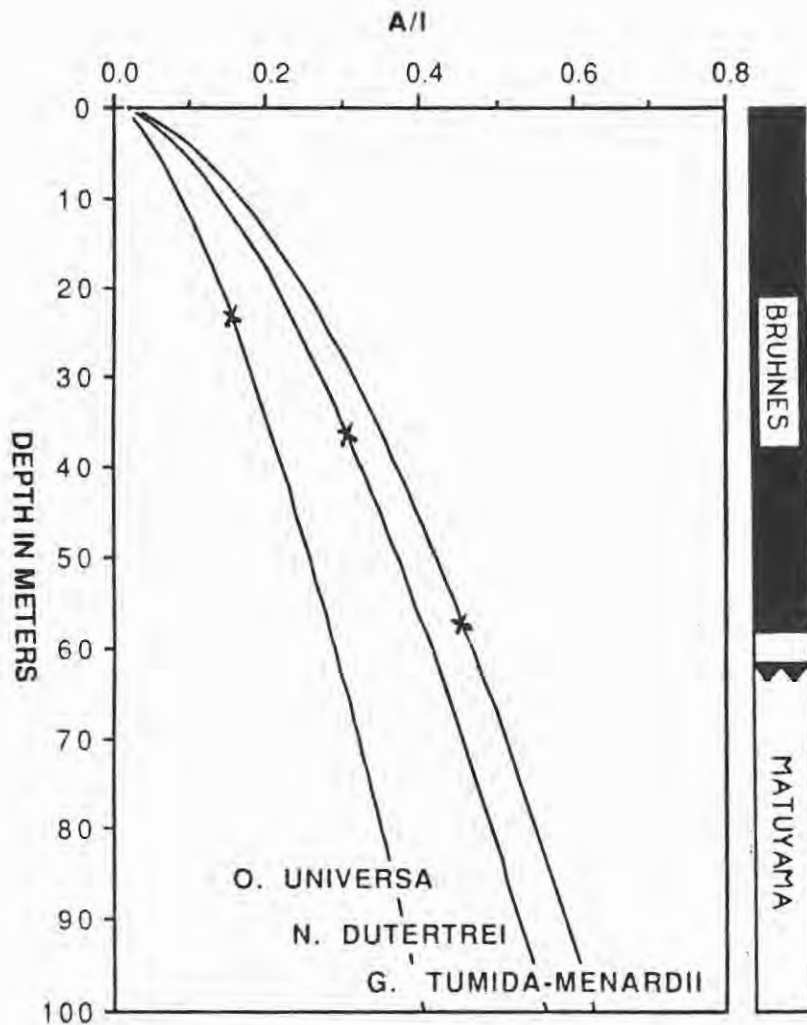


Figure 7.3.b: Non-concurrent A/I ratios of three species (where *Orbulina universa* = 0.15, *Neogloboquadrina dutertrei* = 0.28, and the *Globorotalia tumida-menardii* complex = 0.45) plotted on the epimerization curves predetermined for ODP Site 625B. These ratios are found at different depths in the core, and do not represent the same age.

or indicate reworking of some of the species in the sample. In any case, the data should be rejected and no age should be assigned to the sample.

Proposed Taxonomic Study

It has been shown that different species of foraminifera have diagnostic amino acid compositions. However, due to the time constraints associated with this project, it was not possible to perform an extensive statistical analysis of the amino acids as they relate to taxonomy. It is hoped that future examination of the data presented in this thesis will reveal interesting taxonomic trends with time in certain species.

REFERENCES

- Bada, J. L., 1985, Racemization of amino acids, *in* Garret, G. C., ed., *Chemistry and Biochemistry of the amino acids*: London, Chapman and Hall, p. 399-414.
- Bada, J. L. and Man, E. H., 1980, Amino acid diagenesis in Deep Sea Drilling Project cores: kinetics and mechanisms of some reactions and their applications in geochronology and in paleotemperature and heat flow determinations: *Earth Science Reviews*, v. 16, p. 21-55.
- Bada, J. L. and Schroeder, R. A., 1972, Racemization of isoleucine in calcareous marine sediments: kinetics and mechanism: *Earth and Planetary Science Letters*, v. 15, p. 1-11.
- Bada, J. L., Luyendyk, B. P., and Maynard, J. B., 1970, Marine sediments: dating by the racemization of amino acids: *Science*, v. 170, p. 730-732.
- Bé, A. W. H., 1977, An ecological, zoogeographic and taxonomic review of recent planktonic foraminifera, *in* Ramsay, A. T. S., ed., *Oceanic micropaleontology*: New York, Academic Press, p. 1-100.
- Berger, W.H., 1968, Planktonic foraminifera: selective solution and paleoclimatic interpretation: *Deep Sea Research*, v. 15, p. 31-43.

- Berggren, W. A., Kent, D. V., and Van Couvering, J. A., 1985, The Neogene: Part 2, Neogene geochronology and chronostratigraphy, in Snelling, N. J., ed., The chronology of the geologic record: Geological Society of America Memoir No. 10, p. 211-260.
- Ericson, D. B., and Wollin, G., 1968, Pleistocene climates and chronology in deep sea sediments: *Science*, v. 162, p. 1227-1234.
- Gardner, J.V., 1975, Late Pleistocene carbonate dissolution cycles in the eastern equatorial Atlantic: Cushman Foundation Foraminiferal Research, Special Publication No. 13, p. 129-141.
- Gartner, S., and Huang, T.C., 1986, Pliocene-Pleistocene biochronology, and climate and sedimentary cycles of the northern Gulf of Mexico: Geological Society of America 99th Annual Meeting and Exposition, Abstracts with Programs, p. 143.
- Hare, P. E., 1962, The amino acid composition of the organic matrix of some west coast species of Mytilus: Unpublished Ph.D. Thesis, California Inst. Tech., 109 p.
- Hare, P. E., 1963, Amino acids in the proteins from aragonite and calcite in the shells of Mytilus californianus: *Science*, v. 139, p. 216-217.
- Hare, P. E., and Hoering, T. C., 1973, Separation of amino acid optical isomers by gas chromatography: Carnegie Institution of Washington Yearbook, v. 72, p. 690-694.
- Hare, P. E., and Mitterer, R. M., 1967, Nonprotein amino acids in fossil shells: Carnegie Institution of Washington Yearbook, v. 65, p. 362-364.

- Hare, P. E., and Mitterer, R. M., 1969, Laboratory simulation of amino acid diagenesis in fossils: *Carnegie Institution of Washington Yearbook*, v. 67, p. 205-208.
- Hare, P. E., Hoering, T. C., and King, K. Jr., eds., 1980, *Biogeochemistry of amino acids*: New York, John Wiley, Inc., 558 p.
- Hare, P. E., St. John, P. A., and Engel, M. H., 1985, Ion exchange separation of amino acids, *in* Garrett, G. C., ed., *Chemistry and biochemistry of amino acids*: London, Chapman and Hall, p. 415-425.
- Hearty, P. J., Miller, G. H., Sterns, C. E., and Szabo, B. J., 1986, Aminostratigraphy of Quaternary shorelines in the Mediterranean Basin: *Geological Society America Bulletin*, v. 97, p. 850-858.
- Johnson, G. W., 1988, Pleistocene planktonic foraminiferal biostratigraphy and paleoecology: Northeast Gulf of Mexico: Unpublished M.S. Thesis, University of Delaware, Newark, DE, 252 p.
- Katz, B. J., and Man, E. H., 1980, The effects and implications of ultrasonic cleaning on the amino acid geochemistry of foraminifera, *in* Hare, P. E., Hoering, T. C., and King, K. Jr., eds., *Biogeochemistry of amino acids*: New York, John Wiley, Inc., p. 215-222.
- Katz, B. J., Harrison, C. G. A., and Man, E. H., 1979, The effects of the geothermal gradient on amino acid racemization: *Earth and Planetary Science Letters*, v. 44, p. 279-286.
- Kennedy, G. L., LaJoie, K. R., and Wehmiller, J. F., 1982, Aminostratigraphy and faunal correlations of late Quaternary marine terraces, Pacific coast USA: *Nature*, v. 299, p. 545-547.

- Kennett, J. P., and Srinivasan, M. S., 1983, Neogene planktonic foraminifera: Stroudsburg, Pennsylvania, Hutchinson Ross Publishing Company, 265 p.
- King, K. Jr., 1980, Application of amino acid biogeochemistry for marine sediments, *in* Hare, P. E., Hoering, T. C., and King, K. Jr., eds., Biogeochemistry of amino acids: New York, John Wiley, Inc., p. 377-392.
- King, K. Jr., and Hare, P. E., 1972, Species effects in the epimerization of L-isoleucine in fossil planktonic foraminifera: Carnegie Institution of Washington Yearbook, v. 71, p. 596-598.
- King, K. Jr., and Hare, P. E., 1972a, Amino acid composition of planktonic foraminifera: a paleobiochemical approach to evolution: Science, v. 175, p. 1461-1463.
- King, K. Jr., and Hare, P. E., 1972b, Amino acid composition of the test as a taxonomic character for living and fossil planktonic foraminifera: Micropaleontology, v. 18, p. 285-293.
- King, K. Jr., and Neville, C., 1977, Isoleucine epimerization for dating marine sediments: importance of analyzing monospecific foraminiferal samples: Science, v. 195, p. 1333-1335.
- Kriausakul, N., and Mitterer, R. M., 1978, Isoleucine epimerization in peptides and proteins: kinetic factors and applications to fossil proteins: Science, v. 201, p. 1011-1014.
- Kvenvolden, K. A., Peterson E., and Brown, F. S., 1970, Racemization of amino acids in sediments from Saanich Inlet, British Columbia: Science, v. 169, p. 1079.

- Kvenvolden, K. A., Peterson, E., Wehmiller, J., and Hare, P. E., 1973, Racemization of amino acids in marine sediments determined by gas chromatography: *Geochimica et Cosmochimica Acta*, v. 37, p. 2215-2225.
- Macko, S. A., and Aksu, A. E., 1986, Amino acid epimerization in planktonic foraminifera suggests slow sedimentation rates for Alpha Ridge, Arctic Ocean: *Nature*, v. 322, p. 730-733.
- Martin, R.E., Johnson, G.W., and Spatz, B., 1987, Plio- Pleistocene planktonic foraminifera biostratigraphy, paleoceanography, and sediment accumulation rates, northeast Gulf of Mexico: *American Association of Petroleum Geologists Bulletin*, v. 71, p. 590.
- Masters, P. M., and Bada, J. L., 1977, Racemization of isoleucine in fossil molluscs from Indian middens and interglacial terraces in southern California: *Earth and Planetary Science Letters*, v. 37, p. 173-183.
- McCoy, W. D., 1987, The precision of amino acid geochronology and paleothermometry: *Quaternary Science Reviews*, v. 6, p. 43-54.
- Miller, B.B., McCoy, W.D., and Bleuer, N.K., 1987, Stratigraphic potential of amino acid ratios in Pleistocene terrestrial gastropods: an example from west-central Indiana, U.S.A.: *Boreas*, v. 16, p.133-138.
- Miller, G.H., 1985, Aminostratigraphy of Baffin Island shell-bearing deposits, *in* Andrews, J.T., ed., *Quaternary environments: Baffin Island, Baffin Bay and West Greenland, United Kingdom*, George Allen and Unwin, p. 394-427.

- Miller, G.H., and Hare, P.E., 1980, Amino acid geochronology: integrity of the carbonate matrix and potential of molluscan fossils, *in* Hare, P. E., Hoering, T. C., and King, K. Jr., eds., *Biogeochemistry of amino acids*: New York, John Wiley, Inc., p. 414-443.
- Miller, G.H., and Mangerud, J., 1985, Aminostratigraphy of European marine interglacial deposits: *Quaternary Science Reviews*, v. 4, p. 215-278.
- Miller, G.H., Jull, A.J.T., Linick, T., Sutherland, D., Sejrup, H.P., Brigham, J.K., Bowen, D.Q., Mangerud, J., 1987, Racemization-derived late Devensian temperature reduction in Scotland: *Nature*, v. 326.
- Miller, G.H., Sejrup, H.P., Mangerud, J., and Anderson, B., 1983, Amino acid ratios in Quaternary molluscs and foraminifera from western Norway: correlation, geochronology and paleotemperature estimates: *Boreas*, v. 12, p. 107-124.
- Miller, G.H., Wendorf, F., Ernst, R., Schild, R., Close, A.E., Friedman, I., Schwarcz, H.P., 1989, Dating lacustrine episodes in the Eastern Sahara by the epimerization of isoleucine in ostrich eggshells: *in press*.
- Mitchum, R.M., Jr., 1978, Seismic stratigraphic investigation of West Florida Slope, Gulf of Mexico, *in* Bouma, A.H., Moore, G.T., and Coleman, J.M., eds., *Framework, facies and oil-trapping characteristics of the upper continental margin*: American Association of Petroleum Geologists Studies in Geology, v. 7, p. 193-223.
- Mitterer, R.M., and Kriaušakul, N., 1984, Comparison of rates and degrees of isoleucine epimerization in dipeptides and tripeptides: *Organic Geochemistry*, v. 7, p. 91-98.

- Mueller, P.J., 1984, Isoleucine epimerization in Quaternary planktonic foraminifera: effects of diagenetic hydrolysis and leaching, and Atlantic-Pacific intercore correlations: *Meteor Forsch.-Ergebnisse, Reihe C.*, No. 38, p. 25-47.
- Neff, E.D., 1985, Pre-late Pleistocene paleoclimatology and planktonic foraminiferal biostratigraphy of the northeast Gulf of Mexico: M.S. Thesis, University of South Carolina, Columbia, SC, 123 p.
- Nowlin, W.D., 1971, Water masses and general circulation of the Gulf of Mexico: *Oceanology International*, v. , p. 28-33.
- Parker, F.L., 1962, Planktonic foraminiferal species in Pacific sediments: *Micropaleontology*, v. 8, p. 219-254.
- Rabinowitz, P.D., Garrison, L.E., Merrell, W.J., and Kidd, R.B., 1985, Ocean Drilling Program Leg 100 report: unpublished Hole summary, 87 p.
- Schroeder, R.A., 1975, Absences of β -alanine and γ -aminobutyric acid in cleaned foraminiferal shells: implications for use as a chemical criterion to indicate removal of non-indigenous amino acid contaminants: *Earth and Planetary Science Letters*, v. 25, p. 274-278.
- Schroeder, R.A., and Bada, J.L., 1976, A review of the geochemical applications of the amino acid racemization reaction: *Earth Science Reviews*, v. 12, p. 347-391.
- Sejrup, H.P., Rokeongen, K., and Miller, G.H., 1984a, Isoleucine epimerization in Quaternary benthonic foraminifera from the Norwegian continental shelf: a pilot study: *Marine Geology*, v. 56, p. 227-239.

- Sejrup, H.P., Miller, G.H., Brigham-Grette, J., Lovlie, R., and Hopkins, D., 1984b, Amino acid epimerization implies rapid sedimentation rates in Arctic Ocean cores: *Nature*, v. 310, p. 772-775.
- Shackleton, N.J., and Opdyke, N.D., 1973, Oxygen isotope and paleomagnetic stratigraphy of equatorial Pacific core V28-238: oxygen isotope temperatures and ice volumes on a 10^5 and 10^6 year time scale: *Quaternary Research*, v. 3, p. 39-55.
- Snyder, S.W., 1978, Distribution of planktonic foraminifera in surface sediments of the Gulf of Mexico: *Tulane Studies in Geology and Paleontology*, v. 14, p. 1-80.
- Spotz, B.L., 1989, Late Miocene-Pliocene planktonic foraminiferal biostratigraphy and paleoceanography, northeast Gulf of Mexico: Unpublished M.S. thesis, University of Delaware, Newark, DE, 173 p.
- Stainforth, R.M., Lamb, J.L., Luterbacher, K., Beard, H.J., and Jeffords, R.M., 1975, Cenozoic planktonic foraminiferal zonation and characteristics of index foraminifera: *University of Kansas Paleontological Contributions*, Article 62, 425 p.
- Stathoplos, L., and Hare, P.E., 1988, Amino acid analysis of individual fossil planktonic foraminiferal tests: *Annual Report of the Director Geophysical Laboratory- Carnegie Institute of Washington* p. 127-132.
- Wehmiller, J.F., 1971, Amino acid diagenesis in fossil calcareous organisms: PhD. Dissertation, Columbia University, New York, NY, 329 p.

- Wehmiller, J.F., 1977, Amino acid studies of the Del Mar, California Midden site: apparent rate constants, ground temperature models and chronological implications: *Earth Planetary Science Letters*, v. 37, p. 184-196.
- Wehmiller, J.F., 1980, Intergeneric differences in apparent racemization kinetics in mollusks and foraminifera: implications for models of diagenetic racemization, *in* Hare, P. E., Hoering, T. C., and King, K. Jr., eds., *Biogeochemistry of amino acids*: New York, John Wiley, Inc., p. 341-355.
- Wehmiller, J.F., 1982, A review of amino acid racemization studies in Quaternary mollusks: stratigraphic and chronologic applications in coastal and interglacial sites, Pacific and Atlantic coasts, U.S., U.K., Baffin Island and tropical islands: *Quaternary Science Reviews*, v. 1, p. 83-120.
- Wehmiller, 1984, Interlaboratory comparison of amino acid enantiomeric ratios in fossil Pleistocene mollusks: *Quaternary Research*, v. 22, p. 109-121.
- Wehmiller, J.F., 1984, Relative and absolute dating of Quaternary mollusks with amino acid racemization: evaluation, applications and questions, *in* Mahaney, W.C., ed, *Quaternary dating methods*: Amsterdam, Elsevier, p. 171-193.
- Wehmiller, J.F., 1986, Amino acid racemization geochronology, *in* Hurford, A.J., Jaeger, E., and Ten Cate, J.A.M., eds., *Dating young sediments-proceedings of the workshop in Beijing*: People's Republic of China, p. 139-158.
- Wehmiller, J.F., 1989, Applications of organic geochemistry for Quaternary research: aminostratigraphy and aminochronology, *in* Engel and Macko, eds., *Organic Geochemistry*, in preparation.

- Wehmiller, J.F., and Belknap, D.F., 1978, Alternative kinetic models for the interpretation of amino acid enantiomeric ratios in Pleistocene mollusks: examples from California, Washington, and Florida: *Quaternary Research*, v. 9, p. 330-348.
- Wehmiller, J.F., and Hare, P.E., 1971, Racemization of amino acids in marine sediments: *Science*, v. 173, p. 907-911.
- Wehmiller, J.F., Belknap, D.F., Boutin, B.S., Mirecki, J.E., Rahaim, S.D., York, L.L., 1988, A review of the aminostratigraphy of Quaternary mollusks from US Atlantic coastal plain sites, in Easterbrook, D.J., ed., *Quaternary dating methods*, Geological Society of America special paper #227, p. 69-110..
- Wehmiller, J.F., Hare, P.E., and Kujala, G.A., 1976, Amino acids in fossil corals: racemization (epimerization) reactions and their implications for diagenetic models and geochronological studies: *Geochimica et Cosmochimica Acta*, v. 40, p. 736-776.
- Williams, K.M., and Smith, G.G., 1977, A critical evaluation of the application of amino acid racemization to geochronology and geothermometry: *Origins of Life*, v. 8, p. 91-144.

APPENDIX A: Procedure for Wet Sieving

1. Core samples were placed in a low temperature oven for 12 hours to obtain a bulk-sediment dry weight.
2. Dried core samples were placed in a clean beaker and soaked for several hours in distilled water. Ultrasonics were used for a maximum of three minutes to disaggregate clumps of sediment.
3. Samples were washed over a nest of 63 μm and 125 μm sieves. (A large portion of the <63 μm fraction was saved, labeled, and is now stored at the University of Delaware).
4. Sieves were turned upside down and the captured residue was rinsed into filter paper. (Sieves were ultrasonically cleaned for 3 minutes between processing of each sample to minimize the possibility of cross-contamination.)
5. The filter paper was air-dried over night.
6. Filtered residue was weighed, placed into labeled vials, and stored in a cool, dry, dark place.

**APPENDIX B: Sample Calculation for Determining the Number of
Nanomoles Amino Acid/Gram Carbonate Material**

1) Averages of the integrated areas beneath each amino acid (abbreviated, AA) peak for all injections of a sample were determined.

2) Averages of the integrated areas beneath each amino acid peak for all injections of the quantitative standards run before and after the sample in question were determined.

3) The number of nanomoles amino acid in the sample were determined by standardizing to the known concentrations in the quantitative standard and solving for X in the following equation:

$$\frac{(\text{area of AA peak})_{\text{standard}}}{(.25 \text{ nanomoles AA})_{\text{standard}}} = \frac{(\text{area of AA peak})_{\text{sample}}}{(X \text{ nanomoles AA})_{\text{sample}}}$$

4) The number of grams of shell material analyzed on the HPLC were determined by multiplying the original sample mass by the dilution factor, or solving for Y in the following equation:

$$Y = \left(\frac{0.05 \text{ ml sample injected onto the HPLC}}{\text{number ml pH}_2 \text{ buffer added for dilution}} \right) \left(\begin{array}{c} \text{original} \\ \text{sample} \\ \text{mass} \end{array} \right)$$

5) The number of nanomoles amino acid/gram carbonate material is determined by dividing Y into X from the equations above.

APPENDICES C-H: Raw data of samples analyzed for amino acids, including cleaning method (see Table 3.1 for a description of abbreviations for the cleaning methods used), Delaware laboratory number, core-sample, number of runs on HPLC, method of drying used during core-sample processing (heat or air), depth in core, age, and absolute abundances of some amino acids. Absolute abundances are the means of peak areas from consecutive chromatograms (providing a sample has been run more than once), and are presented in units of nanomoles amino acid/gram carbonate. Reproducibility of consecutive chromatograms is usually within 5% (Wehmiller, 1980).

APPENDIX C: Globigerinoides ruber

APPENDIX D: Orbulina universa

APPENDIX E: Neogloboquadrina dutertrei

APPENDIX F: The Globorotalia tumida-menardii Complex

APPENDIX G: Mixed Foraminiferal Assemblage

APPENDIX H: Interlaboratory Comparison Powders

The following symbols are used throughout Appendices C-H for abbreviated notation:

* - A/I ratios were determined from measuring the peak heights directly from the chromatograms by hand.

- Samples hydrolyzed in 12N HCl, instead of 6N HCl.

F = Free analysis of amino acids, unless already specified.

P = ILC-C powder picked as if a foraminifera sample.

Appendix C - *Globigerinoides ruber*

Amino Acid Abundances (nmoles/gram carbonate)

	Cleaning	Delaware Number	Core Sample	Number of Runs	Heat/Air Dry	Depth (m)	Age (ka)	Aspartic	Threonine	Serine	Glutamic
1	A	880160	12/3:50-52	1	air	95.50	1807	45.6	7.8	7.8	89.6
2	A	880161	12/4:0-2	1	air	96.50	1834	2951.6	3149.4	1903.3	4857.8
3	B	8755 *	1/1:50-52	1	heat	0.50	4	62.6	16.3	14.5	33.8
4	B	8756 *	2/4:50-52	1	heat	13.00	82	229.8	69.8	62.5	142.9
5	B	8757 *	2/6:0-2	1	heat	15.50	114	133.5	34.2	26.4	88.5
6	B	880163	12/3:50-52	1	air	95.50	1807	135.0	16.4	20.9	151.2
7	D: 60	880612	2/1:56-58	1	air	8.50	55	700.6	257.5	195.2	579.7
8	D: 60	880613	3/2:43-45	1	air	19.43	214	1349.2	109.1	51.9	116.3
9	D: 60	880614	4/3:55-57	1	air	30.55	365	811.6	204.0	194.0	545.0
10	D: 60	880324	4/5:52-54	1	air	33.52	405	776.6	233.4	448.0	735.2
11	D: 60	880615	5/3:52-54	2	air	40.00	492	740.0	117.4	222.5	544.2
12	D: 60	880616	6/5:97-99	2	air	48.50	603	720.2	105.9	189.1	518.5
13	D: 60	880325	7/1:50-52	1	air	51.00	651	705.0	158.3	141.4	697.7
14	D: 60	880326	7/3:50-52	1	air	54.00	712	754.6	243.0	213.7	1191.2
15	D: 60	880327	7/5:50-52	1	air	57.00	773	447.8	66.9	107.5	342.7
16	D: 60	880328	8/1:50-52	1	air	59.00	814	33.7	120.5	93.1	35.8
17	D: 60	880329	8/3:50-52	1	air	62.00	875	545.4	25.1	173.4	458.0
18	D: 60	880330	8/5:50-52	1	air	65.00	937	683.7	92.4	400.5	86.7
19	D: 60	880343	10/6:0-2	2	air	83.00	1467	271.0	1675.3	1675.3	308.5
20	D: 60	880344	11/1:0-2	1	air	84.00	1495	428.3	2511.1	2511.1	472.4
21	D: 60	880345	11/1:100-102	1	air	85.00	1522	458.8	960.3	960.3	623.8
22	D:15	880312	9/1:0-2	1	air	68.00	1006	385.7	490.1	267.1	356.9
23	D:15	880313	9/1:50-52	2	heat	68.50	1022	424.9	22.4	208.0	393.1
24	D:15	880314	9/1:100-102	2	air	69.00	1038	411.1	62.8	130.7	304.5
25	D:15	880315	9/2:0-2	1	heat	69.25	1046	1536.7	214.9	1219.6	1884.7
26	D:15	880316	9/2:50-52	1	air	69.50	1055	1201.7	212.6	402.8	1024.6
27	D:15	880317	9/2:100-102	1	heat	70.00	1071	2131.4	196.0	2203.3	2788.7
28	D:15	880331	9/4:50-52	1	air	72.50	1151	759.0	51.9	181.7	684.5
29	D:15	880332	9/6:50-52	1	air	75.50	1248	896.9	434.9	227.5	1000.7
30	D:15	880333	10/1:50-52	1	air	76.50	1280	1013.0	574.3	300.4	1886.8
31	D:15	880334	10/3:50-52	1	air	79.00	1356	962.3	2947.5	1541.6	1665.7
32	D:15	880335	10/3:50-52	1	air	82.00	1439	929.1	3510.8	1836.3	1111.6

Appendix C - *Globigerinoides ruber* (continued)
 Amino Acid Abundances (nmoles/gram carbonate)

	Glycine	Alanine	Valine	Methionine	Allo-Isoleucine	Isoleucine	Leucine	Tyrosine	Phenylalanine	Allo/Iso (Area)	Allo/Iso (Height)
1	157.4	102.5	31.1	0.0	4.4	15.7	25.4	0.0	0.0	0.282	0.313
2	3388.7	3246.5	1220.1	193.9	51.4	614.5	1559.9	47.4	836.4	0.084	0.101
3	43.6	26.4	17.2	24.6	1.4	11.0	15.9	0.0	6.7	0.060	0.125
4	162.6	113.5	14.6	124.3	5.1	54.5	74.3	44.5	38.3	0.093	0.096
5	83.8	61.4	30.4	59.1	7.1	27.1	34.3	0.0	2.2	0.263	0.254
6	141.4	108.5	64.8	0.0	9.3	26.4	42.6	0.0	25.6	0.350	0.427
7	667.0	324.8	289.5	5.8	7.8	155.6	197.0	0.0	0.9	0.050	0.060
8	831.8	968.7	354.9	365.0	23.9	191.3	276.8	0.0	157.6	0.125	0.143
9	771.9	302.9	232.5	2.7	19.5	115.0	165.4	0.0	94.5	0.169	0.193
10	1437.4	621.8	263.0	0.0	20.0	130.6	228.4	16.5	117.1	0.153	0.182
11	546.5	288.1	236.6	0.0	22.6	116.8	179.8	0.0	98.6	0.193	0.218
12	553.2	277.2	213.4	0.0	22.4	107.4	168.3	0.0	91.6	0.208	0.250
13	825.2	491.8	284.4	12.2	24.9	151.3	236.4	0.0	100.5	0.165	0.195
14	1265.2	849.2	576.0	7.4	20.4	295.6	667.5	0.0	0.0	0.069	0.085
15	481.3	271.0	138.2	7.0	14.8	70.6	106.4	16.9	54.9	0.209	0.253
16	326.2	257.8	171.9	8.8	18.1	87.8	126.4	32.4	63.4	0.206	0.246
17	614.9	349.4	170.3	9.3	18.0	85.7	144.8	0.0	69.4	0.210	0.241
18	164.1	87.1	291.3	0.0	22.4	146.6	254.2	27.0	131.0	0.153	0.188
19	447.6	166.0	118.7	2.3	7.1	62.6	135.8	0.0	55.0	0.113	0.126
20	875.8	246.9	160.5	3.3	11.8	105.3	194.3	0.0	92.7	0.112	0.137
21	965.0	333.6	216.9	8.9	10.1	122.9	239.8	0.0	13.7	0.082	0.098
22	695.6	248.4	102.9	10.1	13.3	47.5	102.6	0.0	0.0	0.281	0.336
23	586.8	192.3	165.4	9.0	18.6	86.9	126.7	0.0	0.0	0.215	0.254
24	337.4	203.9	139.2	5.9	15.8	76.7	120.5	0.0	0.0	0.206	0.242
25	2525.2	1307.0	799.4	7.6	58.2	407.6	762.8	101.6	324.5	0.143	0.168
26	1686.7	829.0	433.1	14.5	49.0	221.7	322.0	0.0	0.0	0.221	0.266
27	6201.1	2402.4	1027.5	47.3	40.8	561.7	1059.0	90.1	444.7	0.073	0.090
28	1248.0	562.7	253.1	1.0	26.2	122.7	205.1	20.1	94.7	0.214	0.247
29	2302.2	907.4	344.2	20.1	25.7	196.6	330.3	14.5	160.5	0.131	0.163
30	2371.2	1234.5	820.6	8.7	24.8	437.8	834.2	23.5	330.6	0.057	0.069
31	1969.6	1486.6	520.6	41.0	24.6	295.1	549.5	39.6	261.3	0.083	0.105
32	3413.6	1245.0	549.2	32.9	13.9	247.7	534.2	0.0	236.5	0.056	0.090

Appendix C - *Globigerinoides ruber* (continued)
 Amino Acid Abundances (nmoles/gram carbonate)

	Cleaning	Delaware Number	Core Sample	Number of Runs	Heat/Air Dry	Depth (m)	Age (ka)	Aspartic	Threonine	Serine	Glutamic
33	D:15	880336	11/2:50-52	1	air	86.00	1550	222.8	0.0	0.0	122.6
34	D:15	880337	11/4:50-52	1	air	89.00	1633	1124.9	2274.1	1189.4	1443.5
35	D:15	880338	11/6:50-52	1	air	91.50	1702	969.8	958.2	501.2	1200.7
36	D:15	880339	12/2:100-102	1	air	94.50	1782	1140.4	2570.5	1344.5	1407.9
37	E	880661	1/1:100-102	2	heat	1.00	9	813.4	1907.6	1210.3	1020.1
38	E	880662	2/5:50-52	2	heat	14.50	95	514.0	16.2	22.1	319.5
39	E	880621	7/2:0-2	2	air	52.00	671	404.6	27.5	89.5	298.2
40	E	880624	7/4:100-102	2	air	56.00	753	388.1	119.3	68.3	273.1
41	E	880627	8/2:0-2	1	air	60.00	835	429.6	67.4	79.7	330.3
42	E	880598	9/3:0-2	1	air	70.50	1087	1792.5	1003.3	476.8	2052.2
43	E	880599	10/2:100-102	1	air	77.00	1300	1294.9	5.7	552.5	1057.0
44	E	880600	11/3:0-2	1	air	87.00	1578	851.1	537.6	255.5	741.3
45	E	880601	12/2:0-2	1	air	93.50	1755	654.9	38.8	345.0	552.9
46	F	880622 #	7/2:100-102	2	air	53.00	692	1102.9	14023.3	2798.8	1342.9
47	F	880625 #	7/6:0-2	2	air	58.00	794	581.3	578.7	115.5	600.6
48	F	880628	8/2:100-102	2	air	61.00	855	560.4	157.3	56.0	460.4
49	G	880623 #	7/4:0-2	2	air	55.00	732	441.7	79.3	48.6	302.1
50	G	880626	7/6:100-102	1	air	58.50	804	658.7	8.1	156.4	688.3
51	G	880629	8/4:0-2	1	air	63.00	896	536.7	173.3	68.9	473.3

Appendix C - *Globigerinoides ruber* (continued)
 Amino Acid Abundances (nmoles/gram carbonate)

	Glycine	Alanine	Valine	Methionine	Allo- Isoleucine	Isoleucine	Leucine	Tyrosine	Phenyl- alanine	Allo/Iso (Area)	Allo/Iso (Height)
33	295.1	90.3	74.5	0.0	16.1	44.4	53.5	0.0	29.6	0.363	0.460
34	2064.4	1167.2	465.6	48.5	22.4	241.0	457.6	13.1	245.6	0.093	0.119
35	2865.6	900.5	378.9	15.2	23.9	208.5	400.7	7.0	180.5	0.114	0.136
36	3403.2	982.7	443.3	20.6	22.3	242.4	465.1	0.0	217.8	0.092	0.119
37	672.4	468.4	441.6	0.0	1.1	218.8	495.8	25.8	193.3	0.005	0.008
38	274.8	202.3	139.7	0.0	7.8	73.2	97.2	23.4	58.9	0.107	0.127
39	355.8	181.6	137.0	0.0	13.9	77.2	112.9	72.8	0.0	0.180	0.203
40	243.9	153.0	401.4	2.2	36.6	142.8	207.5	1.5	114.7	0.256	0.288
41	307.6	205.8	210.5	6.1	25.2	119.0	166.8	0.0	88.3	0.211	0.234
42	2612.6	1523.6	709.5	5.6	46.3	375.8	668.9	32.4	340.7	0.123	0.145
43	2556.7	824.4	372.7	0.0	28.8	200.5	368.9	0.0	179.7	0.144	0.169
44	1131.3	404.4	285.4	0.0	24.9	156.2	308.0	0.0	140.1	0.160	0.175
45	1348.5	429.9	193.1	0.0	17.0	103.5	191.8	0.0	93.5	0.164	0.179
46	1674.7	905.5	1131.4	2.7	25.8	634.9	1273.8	12.7	494.7	0.041	0.048
47	1386.1	423.2	259.9	1.7	18.9	143.5	232.3	0.0	123.6	0.132	0.152
48	395.3	292.0	190.6	5.8	25.6	92.6	129.7	30.0	86.0	0.276	0.325
49	495.9	233.8	401.4	2.2	36.6	142.8	207.5	1.5	114.7	0.256	0.288
50	1147.9	483.5	262.1	2.6	25.9	133.8	201.0	5.1	127.9	0.194	0.226
51	335.4	285.3	190.6	5.8	25.6	92.6	129.7	30.0	86.0	0.276	0.325

Appendix D - Orbulina univerrse

Amino Acid Abundances (nmoles/gram carbonate)

	Cleaning	Delaware Number	Core Sample	Number of Runs	Heat/Air Dry	Depth (m)	Age (ka)	Aspartic	Threonine	Serine	Glutamic
1	D: 60	880607	3/2: 43-45	2	air	19.43	214	839.7	340.2	313.3	674.2
2	D: 60	880608	5/3: 52-54	2	air	40.00	492	495.0	105.7	146.6	387.4
3	D: 60	880609	7/1: 50-52	2	air	51.00	651	477.9	1397.3	471.8	452.9
4	D: 60	880384	8/2: 0-2	1	air	60.00	835	391.6	352.5	342.7	308.4
5	D: 60	880385	9/2: 50-52	1	air	69.00	1038	338.4	165.4	548.0	275.1
6	D: 60	880386	10/4: 0-2	3	air	80.00	1383	566.2	49.4	636.3	665.1
7	D: 60	880610	11/5: 0-2	2	air	89.75	1657	469.8	912.7	392.2	433.3
8	D: 60	880611	12/6: 0-2	2	air	99.50	1919	442.2	514.7	221.2	442.7
9	E	880663	2/3: 100-102	2	heat	12.00	76	571.1	438.8	438.8	316.8
10	E	880664	2/4: 101-103	2	air	13.50	85	560.3	34.0	83.0	400.7
11	E	880665	3/4: 53-55	2	air	22.53	256	556.8	37.6	37.6	448.4
12	E	880666	4/2: 7-9	2	air	29.00	344	493.7	3.3	30.2	320.9
13	E	880667	9/3: 0-2	2	air	70.50	1087	425.0	15.1	32.3	303.8
14	E	880673	13/5: 50-52	2	heat	107.50	2156	296.1	5.9	28.1	214.6
15	E	880678	17/6: 50-52	2	heat	140.00	3110	190.4	19.3	19.3	145.7
16	E	880674	16/6: 100-102	2	heat	142.00	3169	358.1	43.4	40.5	257.2
17	E	880682	21/5: 100-102	2	heat	174.00	4110	230.6	25.2	25.2	151.6

Appendix D - *Orbulina uniyersa* (continued)
 Amino Acid Abundances (nmoles/gram carbonate)

	Glycine	Alanine	Valine	Methionine	Allo- Isoleucine	Isoleucine	Leucine	Tyrosine	Phenyl- alanine	Allo/Iso (Area)	Allo/Iso (Height)
1	1086.6	512.7	333.2	4.2	16.6	186.9	270.9	0.0	150.2	0.089	0.108
2	548.8	279.8	156.6	0.0	18.3	82.6	127.0	4.4	71.2	0.222	0.254
3	640.1	401.8	221.1	11.8	16.3	143.4	220.3	0.0	105.9	0.113	0.138
4	395.7	266.4	155.0	6.4	14.4	91.7	161.4	100.0	51.8	0.157	0.173
5	479.9	241.4	117.2	6.4	16.1	54.2	133.5	64.0	51.7	0.296	0.317
6	869.0	361.8	230.6	5.0	23.1	158.0	276.3	22.1	144.3	0.146	0.165
7	427.5	268.7	241.7	0.0	16.6	127.2	258.5	9.0	99.3	0.131	0.154
8	837.4	311.3	159.8	0.0	16.2	92.0	161.0	0.0	78.6	0.176	0.208
9	397.4	250.8	182.2	0.0	11.6	94.6	147.1	38.1	73.1	0.122	0.139
10	414.8	272.5	183.3	0.0	8.5	110.7	159.2	14.9	89.2	0.077	0.091
11	331.0	310.3	167.5	0.0	13.0	88.9	160.1	9.3	82.8	0.146	0.160
12	317.6	205.6	161.1	0.0	17.4	83.5	119.2	1.3	77.3	0.208	0.228
13	285.6	219.5	131.8	0.0	19.7	62.5	110.7	51.5	40.7	0.315	0.344
14	207.7	144.9	92.6	0.0	18.8	47.0	77.6	0.0	41.8	0.400	0.435
15	149.9	91.8	56.6	0.0	11.7	27.1	47.8	0.0	23.2	0.434	0.511
16	245.7	162.3	97.6	0.0	27.8	43.2	85.4	73.7	0.0	0.550	0.647
17	117.1	105.5	68.1	0.0	15.3	24.9	44.8	0.0	23.4	0.614	0.635

Appendix E - Neoglobodrina dutertrei
 Amino Acid Abundances (nmoles/gram carbonate)

	Cleaning	Delaware Number	Core Sample	Number of Runs	Heat/Air Dry	Depth (m)	Age (ka)	Aspartic	Threonine	Serine	Glutamic
1	D: 60	880604	2/5:44-46	2	air	14.44	93	667.9	218.0	140.5	437.0
2	D: 60	880605	3/2:43-45	2	air	19.43	214	760.8	108.6	443.1	702.4
3	D: 60	880606	5/3:52-54	3	air	40.00	492	522.9	121.1	93.4	388.4
4	D: 60	880346	8/2:0-2	2	air	60.00	630	353.3	162.5	459.1	304.7
5	D: 60	880347	9/2:50-52	2	air	69.50	1055	375.3	26.8	283.7	375.3
6	D: 60	880348	10/4:0-2	4	air	80.00	1383	381.9	997.0	581.8	402.7
7	E	880646	1/1:100-102	2	heat	1.00	9	594.4	441.5	109.2	248.4
8	E	880647	2/4:101-103	2	air	13.50	85	789.6	3891.8	896.2	424.4
9	E	880648	2/5:44-46	2	air	14.44	93	617.3	157.7	128.3	448.1
10	E	880649	2/5:50-52	2	heat	14.50	95	558.3	123.6	107.5	269.8
11	E	880650	3/4:53-55	2	air	22.50	256	549.0	218.2	63.0	423.1
12	E	880651	5/3:52-54	2	air	40.00	492	472.7	83.6	72.0	383.4
13	E	880652	6/7:6-8	2	air	50.00	630	455.8	103.9	42.0	344.6
14	E	880654	8/2:0-2	2	air	60.00	835	531.6	57.6	37.1	459.2
15	E	880655	8/3:50-52	2	air	62.00	875	715.5	68.3	68.3	483.8
16	E	880596	10/6:0-2	2	air	83.00	1467	407.2	50.8	52.1	317.1
17	E	880597	11/3:100-102	2	air	88.00	1592	479.7	50.3	77.6	418.4
18	E	880657	12/6:0-2	2	air	99.50	1917	272.3	28.7	47.7	197.8
19	E	880671	13/5:50-52	2	heat	107.50	2146	334.6	29.9	80.4	287.1
20	E	880672	16/6:100-102	2	heat	134.00	2903	434.8	1.9	21.8	320.1
21	E	880680	17/6:50-52	2	heat	144.00	3074	362.9	18.1	24.9	278.6
22	E	880682	21/5:100-102	2	heat	184.00	4046	238.3	17.4	17.4	153.3

Appendix E - Neogloboquadrina dutertrei (continued)
 Amino Acid Abundances (nmoles/gram carbonate)

	Glycine	Alanine	Valine	Methionine	Allo- isoleucine	Isoleucine	Leucine	Tyrosine	Phenyl- alanine	Allo/Iso (Area)	Allo/Iso (Height)
1	458.6	397.3	257.2	0.0	23.8	136.1	178.0	0.0	133.8	0.175	0.197
2	778.6	457.0	394.1	0.0	26.8	209.5	395.8	9.3	218.8	0.128	0.141
3	409.5	327.2	198.1	0.0	30.5	92.9	137.5	5.1	91.6	0.329	0.364
4	265.8	253.9	156.2	0.0	20.7	75.9	118.4	1.6	59.9	0.272	0.291
5	797.0	374.3	134.5	8.7	18.4	64.5	111.9	5.8	18.5	0.285	0.314
6	723.6	304.3	118.6	2.8	17.3	62.8	143.5	10.7	53.7	0.276	0.300
7	458.9	382.0	218.9	1.5	5.1	136.0	194.0	28.1	146.3	0.038	0.050
8	653.8	453.1	434.0	0.0	22.1	208.4	401.2	47.0	231.7	0.106	0.120
9	334.6	319.7	218.0	0.0	19.0	117.7	180.8	4.8	137.1	0.161	0.189
10	388.0	367.0	213.1	0.0	21.5	115.3	164.6	17.0	133.1	0.187	0.204
11	209.0	317.4	185.4	0.0	26.2	102.0	139.0	5.2	104.7	0.256	0.290
12	392.7	297.2	184.8	0.0	29.0	89.4	132.2	5.3	90.3	0.325	0.364
13	286.6	268.0	166.6	0.0	29.2	77.1	114.9	0.0	103.8	0.381	0.437
14	372.2	372.4	206.3	0.0	36.6	91.1	142.3	0.0	119.0	0.402	0.430
15	449.3	446.7	264.4	0.0	50.6	107.0	177.3	0.0	120.7	0.473	0.492
16	365.1	287.9	156.0	1.2	32.1	68.6	109.1	0.0	0.0	0.467	0.503
17	548.5	351.6	190.8	0.0	37.2	80.8	129.2	2.1	77.0	0.460	0.508
18	169.0	180.2	91.5	0.0	24.4	27.6	68.9	0.0	37.5	0.756	0.748
19	234.8	247.0	129.9	0.0	27.8	49.4	114.7	0.0	64.0	0.564	0.588
20	227.3	290.5	157.4	0.0	41.3	57.7	110.1	0.0	74.0	0.717	0.744
21	243.8	252.8	131.6	0.0	32.9	54.4	90.6	0.0	56.4	0.604	0.673
22	137.2	158.8	76.5	0.0	22.5	26.6	50.0	0.0	32.4	0.843	0.889

Appendix F- *Globorotella tumida-menardii* Complex
 Amino Acid Abundances (nmoles/gram carbonate)

	Cleaning	Delaware Number	Core Sample	Number of Runs	Heat/Air Dry	Depth (m)	Age (ka)	Aspartic	Threonine	Serine	Glutamic
1	E	880637	1/1:50-52	2	heat	0.50	4	667.9	1461.4	409.4	442.7
2	E	880658	1/1:100-102	4	heat	1.00	9	594.6	1474.4	673.8	590.9
3	E	880638	2/5:44-46	2	air	14.40	93	461.9	166.1	101.5	329.7
4	E	880659	2/5:50-52	4	heat	14.50	95	486.4	92.2	69.5	385.8
5	E	880639	3/4:53-55	2	air	22.50	256	414.9	75.9	66.0	287.3
6	E	880640	4/7:5-7	2	air	36.50	445	384.5	176.5	31.3	264.8
7	E	880641	6/7:6-8	2	air	50.00	630	440.6	166.6	46.7	365.2
8	E	880669	7/1:50-52	2	air	51.00	651	370.3	16.7	29.1	267.6
9	E	880642	8/6:100-102	2	air	67.00	977	240.6	33.0	24.9	217.2
10	E	880643	10/6:0-2	2	air	83.00	1467	263.4	33.6	26.3	241.1
11	E	880644	12/6:0-2	2	air	99.50	1917	302.5	16.2	45.4	291.4

Appendix F- *Globorotalla tumida-menardii* Complex (continued)
 Amino Acid Abundances (nmoles/gram carbonate)

	Glycine	Alanine	Valine	Methionine	Allo- Isoleucine	Isoleucine	Leucine	Tyrosine	Phenyl- alanine	Allo/Iso (Area)	Allo/Iso (Height)
1	531.2	403.2	253.3	0.0	10.6	149.2	186.5	17.2	146.2	0.071	0.082
2	584.0	442.5	340.9	4.0	2.5	173.3	374.2	35.6	606.5	0.015	0.020
3	359.0	331.0	194.2	0.0	20.1	106.4	131.4	11.9	102.7	0.189	0.214
4	395.3	347.6	185.4	0.0	19.2	98.6	118.7	41.1	80.7	0.196	0.216
5	300.5	297.5	156.3	0.0	25.0	69.6	110.1	13.2	76.6	0.360	0.387
6	263.4	265.1	147.7	0.0	29.2	74.0	100.0	109.7	0.0	0.394	0.433
7	251.5	300.5	194.9	0.0	31.3	95.3	154.8	133.1	0.0	0.328	0.366
8	230.3	246.2	143.9	0.0	25.9	60.8	97.9	59.9	0.0	0.426	0.438
9	190.3	186.7	100.9	0.0	22.4	43.0	68.1	64.4	0.0	0.521	0.588
10	195.6	206.8	107.6	0.0	24.2	40.2	74.3	62.8	0.0	0.602	0.630
11	249.5	217.1	123.3	0.0	30.0	49.7	90.3	81.5	0.0	0.605	0.654

**Appendix G - Mixed Foraminiferal Species
Amino Acid Abundances (nmoles/gram carbonate)**

	Cleaning	Delaware Number	Core Sample	Number of Runs	Heat/Air Dry	Depth (m)	Age (ka)	Aspartic	Threonine	Serine	Glutamic
TOTAL FRACTION											
1	E	880684	1/1:47-49	2	air	0.50	4	1202.5	512.8	512.8	692.3
2	E	880685	2/5:6-8	2	air	14.60	97	580.7	36.1	31.5	342.3
3	E	880686	3/6:3-5	2	air	25.30	294	528.0	22.1	77.1	461.8
4	E	880687	4/6:6-8	2	air	34.50	418	445.6	22.2	10.5	289.6
5	E	880688	7/1:50-52	2	air	51.00	651	493.0	17.7	18.4	322.5
6	E	880689	8/2:100-102	2	air	61.00	855	433.8	13.9	9.2	308.7
7	E	880690	10/2:0-2	2	air	77.00	1314	327.1	10.9	14.3	235.1
8	E	880692	11/3:100-102	2	air	87.50	1592	505.2	9.5	9.5	326.8
9	E	880693	12/5:50-52	2	air	98.50	1886	380.8	156.1	170.2	260.5
FREE FRACTION											
1	E	880694	1/1:47-49	4	air	0.50	4	24.5	1623.0	214.9	8.2
2	E	880695	2/5:6-8	2	air	14.60	97	123.9	6.7	35.5	33.7
3	E	880697	4/6:6-8	2	air	34.50	418	195.9	336.4	37.1	50.1
4	E	880698	7/1:50-52	2	air	51.00	651	408.1	342.5	35.1	96.1
5	E	880700	8/2:100-102	2	air	61.00	855	218.1	465.4	61.6	54.3
6	E	880701	10/2:0-2	2	air	77.00	1314	212.6	114.9	15.2	46.5
7	E	880702	11/3:100-102	2	air	87.50	1592	197.1	0.0	0.0	43.5
8	E	880711	12/5:50-52	2	air	98.50	1886	360.3	71.6	75.3	251.4

Appendix G - Mixed Foraminiferal Species (continued)
 Amino Acid Abundances (nmoles/gram carbonate)

	Glycine	Alanine	Valine	Methionine	Allo- Isoleucine	Isoleucine	Leucine	Tyrosine	Phenyl- alanine	Allo/Iso (Area)	Allo/Iso (Height)
TOTAL FRACTION											
1	961.1	526.5	313.1	2.4	1.8	179.3	259.4	17.2	184.8	0.010	0.014
2	322.7	296.5	167.1	0.0	15.2	90.9	109.8	15.6	87.7	0.167	0.197
3	372.5	334.7	217.7	0.0	23.5	117.5	189.6	154.9	0.0	0.200	0.223
4	261.7	252.0	151.9	0.0	25.2	70.0	93.1	102.3	0.0	0.359	0.395
5	266.9	251.7	145.3	0.0	24.9	69.5	94.0	10.3	61.9	0.357	0.371
6	244.2	249.0	138.1	0.0	20.6	69.1	93.6	0.0	57.5	0.297	0.319
7	203.6	206.4	114.5	0.0	19.8	53.8	78.3	0.0	39.1	0.367	0.407
8	265.2	278.0	181.7	0.0	39.5	73.3	111.8	17.9	68.1	0.539	0.564
9	254.7	217.7	114.3	0.0	27.6	44.1	81.0	6.0	44.7	0.640	0.686
FREE FRACTION											
1	68.7	29.5	10.9	0.0	0.0	0.0	4.3	0.0	6.4	0.000	0.000
2	135.3	124.1	45.5	0.0	12.0	13.6	27.6	18.5	11.4	0.879	0.921
3	143.6	158.2	64.3	0.0	17.8	18.5	38.2	0.0	27.4	0.960	0.960
4	232.6	273.1	109.0	0.0	28.2	29.7	65.6	20.1	40.8	0.949	0.980
5	106.2	147.4	62.2	0.0	18.6	17.6	37.7	4.9	21.9	1.056	1.111
6	108.6	142.4	62.3	0.8	20.0	18.0	38.4	6.6	21.7	1.112	1.128
7	73.5	102.7	52.4	0.0	15.3	14.4	28.9	6.7	15.9	1.065	1.104
8	204.0	198.8	123.8	0.0	28.6	49.7	77.9	9.3	52.0	0.576	0.609

Appendix H - Interlaboratory Comparison Powders
 Amino Acid Abundances (nmoles/gram carbonate)

	Cleaning	Delaware Number	Number of Runs	Aspartic	Threonine	Serine	Glutamic	Glycine	Alanine	Valine	Methionine
ILC-B POWDERS											
1	A	880159	3	644.0	176.8	43.2	546.8	344.3	465.5	289.4	0.5
2	B	880162	2	649.5	258.4	56.2	612.7	404.5	551.0	341.1	20.1
3	D: 15	880311	2	141.5	140.1	55.4	186.7	61.3	89.8	171.4	13.4
4	D: 15	880340	2	691.5	65.2	24.8	373.2	261.0	413.7	193.2	0.8
5	D: 60	880322	2	603.6	84.3	49.8	300.1	249.1	336.0	147.2	0.0
6	D: 60	880350	2	602.5	739.9	61.1	605.0	458.5	586.0	344.1	2.3
7	D: 60	880383	3	711.5	266.3	73.8	598.8	470.1	575.8	317.7	0.0
8	D: 60	880603	2	614.2	225.2	312.1	416.0	253.2	351.3	197.9	0.0
9	D: 60	880617	2	423.7	141.7	47.3	287.0	184.3	240.7	134.6	0.0
10	E	880602	2	892.0	397.9	143.5	699.2	469.5	507.3	384.9	2.0
11	E	880620	4	727.7	275.5	67.6	575.5	415.2	476.3	312.1	0.2
12	E	880633	2	750.3	232.7	55.0	548.4	372.5	491.1	284.0	0.0
13	E	880634 #	2	634.6	260.0	42.4	538.4	355.2	455.6	283.9	0.0
14	E	880636	5	700.1	161.7	30.6	536.2	338.3	449.3	242.4	0.0
15	E	880645	2	616.1	213.1	30.2	577.7	319.8	438.1	232.4	0.7
16	E	880653	2	895.5	309.9	119.6	615.9	376.2	515.5	274.4	0.5
17	E	880660	2	576.6	57.8	8.4	333.5	227.0	307.0	177.9	0.0
18	E	880668	2	701.9	30.5	23.7	374.1	268.0	380.2	157.1	2.3
19	E	880676	2	805.4	79.7	10.0	558.5	304.9	467.2	291.3	0.0
20	E	880683	2	419.7	35.4	11.4	460.8	339.9	438.3	223.8	0.0
21	E	880691	2	618.5	27.9	14.6	383.6	281.9	350.0	199.6	0.0
22	E	880699 F	2	424.9	49.3	49.3	111.4	231.4	371.3	146.3	26.5
23	G	880630	2	699.8	145.8	53.4	421.0	191.2	275.4	247.5	2.7
ILC-C POWDERS											
1	D: 60	880341	2	334.6	29.0	31.9	318.6	250.4	383.6	180.4	15.5
2	D: 60	880349 P	2	353.6	5.0	153.3	355.9	303.8	394.6	195.2	3.0

Appendix H - Interlaboratory Comparison Powders (continued)
 Amino Acid Abundances (nmoles/gram carbonate)

	Allo- Isoleucine	Isoleucine	Leucine	Tyrosine	Phenyl- alanine	Allo/Iso (Area)	Allo/Iso (Height)
ILC-B POWDERS							
1	61.8	119.2	233.1	211.3	198.6	0.518	0.554
2	68.4	143.5	254.3	199.9	212.1	0.477	0.519
3	29.2	57.2	126.9	119.2	118.6	0.509	0.540
4	38.2	83.6	153.5	122.6	129.8	0.458	0.503
5	30.2	64.2	146.6	106.9	116.7	0.471	0.524
6	59.9	141.8	252.4	99.5	62.1	0.423	0.467
7	59.1	136.7	255.2	166.9	217.3	0.432	0.467
8	36.0	82.5	156.8	99.0	129.1	0.436	0.473
9	22.5	56.9	103.4	54.5	89.7	0.395	0.431
10	52.5	147.5	350.1	230.3	281.1	0.396	0.388
11	51.1	130.3	243.6	56.6	149.0	0.392	0.429
12	51.4	124.8	223.5	95.4	178.0	0.412	0.456
13	56.2	128.2	207.1	41.2	174.2	0.438	0.485
14	53.0	111.2	197.3	103.9	180.1	0.477	0.506
15	52.0	103.9	186.0	93.7	179.2	0.501	0.535
16	68.2	120.8	230.0	208.3	222.0	0.547	0.584
17	34.2	68.9	153.2	66.4	122.2	0.496	0.502
18	20.9	46.3	152.1	121.1	109.2	0.465	0.435
19	47.6	99.8	234.4	117.9	190.7	0.477	0.501
20	45.6	97.5	171.3	74.5	150.2	0.465	0.488
21	35.1	80.9	146.3	68.7	120.5	0.432	0.470
22	38.0	41.8	118.5	87.6	83.6	0.909	1.019
23	50.8	107.8	203.7	135.7	167.7	0.471	0.496
ILC-C POWDERS							
1	54.5	58.4	122.2	57.4	29.1	0.933	1.014
2	54.6	65.3	138.6	52.3	31.6	0.836	0.922

Bed Johnson 625 DART

on Geosci Server

HEAT OR AIR	COMMENTS	SAMPLE	LAB NO
		12/3 : 50 R	880160
	NOT CLEANED	12/4 : 0 R	880161
		12/3 : 50 R	880163
	2 RUNS	11/5 : 0 MIX	880190
		11/5 : 0 MIX	880190
		11/5 : 0 MIX	880191
		11/5 : 0 MIX	880192
		11/5 : 0 MIX	880193
		ILC-B	880311
		9/1 : 0 R	880312
	1 INJECT	9/1 : 50 R	880313
	2ND INJECT	9/1 : 50 R	880313
	AVG OF 2	9/1 : 50 R	880313
		9/1 : 100 R	880314
		9/2 : 0 R	880315
		9/2 : 50 R	880316
HEAT	UNCERTAIN SECTION	9/2 : 100 R	880317
		9/2 : 100 * R	880318
		ILC-B 1	880322
		4/5 : 52 RR	880323
		4/5 : 52 WR	880324
		7/1 : 50 R	880325
		7/3 : 50 R	880326
		7/5 : 50 R	880327
		8/1 : 50 R	880328
		8/3 : 50 R	880329
		8/5 : 50 R	880330
		9/4 : 50 R	880331
		9/6 : 50 R	880332
		10/1 : 50 R	880333
		10/3 : 50 R	880334
		10/5 : 50 R	880335
		11/2 : 50 R	880336
		11/4 : 50 R	880337
		11/6 : 50 R	880338
		12/2 : 100 R	880339
		ILC B - 2	880340
		ILC - C 1	880341
		8/2 : 0 D	880346
		9/2 : 50 D	880347
		10/4 : 0 D	880348
		ILC - C 2	880349
		ILC - B 3	880350
		WATER BLNK 2	880377
		WATER BLNK 3	880378
		10/6 : 0 - R	880343
		11/1 : 0 - R	880344
		11/1 : 100 - R	880345

Ben

ASP	THR	SER	GLU	GLY	ALA	VAL	MET	ALLO
45.638	7.84	284.091	89.567	157.355	102.475	31.087	0	4.43
2951.561	9101.159	0	4857.806	3388.742	3246.45	1220.065	193.935	51.352
172.404	36.478	0	161.274	157.602	121.087	73.442	0	10.345
509.873	48.279	0	609.019	474.199	532.18	285.969	0	54.665
405.99	52.28	0	221.396	289.13	317.109	180.864	1.219	37.74
369.273	15.318	0	429.731	325.041	341.466	201.409	1.487	45.077
449.289	0	0	398.671	297.372	340.764	227.82	0	36.413
405.528	7.518	0	401.471	294.007	344.88	219.898	0	39.047
141.53	237.178	2.489	186.703	72.882	77.922	171.448	13.383	29.178
385.738	0	534.241	356.894	695.593	248.437	102.949	10.084	13.329
539.307	22.017	269.028	500.849	770.837	217.586	211.052	10.548	23.59
310.514	22.763	146.872	285.313	402.674	167.052	119.789	7.525	13.671
424.91	22.39	207.95	393.081	586.755	192.319	165.421	9.037	18.63
411.117	62.758	130.659	304.452	337.425	203.913	139.204	5.903	15.79
1536.718	214.864	1219.576	1884.72	2525.18	1306.975	799.361	7.648	58.198
1201.744	212.645	402.834	1024.593	1686.713	829.048	433.089	14.537	49.022
2131.435	196.04	2203.314	2788.711	6201.052	2402.379	1027.473	47.328	40.756
959.962	129.405	355.614	820.679	1046.079	536.824	333.984	7.346	41.58
603.628	84.347	49.77	300.098	249.147	336.022	147.236	0	30.223
761.954	192.199	207.583	561.205	532.787	351.206	215.66	0	20.884
776.616	233.352	447.995	735.167	1437.413	621.816	263.002	11.209	19.953
704.972	158.339	141.403	697.7	825.208	491.825	284.431	12.195	24.91
754.609	5410.6	0	1191.196	1265.173	849.244	575.979	7.352	20.373
447.755	66.943	107.526	342.712	481.28	271.01	138.241	6.961	14.756
33.707	240.971	0	35.801	326.221	257.841	171.949	8.812	18.129
545.355	25.13	173.408	458.039	614.863	349.391	170.338	9.309	17.966
683.651	92.442	400.489	86.703	164.118	87.145	291.306	0	22.406
758.954	199.88	242.554	684.483	1248.012	562.655	253.069	1.032	26.238
896.892	0	607.33	1000.735	2302.2	907.434	344.172	20.111	25.661
1012.97	44264.71	0	1886.768	2371.187	1234.464	820.572	8.682	24.824
962.304	0	4116.389	1665.737	1969.634	1486.609	520.587	40.964	24.551
929.103	0	0	1111.622	3413.642	1245.033	549.226	0	13.876
222.847	0	0	122.625	295.079	90.317	74.496	0	16.115
1124.922	0	0	1443.544	2064.373	1167.189	465.595	48.52	22.431
969.76	0	1338.182	1200.671	2865.588	900.454	378.928	15.168	23.859
1140.413	0	0	1407.889	3403.171	982.747	443.329	20.606	22.303
691.494	251.372	33.141	373.207	260.968	413.725	193.248	0.776	38.231
334.554	21.16	37.843	318.634	250.38	383.598	180.361	15.473	54.537
354.892	120.843	634.146	305.93	267.295	253.676	156.719	0	20.763
375.339	19.542	336.857	375.287	796.951	374.307	134.474	8.681	18.403
302.113	2395.754	0	311.089	563.852	245.378	98.635	4.494	15.052
353.627	3.621	182.062	355.909	303.817	394.641	195.174	3.012	54.594
602.482	539.238	72.522	604.964	458.478	585.961	344.12	2.277	59.94
46.216	0	682.818	23.494	55.101	12.851	0	0	0
46.216	0	682.818	23.494	55.101	12.851	0	0	0
271.021	2168.861	0	308.526	447.627	165.996	118.72	2.33	7.08
428.318	3250.91	0	472.402	875.845	246.909	160.458	3.283	11.776
458.811	0	4220.023	623.831	965.016	333.649	216.905	8.91	10.08

ISO	LEU	TYR	PHE	A/I A	A/I H
15.698	25.428	0	0	0.282	0.313
614.461	1559.923	47.425	836.426	0.084	0.101
29.52	47.404	0	28.399	0.35	0.427
108.745	151.22	19.354	85.664	0.503	0.568
75.502	103.851	19.172	59.239	0.5	0.578
82.974	105.877	15.024	64.897	0.543	0.601
65.362	86.107	7.836	48.557	0.557	0.634
71.695	92.151	2.441	23.609	0.545	0.632
57.249	126.938	119.197	118.596	0.509	0.54
47.45	102.625	0	0	0.281	0.336
110.399	159.095	0	0	0.214	0.267
63.462	94.336	0	0	0.215	0.241
86.931	126.716	0	0	0.215	0.254
76.659	120.458	0	0	0.206	0.242
407.584	762.763	101.614	324.492	0.143	0.168
221.743	322.027	0	0	0.221	0.266
561.711	1059.021	90.054	444.709	0.073	0.09
177.22	269.456	0	0	0.235	0.273
64.222	146.6	106.875	116.674	0.471	0.524
114.4	162.323	0	0	0.183	0.221
130.604	228.39	16.549	117.064	0.153	0.182
151.333	236.427	0	100.458	0.165	0.195
295.61	667.471	0	0	0.069	0.085
70.564	106.425	16.886	54.932	0.209	0.253
87.794	126.36	32.389	63.38	0.206	0.246
85.719	144.828	0	69.448	0.21	0.241
146.6	254.215	27.035	130.993	0.153	0.188
122.735	205.078	20.142	94.728	0.214	0.247
196.619	330.304	14.509	160.5	0.131	0.163
437.78	834.244	23.455	330.626	0.057	0.069
295.064	549.522	39.56	261.296	0.083	0.105
247.673	534.233	0	236.516	0.056	0.09
44.409	53.519	0	29.561	0.363	0.46
240.953	457.577	13.088	245.638	0.093	0.119
208.515	400.732	6.989	180.508	0.114	0.136
242.401	465.105	0	217.767	0.092	0.119
83.555	153.503	122.586	129.821	0.458	0.503
58.425	122.154	57.412	29.105	0.933	1.014
76.098	118.317	1.535	59.355	0.272	0.291
64.535	111.868	5.799	18.534	0.285	0.314
53.23	117.097	5.085	17.881	0.283	0.304
65.332	138.569	52.264	31.563	0.836	0.922
141.76	252.438	99.476	62.1	0.423	0.467
10.611	15.535	0	0	0	0
10.611	15.535	0	0	0	0
62.645	135.79	0	54.961	0.113	0.126
105.342	194.269	0	92.721	0.112	0.137
122.906	239.847	0	13.733	0.082	0.098